Functional analysis of the von Hippel-Lindau tumour suppressor in mice

Inauguraldissertation

zur
Erlangung der Würde eines Doktors der Philosophie
vorgelegt der
Philosophisch-Naturwissenschaftlichen Fakultät
der Universität Basel
von

Pia Ballschmieter

aus Ranco (Italien)

Zürich 2005

Genehmigt von der Philosophisch-Naturwissenschaftlichen Fakultät auf Antrag von Prof. Dr. Thomas Bickle, Prof. Dr. Wilhelm Krek und Prof. Dr. Holger Moch.

Basel, den 14. Dezember 2004

Prof. Dr. Hans-Jakob Wirz
(Dekan)

Table of contents

Abstract

Von Hippel-Lindau (VHL) disease is a dominantly inherited cancer syndrome characterized by the development of multiple tumours, among which the most common are tumours of blood vessels called hemangioblastomas (HB) that can be found in the retina and the central nervous system (CNS). The disease is caused by germline mutations in the VHL tumour suppressor gene and tumour development is linked to somatic inactivation of the remaining wild-type allele.

The best documented role of pVHL is as the substrate recognition component of a Skp1/cullin/F-box (SCF)-like E3 ubiquitin protein ligase complex that ubiquitinates the oxygen-sensitive α-subunit of hypoxia inducible factors HIF-1 and HIF-2 under normoxia and targets them for proteasomal degradation, thereby inactivating HIF. Loss of VHL function leads to the constitutive activation of HIF and subsequent up-regulation of hypoxia-inducible mRNAs encoding angiogenic growth factors such as vascular endothelial growth factor (VEGF), Erythropoietin (EPO) and glucose transporter 1 (GLUT1). Up-regulation of these factors characterizes VHL-associated tumours at the molecular level.

VHL gene expression studies on human fetal and adult tissues showed VHL mRNA to be ubiquitously detectable. Expression was not restricted to specific areas known to undergo abnormal differentiation as part of the VHL syndrome such as kidney, cerebellum and pancreas, but it was also present, among others, in the heart, lung and prostate. In addition VHL gene expression was evident in all derivatives of the three germ cell layers also during mouse embryogenesis, being most prominent in epithelial components of the lung, kidney and eye.

Expression studies of the VHL protein (pVHL) utilizing poly- and monoclonal antibodies against human VHL revealed wide cytoplasmic expression in human adult tissues. However, little is known about VHL expression patterns during development and in particular, the detailed distribution of VHL within specific tissues.

To investigate pVHL expression during murine development and adulthood a mouse pVHL-specific antibody was raised and utilized in a detailed immunohistochemical study focusing on the development of two tissues that play a very important role in the course of VHL disease, namely the retina and cerebellum.

Studying VHL disease, as any other disease, in humans is a difficult task that can be circumvented by the usage of genetically engineered mice that phenotypically mimic the

disease. The complete knockout of VHL unfortunately didn't provide a mouse model in which to investigate molecular pathology, gene-gene or protein-tissue interactions or even therapeutic intervention as the animals died early during gestation. In an attempt to create a mouse model that circumvented the block encountered in the complete knockout, we used Cre/loxP technology to design a strategy for creating a conditional VHL knockout, i.e. mice having exon 1 flanked by loxP sites (floxed). As our intent was not crowned with success and the floxed VHL mice were published in the meantime by another laboratory we could benefit by using these mice to specifically knock-out VHL in tissues we found to be interesting due to expression studies that had been undertaken as part of this thesis.

In the thesis presented herein the expression of pVHL in the retina and the cerebellum is described and the potential value of localizing VHL to previously unidentified cells is discussed (chapter 8). Moreover, an outline of an unsuccessful endeavour to create a conditional knockout is provided (chapter 7). Nevertheless, given the availability of such mice from a different laboratory, we undertook a cell-specific deletion approach to substantiate our immunohistochemical observations in vivo as presented in chapter 9.

Abbreviations

APMO	adnexal papillary cystadenoma of probable mesonephric origin
ARNT	aryl hydrocarbon receptor nuclear translocator
BAC	bacterial artificial chromosome
BCS	bovine calf serum
bp	base pair
BrdU	5-Bromo-2'-deoxyuridine
cDNA	complementary desoxyribonucleic acid
CDK	cyclin-dependent kinase
CDKI	cdk inhibitor
Ci	curie
CNS	central nervous system
CRALBP	cellular retinaldehyde-binding protein
Cre	causes recombination
C-TAD	C-terminal transactivation domain
Cul	cullin
CT	C-terminal
DAPI	4'6'-Diamidine-2'-Phenylindole Dihydrochloride
DMEM	Dulbecco´s modified Eagle´s Medium
DMSO	dimethylsulfoxide
DNA	deoxyribonucleic acid
DT-A	Diphtheria toxin A
DTT	dithiothreitol
dNTP	desoxyribonucleoside-triphosphate
ECL	enhanced chemi-luminescence
EDTA	ethylenediamine tetra-acetic acid
EGL	external granular (germinal) layer
ELST	endolymphatic sac tumour
EPAS	endothelial PAS domain protein
EPO	erythropoietin
ES cells	embryonic stem cells
EtOH	ethanol
FCS	fetal calf serum
FIH	factor inhibiting HIF
FITC	Fluorescein
FRT	Flp recombinase target
G418	geneticin
GABA	γ-aminobutyric acid
GCL	ganglion cell layer
GFAP	glial fibrillary acidic protein
GL	granular layer
HB	hemangioblastoma
HBSS	Hank's balanced salt solution
HEPES	N-2-Hydroxyethylpiperazine-N'-2-ethanesulfonic acid
HIF	hypoxia inducible factor
H_2O	water
HRE	hypoxia responsive element
HSV	herplex simplex virus

INL	inner nuclear layer
KAc	potassium acetate
kb	kilo-base (i.e. 1000 nucleotides)
KCl	potassium chloride
kD	kilo-dalton
KLH	keyhole limpet haemocyanin
LB	Luria Bertami medium
LIF	leukaemia inhibitory factor
loxP	locus of crossover (x) in P1
M	molar
m	milli (10^{-3})
µ	micro (10^{-6})
MEF	mouse embryo fibroblast
$MgCl_2$	magnesium chloride
ML	molecular layer
MMP	matrix metalloproteinase
mRNA	messenger ribonucleic acid
NaAc	sodium acetate
NaCl	sodium chloride
Na_2HPO_4	sodium hydrogen phosphate
NaH_2PO_4	sodium dihydrogen orthophosphate
NaOH	sodium hydroxide
Neo	neomycin
NGS	normal goat serum
NT	N-terminal
N-TAD	N-terminal transactivation domain
OD	optical density
ODD	oxygen-dependent degradation domain
ONL	outer nuclear layer
PBS	phosphate-buffered saline
PCE	papillary cystadenomas of the epididymis
PCR	polymerase chain reaction
PDGF	platelet-derived growth factor
Pheo	pheochromocytoma
PMSF	phenyl-methyl-sulphonyl-fluoride
RCC	renal cell carcinoma
RT	room temperature
RT-PCR	reverse transcriptase PCR
SDS	sodium dodecyl sulfate
TEMED	N,N,N',N'-Tetramethylethylenediamine
TGF	transforming growth factor
TIMP	their tissue inhibitors of matrix metalloproteinases
Tk	thymidine kinase
Tris	Tris(hydroxymethyl)aminomethane (Tris base)
U	unit of enzyme activity
UTR	untranslated region
VEGF	vascular endothelial growth factor
VHL	von Hippel- Lindau
WT	wild-type

Chapter 1

Von Hippel-Lindau Disease

Von Hippel-Lindau (VHL) disease is a dominantly inherited family cancer syndrome that predisposes affected individuals to a variety of tumours including those of blood vessels (hemangioblastomas; HB) of the retina and the central nervous system (CNS), clear-cell carcinomas of the kidney (RCC), adrenal gland tumours (pheochromocytomas), endolymphatic sac tumours (ELST), and epididymal and broad ligament cystadenomas (AMPO) (FIG.1) (Lonser, 2003; Kaelin, 2002; Singh, 2001). The disease results from germline mutations and subsequent biallelic inactivation of the VHL gene as a prerequisite for tumour formation and affects 1 in 36 000-45 500 live births (Kondo & Kaelin, 2001; Maher & Kaelin, 1997; Maher *et al.*, 1991; Neumann *et al.*, 1991).

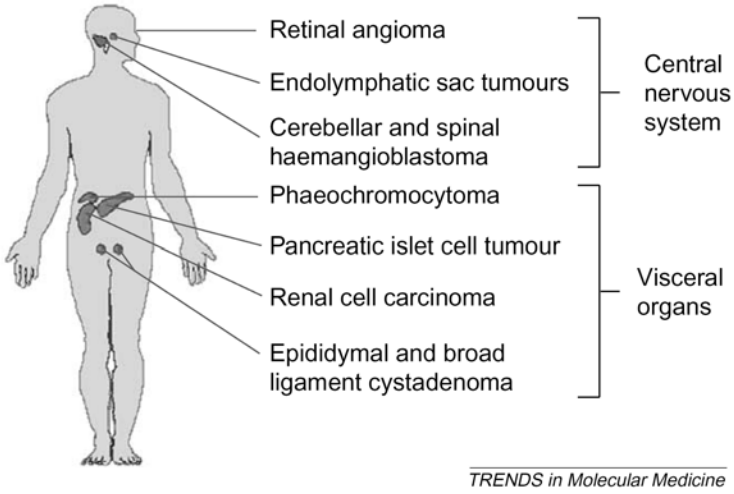

Figure 1: Location of the principal neoplasms seen in VHL disease (Barry & Krek, 2004).

The VHL disease was named after Eugen von Hippel, a german ophthalmologist, who first described eye angiomas and the familial occurrence of these retinal blood vessel tumours in 1904 (von Hippel, 1904), and Arvid Lindau, a Swedish neuropathologist, who in 1926 appreciated that these retinal lesions were a marker for a systemic disorder that also involved blood vessel tumours of the central nervous system (Lindau, 1927).

At the molecular level VHL disease presents itself as autosomal (not limited to one sex) recessive as VHL kindreds have a single germline mutation in one (inherited by an affected parent) of the two VHL alleles (Crossey *et al.*, 1994; Maher *et al.*, 1990). Only the somatic loss or inactivation of the remaining wild-type VHL allele (through deletion,

mutation or silencing by promoter methylation) initiates tumour development in accordance with Knudson's two-hit hypothesis of tumourigenesis (FIG. 2B) (Knudson, 1971). Nevertheless, as this somatic event occurs at a very high frequency, resulting in a high penetrance of VHL disease (> 90 %), the VHL disease presents itself clinically as an autosomal dominant disorder. However, one has to keep in mind that in addition to the biallelic deletion of VHL following the already present germline mutation, only cells that are constituents of susceptible target organs (CNS, kidneys etc.) eventually develop tumours.

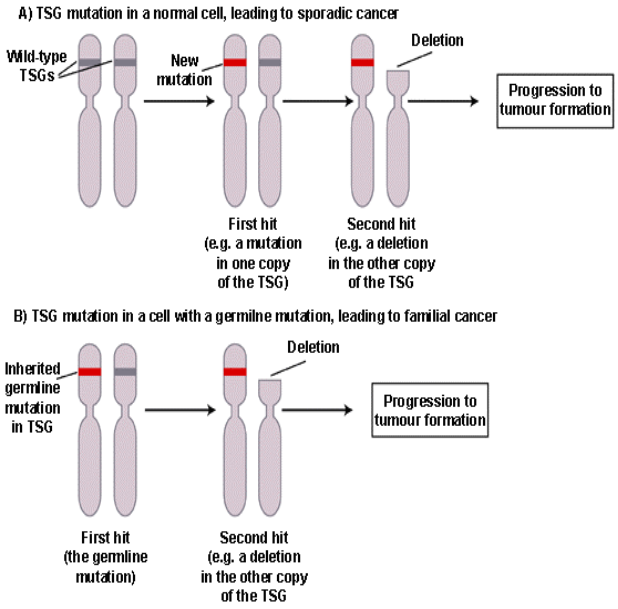

Figure 2. Knudson's two-hit hypothesis for tumourigenesis involving a tumour suppressor gene (TSG). (A) Normal individuals require somatic inactivation of both alleles of a TSG for tumour formation = "two hits" (B) Individuals with an inherited inactivated allele only require inactivation of the corresponding TSG allele for tumour progression = "one hit"

Adapted from Richards et al. 2001

In keeping with the Knudson 2-hit model, VHL gene inactivation has also been shown in some sporadic tumours of the same histological types as observed in VHL disease. VHL protein function is lost in 50-80% of sporadic cases of renal clear-cell carcinomas (Brieger *et al.*, 1999; Gnarra *et al.*, 1994), as well as in some sporadic cases of CNS hemangioblastomas (Lee *et al.*, 1998). In these cases the first hit occurs as a result of somatic mutation or promoter hypermethylation and then requires a second somatic mutation to occur in order for tumours to arise (FIG. 2A) (Maher *et al.*, 1990).

1.1 Clinical manifestations of VHL disease

VHL disease, unlike most other diseases, does not occur exclusively in one organ or at a particular age and has no single primary symptom. The age of onset is variable as it depends on the expression of the disease within an individual and within a family, but the disease normally achieves full penetrance by the age of 65.

Among the large number of tumours that have been shown to be linked to VHL disease the most recurrent ones are retinal and CNS hemangioblastomas, RCC and to a much lesser extent pheochromocytomas (although the latter is used to classify the disease

subtypes as discussed under 1.2). In addition to these "main" features, multiple renal, pancreatic and epididymal cysts can occur and in up to *ca.* 10 % of patients pancreatic islet cell tumours and endolymphatic sac tumours (ELST) of the inner ear are found. While hemangioblastomas are normally benign cystic tumours (although they can still be a cause of considerable morbidity), RCC, pheochromocytoma and pancreatic islet cell tumours can all be malignant.

The main causes of death in VHL disease have been metastases from renal cell carcinomas and neurological complications of CNS hemangioblastomas, though in recent years due to improved surveillance, earlier diagnosis and improved treatments, the prognosis has improved and complications related to these tumours have been reduced.

The phenotypes of VHL disease will be shortly discussed below (for reviews see Lonser *et al.*, 2003; Kaelin, 2002; Singh *et al.*, 2001; Choyke *et al.*, 1995):

1.1.1 Hemangioblastomas

Hemangioblastomas are benign non-metastasising blood vessel tumours that consist of a mixture of so-called "stromal cells" and blood vessels (pericytes and endothelial cells) (FIG. 3). The origin of the stromal cells is still a matter of debate (see also discussion) but it has been shown that these are the neoplastic component (the tumour cells) as they have lost pVHL expression and function, overproducing HIF target gene products such as vascular endothelial growth factor (VEGF) and platelet-derived growth factor B chain (PDGF-β), which are likely to support the proliferation of the endothelial cells and pericytes respectively, transforming growth factor- α (TGF–α) and erythropoietin (EPO). Retinal and central nervous system hemangioblastomas in VHL disease are histologically indistinguishable and are therefore both referred to as hemangioblastomas.

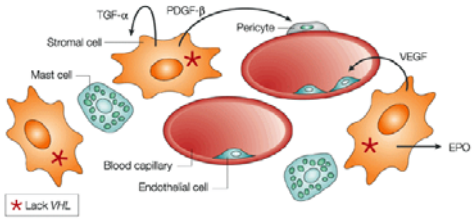

Figure 3. Histopathology of hemangioblastomas (HB). HBs consist of stromal cells and blood vessel cells-pericytes and endothelial cells. In VHL disease the blood vessel cells have been shown to be VHL+/-, whereas the stromal cells are VHL-/-. Due to the lack of VHL function the stromal cells accumulate high levels of hypoxia-inducible factor HIF-1α, which in turn leads to the overproduction of a number for HIF target genes such as TGF- α, EPO, VEGF and PDGF-β. TGF- α probably acts in an autocrine loop.
Adapted from Kaelin, 2002

1.1.1.1 Retinal Hemangioblastomas

Among the manifestation of VHL disease retinal hemangioblastomas (HB; also called angiomas) appear to be among the most common and earliest tumours, seen in as many as

41-60 % of VHL patients. These tumours arise normally in the capillary bed of the retina, in the vascular tissue between the arterioles and venules in the circulatory system (FIG. 4). When capillaries form angiomas in the retina they start out extremely small and difficult to detect/see due to the fact that they form mostly in the periphery or on/near the optic disc far away from the area of central vision. Retinal hemangioblastomas are frequently multiple and if untreated may produce retinal detachment and hemorrhage leading to blindness. Detected early though most retinal angiomas respond to laser therapy or cryotherapy (reviews by Singh *et al.*, 2001; The VHL Handbook under www.vhl.org).

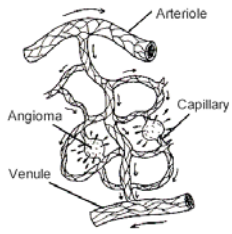

Figure 4. Retinal angioma in VHL disease.

1.1.1.2 Central nervous system hemangioblastomas

The most common tumours in VHL disease affecting 60-80 % of all VHL patients are central nervous system hemangioblastomas (or hemangiomas). These blood vessel tumours of the brain and spinal cord are benign but a major source of morbidity. Many patients with VHL disease ultimately develop multiple CNS hemangioblastomas and the management of brain stem and spinal tumours is often difficult and thus CNS involvement remains an important cause of morbidity and mortality for VHL patients.

The cerebellum is the most frequent site of central nervous system hemangioblastomas (57-60 % of patients) followed by the spinal cord (13-12 %) and brain stem sites. The mean age at onset of cerebellar hemangioblastomas in VHL disease is considerably younger than in sporadic cases.

1.1.2 Renal Clear Cell Carcinomas and renal cysts

Renal Cell Carcinoma (RCC) occurs in 24-47 % of patients with VHL disease and affects a majority of the individuals with VHL disease, if they live long enough. In addition, RCC in VHL disease tends to be associated with renal cysts adding up to increase the finding of a renal lesion to 60 %. Renal cell carcinomas are the major malignant neoplasm in VHL disease and mutations in the VHL gene are the primary cause of inherited renal cancer. Renal cysts are frequent although they rarely produce significant renal impairment, but they can give rise, over time, to RCC.

1.1.3 Pheochromocytomas

Pheochromocytomas are benign tumours of the adrenal gland that arise from neural crest tissue and produce elevated levels of catecholamines (norepinephrine and epinephrine) (Koch *et al*., 2001). Pheochromocytomas are present in about 7-19 % of VHL disease patients and tend to be multiple or bilateral. Although this type of tumour is not that frequent overall, in some families pheochromocytomas are the major manifestation and this has contributed to the classification criteria of the VHL disease as discussed under 1.2.

1.1.4 Pancreatic cysts and neoplasms

Pancreatic lesions in VHL disease are usually classified as nonsecretory (cyst and cystadenoma) or secretory (islet cell tumour) (Neumann *et al.*, 1991). Among these the pancreatic cyst is the most common pancreatic lesion observed in about 15-30 % of patients with VHL disease.

Islet cell tumours consist of nests of polygonal cells with vesicular nuclei and are mostly asymptomatic but lesions can grow rapidly, cause biliary obstruction and metastasise to the liver or more distantly to the bone. An association may exist between islet cell tumours of the pancreas and pheochromocytomas since *ca.* 20 % of the VHL families with a high prevalence of pheochromocytoma will also develop islet cell tumours whereas this tumour is rare in other VHL families.

1.1.5 Endolymphatic sac tumours (ELST)

Slow-growing low-grade papillary adenocarcinomas may occur in up to 11 % of patients and are often bilateral. ELST is a recently recognized feature of VHL disease and may be more common than previously thought (Manski *et al.*, 1997).

1.1.6 Epididymal and broad ligament cystadenoma

Papillary cystadenomas (a benign tumour with multiple cysts inside it, having higher density than a normal cyst) of the epididymis (PCE) are seen in approximately 10-26 % of men with VHL disease (Choyke *et al.*, 1997). (The epididymis is a small, coiled conduit, which lies behind the testicle, in the scrotum, on the path to the vas deferens, the vessel, which carries the sperm from the testicle to the prostate gland.)

A corresponding tumour in women is the adnexal (adjoining) papillary cystadenoma of probable mesonephric origin (APMO) of the broad ligament near the

fallopian tube (the channel carrying eggs from the ovary to the uterus). The broad ligament lies in folds and creases on top of both ovaries and uterine tubes, connecting these structures to the larger body of the uterus.

1.2 Clinical diagnosis and classification of VHL disease

The diagnostic criteria for VHL disease are based upon three elements: retinal capillary or CNS hemangioblastoma, visceral lesions and family history of similar lesions (Melmon & Rosen, 1964). Patients with a family history and a hemangioblastoma (retinal or CNS), pheochromocytoma or RCC are diagnosed with the disease. Those patients with no relevant family history must have at least two CNS hemangioblastomas and a visceral tumour (except epididymal and renal cysts as these are frequent in the general population) to meet the diagnostic criteria.

VHL disease can be classified into two main types, depending on the risk of developing pheochromocytoma (Table 1):

Type 1 families have a greatly reduced risk of pheochromocytomas but can develop all the other tumour types whereas Type 2 families have pheochromocytomas but have either a low risk (2A) or high risk (2B) for renal cell carcinoma. Type 2C families have pheochromocytomas only with no other neoplastic findings of VHL. The correlation of specific mutations and therefore the genotype with a specific VHL phenotype will be further elucidated under 1.3.3.

Classification of VHL disease

Type	Clinical characteristics			Germline VHL mutation
	HB	RCC	Pheo.	
Type 1	+	+	–	Deletions and truncations
Type 2A	+	–	+	Missense e.g. Tyr98His
Type 2B	+	+	+	Missense e.g. Arg167Trp
Type 2C	–	–	+	Missense e.g. Leu188Val

Table 1: Classification of VHL disease types and the most frequently mutated residues connected to the different types. In the germline mutation examples, the amino acid of the specific residue number has been exchanged with the amino acid indicated after the residue number. *Adapted from Richards, 2001*

1.3 The VHL gene and protein function

1.3.1 The human VHL gene

In humans the VHL tumour suppressor gene is located on the short arm of chromosome 3 (3p25-26) (Latif *et al.*, 1993), covering less than 20 kb of genomic DNA and encoding a 4.7 kb mRNA. Alternative splicing yields a small proportion of VHL mRNA that lacks exon 2 (isoform II), which is predicted, if translated, to produce an in-frame deletion of 41 amino acids. The identification of VHL patients with germline deletions in exon 2 resulting in isoform II expression only, suggests though that this isoform is not encoding a fully functional gene product (Gnarra *et al.*; 1994).

The VHL coding sequence is contained within 3 exons (exon 1= 70 bp 5' UTR and 340 bp coding sequence, exon 2= 123 bp coding sequence and exon 3= 179 bp coding sequence and 4 kb 3' UTR) (FIG. 5a). Codons 14 to 53 encode eight copies of an acidic pentameric repeat [Gly-X-Glu-Glu-X; $(GXEEX)_8$] with homology to a procyclic surface membrane protein of *Trypanosoma brucei*. However the functional significance of this region is still unclear. The 642 nucleotides of the VHL gene encode a polypeptide of 213 amino acids with an apparent molecular weight of *ca.* 30 kDa and therefore termed $pVHL_{30}$ (Iliopoulos *et al.*, 1995). Due to alternative translation initiation at an internal methionine located at residue 54, a shorter VHL protein, $pVHL_{19}$, of 160 amino acids and with an apparent molecular weight of 18-19 kDa is also synthesized (Blankenship *et al.*, 1999; Schoenfeld *et al.*, 1998; Iliopoulos *et al.*, 1998) (FIG. 5b). This protein lacks the acidic domain.

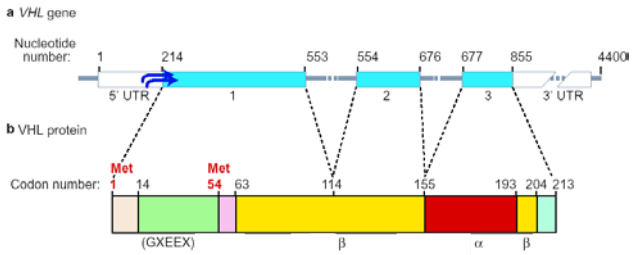

Figure 5. VHL gene (a) and protein (b) structure.

Adapted from Richards, 2001

The VHL gene promoter lies approximately 60 bp upstream from the first methionine codon and is a GC-rich, TATA-less and CCAAT-less promoter with transcription initiating around a putative Sp-1 binding site (Kuzmin *et al.*, 1995). It contains numerous predicted binding sites for transcription factors but it has not yet been revealed how VHL expression is controlled (Zatyka *et al.*, 2002). The 3' untranslated region in human contains 11 so-called Alu repeats and is in part conserved in rodents, however at present, no evidence exists that suggests a VHL-related functional role for these repeats.

1.3.2 The VHL protein (pVHL)

The two VHL gene products $pVHL_{30}$ and $pVHL_{19}$ are both detectable *in vivo* and differ only by the additional presence of the afore-mentioned eight N-terminal acidic repeats characterising solely the longer pVHL form, $pVHL_{30}$. As the functional distinction between the two VHL forms remains elusive to date and as both forms behave similarly in most functional assays, they are very often referred to generically as pVHL. Moreover, almost all inactivating mutations known so far lie within regions of the VHL gene that are common to both proteins leading to the assumption that both forms of pVHL have to be inactivated in order for tumours to arise. However a mutation found in the N-terminal acidic domain, P25L, has been identified in patients with sporadic pheochromocytoma and would suggest that there are different functions related to the two proteins (Van der Harst, *et al.*, 1998). Furthermore the two pVHL forms differ in their subcellular localization: while $pVHL_{19}$ is predominantly nuclear, $pVHL_{30}$ localises to both nuclear and cytoplasmic compartments. In addition it has been shown that when $pVHL_{30}$ resides in the cytoplasm it associates and stabilizes the microtubule network (Hergovich *et al.*, 2003). pVHL has been shown to be subjected to nucleocytoplasmic shuttling mediated by Ran and to be also associated with the endoplasmatic reticulum (ER) (Schoenfeld *et al.*, 2001; Groulx *et al.*, 2000; Lee *et al.*, 1996).

pVHL, comprising both VHL gene products, is a tumour suppressor protein based on both genetic and functional criteria as tumour formation by VHL-defective renal carcinoma cells 786-O in nude mouse xenograft assays is suppressed after reintroduction of wild-type VHL (Gnarra *et al.*, 1996; Iliopoulos *et al.*, 1995).

pVHL has two major, functionally distinct, structural domains: the α- and the β-domain (FIG.5b). While the smaller α-domain consists of 3 α-helices (aa 155-192), the β-domain consists of a seven-stranded β sandwich (aa 63-154) and one α-helix (aa 193-204) (Stebbins *et al.*, 1999). The α-domain is required for binding elongin C (aa 157-171) and the β-domain provides the substrate-docking interface for target proteins, including the HIF-α subunits (see chapter 1.3.5).

1.3.3 Genotype-Phenotype correlations

When germline mutations (mutations present in all cells of an individual including the germ cells and that are therefore heritable) occur in the VHL gene, they confer the genetic risk of tumour formation in concert with somatic second VHL allele loss or DNA

methylation inactivation. Germline VHL mutations have been identified in more than 500 VHL families worldwide and show considerable heterogeneity in both their type and their location within the VHL gene. Two-thirds of VHL patients harbour missense, nonsense, splice site mutations, and micro-deletions and –insertions, while in one-third large deletions of 4-380 kb can be found.

As mentioned before, VHL disease has been classified into subcategories depending on the likelihood of pheochromocytomas to arise in a VHL patient and specific genotype-phenotype correlations are beginning to emerge in affected families (Table 1). Type1 disease is normally associated with mutations that lead to complete loss of the VHL gene product (deletion, frame-shift, nonsense and splice mutations) and the few missense mutations leading to type 1 have been mapped to residues in the hydrophobic core of the β-domain causing probably complete unravelling of the pVHL structure. In contrast, the majority of missense mutations are associated with type 2 disease and mostly map to the binding site for elongin C, to the surface patch in the β-domain involved in binding HIF-α or are predicted to cause relatively localised effects if a structural residue is involved. Type 2C mutations (i.e. associated with pheochromocytoma only) promote HIF-α ubiquitylation in vitro, but are apparently incapable of binding and regulating the assembly of fibronectin (Clifford *et al.*, 2001; Hoffman *et al.*, 2001). This suggests that loss of other VHL functions than HIF-α regulation are necessary for pheochromocytoma susceptibility and raises the possibility that abnormal fibronectin matrix assembly contributes to pheochromocytoma pathogenesis in the setting of VHL disease. Mutations causing type 1, type 2A and type 2B demonstrated variable effects on Hif-α and elongin binding, though resulting all in defective HIF-α regulation and loss of fibronectin binding. In summary HIF deregulation seems to have a causal role in HB and RCC, while there must be another cause for pheochromocytoma pathogenesis. A listing of all found germline and somatic VHL mutations assembled can be viewed under http:// www.umd.be (Beroud *et al.*, 1998).

1.3.4 VHL gene and protein expression

VHL mRNA and protein are ubiquitously expressed implying that tissue-specific expression cannot account for the complex tumour pattern observed in VHL disease. For example, during human embryogenesis, VHL mRNA is expressed from as early as six weeks of gestation in virtually all tissues with particular high levels in urogenital system, brain, spinal cord, sensory ganglia, eyes and bronchial epithelium (Richards *et al.*, 1996). In

addition it has been shown that VHL expression in the kidney is present in the proximal tubule, where RCC is postulated to arise, but also in the loops of Henle, which are normally never affected during the course of VHL disease (Richards *et al.*, 1996; Kessler *et al.*, 1995). The only study focusing on VHL mRNA expression during mouse embryogenesis documented similar widespread expression as in human (Kessler *et al.*, 1995).

Studies investigating the expression of the VHL protein also confirmed widespread VHL expression and demonstrated that pVHL is expressed especially in epithelial cells as those covering the body surface, the alimentary canal, and the respiratory and genitourinary tracts. In addition expression was found in cardiomyocytes, parenchymal cells of visceral organs, secretory cells of the exocrine and endocrine organs, neurons in nervous tissue, lymphocytes in lymphoid tissue and macrophages (Sakashita *et al.*, 1999; Corless *et al.*, 1997; Los *et al.*, 1995).

During the course of the thesis presented herein I was able to show cell-specific expression of VHL in two tissues, namely the retina and the cerebellum by using a newly created antibody recognizing specifically the mouse VHL protein. These new findings will be discussed in chapter 8.

1.3.5 VHL function as part of an E3 ligase complex

pVHL functions as the substrate recognition component of a complex termed VCB-Cul2, a stable multi-protein complex with elongins C and B, Cullin2 (Cul2) and Rbx1 (a RING box protein also called Roc1 and Hrt1) (FIG. 6). (Kamura *et al.*, 1999, Lisztwan *et al.*, 1999; Pause *et al.*, 1997; Kibel *et al.*, 1995; Duan *et al.*, 1995). Cul2 is the scaffold for the E2 enzyme, Rbx1 and elongin C components of the complex. Rbx1 functions to assist in recruiting the E2, while Elongin C bridges Cul2 and the substrate recognition component pVHL, while Elongin B stabilizes the complex. This multi-protein complex, whose correct assembly is directly mediated by association of amino acids 100-155 of pVHL with the chaperonin protein TriC (also called CCT for cytosolic chaperonin-containing TCP-1) (Hansen *et al.*, 2002; Feldman *et al.*, 1999), has E3 ubiquitin-ligase activity and functions in conjunction with an E2 ubiquitin-conjugating enzyme to poly-

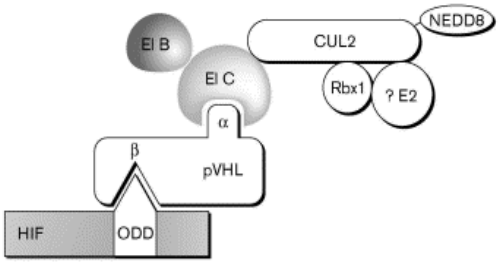

Figure 6. The VCB-Cul2 complex. The von Hippel-Lindau tumour-suppressor protein (pVHL) forms a protein complex (VCB-Cul2) with elongin C (El C), elongin B (El B), Cul-2 (neddylated or not), and Rbx1, which functions as an ubiquitin-protein ligase (E3). The beta domain of pVHL binds directly to the ODD domain of HIF-α subunits and directs their ubiquitination in the presence of oxygen.
Adapted from Ivan & Kaelin, 2001

ubiquitinate proteins which targets them for subsequent degradation via the 26S proteasome (FIG. 7).

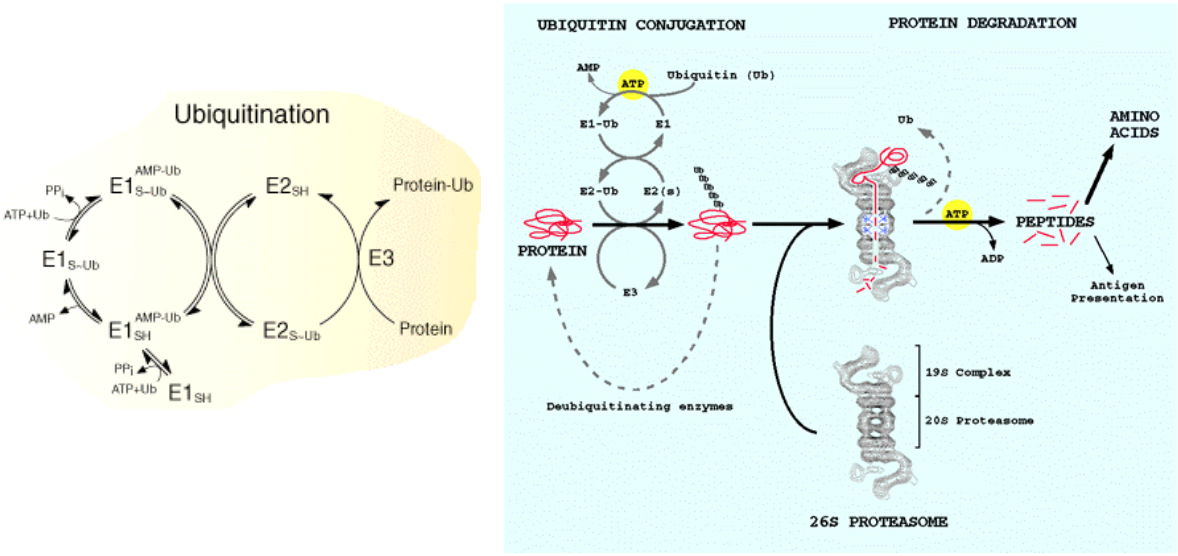

Figure 7. Many proteins that undergo regulated destruction are first covalently modified by the attachment of a polyubiquitin tail, which serves as a signal for degradation by a multiprotein complex of proteolytic enzymes called the proteasome. Substrate-specific poly-ubiquitylation involves the sequential action of the E1 ubiquitin activating enzyme, an E2 ubiquitin-conjugating enzyme and an E3 ubiquitin ligase. Ubiquitination is a multistep process that conjugates ubiquitin moieties to internal lysine residues of proteins and successive conjugation of ubiquitin molecules generates polyubiquitin chains. Polyubiquitinated proteins are then degraded by the 26 S proteasome

To date, the most intensely studied and best-understood substrates of the VCB-Cul2 complex are the α-subunits of the heterodimeric Hypoxia inducible factor (HIF) (see 1.3.5.1) (Iwai *et al.*, 1999). In the presence of oxygen, hydroxylated HIF-α interacts with the β-domain of VHL in the VCB-Cul2 complex, which targets HIF-α for degradation by the ubiquitin-proteasome pathway (Min *et al.*, 2002; Tanimoto *et al.*, 2000). Under hypoxic conditions or in the absence of functional pVHL, HIF-1α and HIF-2α are stabilized and accumulate resulting in elevated transcription of a wide variety of HIF-controlled genes such as VEGF, erythropoietin, glucose transporter GLUT1, TGF-β and TGF-α (Maxwell *et al.*, 1999; Iliopoulos *et al.*, 1996). Overproduction of these angiogenic factors contributes to the highly vascularized tumours that develop in VHL patients.

1.3.5.1 Hypoxia inducible factor (HIF)

The hypoxia-inducible factor HIF-1α is a key regulator of responses to hypoxia through transcriptional activation of a variety of genes linked to processes such as angiogenesis, glucose uptake and metabolism. HIF is a heterodimeric transcription factor consisting of an α-subunit (usually HIF-1α, other family members are HIF-2α and HIF-3 α, which will be discussed at the end of this subchapter) and HIF-1β (also called ARNT for aryl

hydrocarbon receptor nuclear translocator), which are basic helix-loop-helix (bHLH) proteins of the PAS family (named after Per, ARNT and Sim, which were the first members to be recognized). While the nuclear β-subunit is constitutively expressed, the α-subunit is the regulatory component, which is labile under normoxia and targeted by the VCB-Cul2 complex for ubiquitination and subsequent degradation. Under hypoxic conditions though, HIF-α accumulates, becomes phosphorylated, dimerizes with HIF-β and binds to specific DNA sequences, hypoxia-response elements (HRE), in the cis-regulatory regions of hypoxia-inducible genes activating their transcription (general reviews Lee *et al.*, 2004; Maynard & Ohh, 2004).

The interaction of pVHL with HIF-1α requires the latter to be enzymatically hydroxylated at two conserved proline (P) residues, P402 and P564, each within a Leu-X-X-Leu-Ala-Pro sequence motif (Masson *et al.*, 2001). This oxygen dependent hydroxylation is carried out by proline hydroxylases and is required for HIF-α to participate in two essential hydrogen bonds with hydrophilic side chains that are located in the VHL β-domain (Hon *et al.*, 2002; Bruick & McKnight, 2001; Ivan *et al.*, 2001; Epstein *et al.*, 2001; Jaakola *et al.*, 2001;Ohh *et al.*, 2000). In human there are three prolyl hydroxlase isoforms, PHD 1-3, among which PHD2 has been proposed to be the primarily responsible for HIF hydroxylation under normoxia (Berra *et al.*, 2003). The VHL-binding site of HIF-1α lies within a region termed the oxygen-dependent degradation (ODD) domain, which overlaps with the amino-terminal transactivation domain (N-TAD) of HIF-1α, and which confers protein instability in the presence of oxygen. The second transactivation domain of HIF1-α lies in the carboxy-terminus (C-TAD) and activates transcription solely under hypoxia as under normoxia a specific asparagine residue, N893, is hydroxylated by a HIF asparaginyl hydroxylase called FIH (factor inhibiting HIF) (Lando *et al.*, 2002; Mahon *et al.*, 2001). Hydroxylation at this site prevents recruitment of the co-activator proteins p300 and CBP (cyclic-AMP-response-element-binding-protein (CREB)-binding protein). HIF is therefore regulated at the level of protein turnover by prolyl hydroxylation, which serves as a signal for pVHL binding, and at the level of co-activator recruitment by asparaginyl hydroxylation (FIG. 8).

In addition, normoxia also stimulates binding of a protein acetyl-transferase named ARD1 to HIF-1α that acetylates lysine 532 in the ODD domain. This acetylation has been shown to increase the interaction of HIF with VHL promoting its proteasomal degradation, but the mechanism is still unknown (Jeong *et al.*, 2002). The VHL-HIF-α complex has been shown to have in addition another binding partner, the Tat-binding protein TBP-1 (which is

an ATPase subunit within the 19S regulatory particle of the 26S proteasome) that seems to regulate the proteasomal degradation of HIF-α (Corn *et al.*, 2003).

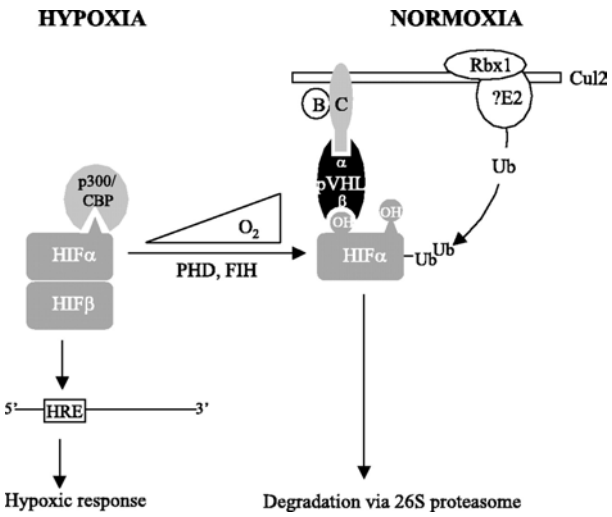

Figure 8. Hydroxylation of HIF-α and the regulation of hypoxia-inducible genes. In the absence of oxygen (left side), HIF-α is bound by the transcriptional coactivators p300/CBP and dimerizes with HIF-β. It then binds to hypoxia-responsive elements (HREs), initiating the transcription of numerous hypoxia-inducible genes. In the presence of oxygen, HIF-α is hydroxylated on conserved pralines bz prolyl hydroxylases (PHDs) and on asparagine at position 803 by the factor inhibiting HIF (FIH) enzyme. Prolyl hydroxylation promotes HIF-α recognition by the b-domain of pVHL and subsequent ubiquitination by the VCB-Cul2 complex, resulting in HIF-α degradation via the 26S proteasome. In addition, the asparaginyl hydroxylation prevents p300/CBP from binding HIF-α, thus also inhibiting transcription of hypoxia-inducible genes. B and C, elongin B and elongin C respectively; Cul2, cullin 2; Ub, ubiquitin.

Adapted from Sufan *et al*., 2004

In human there are in total three HIF-α genes: besides HIF-1α there are the homologues HIF-2α (also called EPAS1 and MOP2) and HIF-3α, which have structural similarities but seem to have different functions (Park *et al.*, 2003). While HIF-1α is ubiquitously expressed, HIF-2α expression is e.g. high in the mouse lung, where it has been implicated in the development of the tubular system, and in vascular endothelial cells where it is involved in vascular remodelling (Wiesener *et al.*, 2003; Brusselmans *et al.*, 2001; Jain *et al.*, 1998; Tian *et al.*, 1997). Interestingly, in the kidney both HIF-1α and HIF-2α are abundantly expressed, but only HIF-2α overexpression promotes growth of renal carcinoma cells and its inhibition is sufficient to suppress this growth (Kondo *et al.*, 2002 and 2003). Therefore, although HIF-1α and HIF-2α are very similar, also binding as dimers with HIF-1β the same DNA sequences, they might have a different tissue or cellular expression resulting possibly in activation of different target genes. The fact that both HIF-1α- and HIF-2α-knockout mice have been shown to be embryonically lethal suggests that the two genes actually have distinct functions (Iyer *et al.*, 1998; Ryan *et al.*, 1998; Tian *et al.*, 1998; Peng *et al.*, 2000). HIF-3α is the least characterized of the three HIF-α subunits and is unique as the gene gives rise to a multitude of splice variants and lacks the N-TAD (Maynard *et al.*, 2003). One of these alternative splice variants of HIF-3α, the inhibitory PAS domain protein (IPAS), has been shown to act as a dominant negative regulator of HIF-1α and HIF-3α might therefore generally act as an antagonist of the HIF system (Makino *et al.*, 2002).

The dysregulation of the HIF transcriptional cascade has extensive effects that make it difficult to distinguish whether, and to what extent, observed matrix-related abnormalities in VHL-defective renal carcinoma cells [including abnormal fibronectin assembly, defective formation of fibrillar adhesions and changes in branching morphogenesis and migration (Esteban-Barragan *et al.*, 2002; Kamada *et al.*, 2001; Davidowitz *et al.*, 2001; Koochekpour *et al.*, 1999; Ohh *et al.*, 1998)] represent effects on pathways that are related or distinct from HIF. In C. elegans it has now been shown recently, by studying and comparing effects of VHL inactivation on gene expression patterns in wild-type versus HIF1-defective backgrounds, that there are HIF-dependent and –independent effects, linking a HIF-independent VHL pathway with extracellular matrix function (Bishop *et al.*, 2004).

1.3.5.2 Other targets of the VCB-Cul2 E3 ligase complex

Additional potential targets of the VBC-Cul2 E3 ligase complex may be:

- the atypical protein kinase C (aPKC) isoforms λ αnd ζ that have been shown to bind to VHL though its β-domain. At least for PKCλ it has been shown that VHL as part of the E3 ligase complex mediates its ubiquitination (Okuda *et al.*, 1999)
- the VHL-interacting de-ubiquitinating (VDU) enzymes 1 and 2 (Li *et al.*, 2002)
- the seventh subunit and the large subunit of RNA polymerase II (Kuznetsova *et al.*, 2003; Na *et al.*, 2003)

1.3.6 Other functions of VHL

VHL role in transcripton (beyond HIF)

Apart form the hypoxia-responsive pathway pVHL is capable of regulating the transcription of certain other genes independently of HIF. Among these are the transcription factor SP1 (Rafty *et al.*, 2002; Cohen *et al.*, 1999) and the pVHL-associated KRAB-A domain-containing protein (VHLaK) transcription repressor (Li *et al.*, 2003).

VHL role in CNS development

Investigation of the putative role of VHL in the CNS development by using rodent progenitor cells showed that neuronal differentiation is induced by VHL gene transduction and correlates with pVHL-expression (Murata *et al.*, 2002; Kanno *et al.*, 2000). In this specific experiment a VHL mRNA antisense oligonucleotide approach inhibited the CNS

progenitor cell differentiation and upregulated their cell cycle fitting to a putative role for VHL in cell-cycle control as also discussed in the next paragraph.

Link between pVHL and cell-cycle control

A potential involvement of VHL in cell cycle control was suggested as it has been shown that cells lacking pVHL, such as the renal cell carcinoma cell line 786-O, overexpress cyclin D1 and downregulate the cyclin-dependent kinase (cdk) inhibitor p27 and exhibit an impaired ability to exit the cell cycle following serum withdrawal (Bindra *et al.*, 2002; Pause *et al.*, 1998). Moreover, forced overexpression of pVHL leads to upregulation of p27 (Kim *et al.*, 1998). But up to this point no evidence was given that there is a direct link between VHL and p27. Moreover different results are emerging making it difficult to understand this potential link (Goda *et al.*, 2003, Wang *et al.*, 2003).

Link between VHL and the extracellular fibronectin matrix

Renal cell carcinoma cells lacking VHL are deficient in proper fibronectin matrix assembly and VHL has been shown to associate directly with fibronectin in order to promote proper matrix assembly (Esteban-Barragan *et al.*, 2002; Ohh *et al.*, 1998). This association is somehow dependent on the neddylation of VHL as a neddylation-defective pVHL mutant fails to promote proper fibronectin matrix assembly (Stickle *et al.*, 2004).

Type 2C mutant, predisposing solely to pheochromocytoma, have been linked to fibronectin assembly, as their binding capacity to fibronectin is impaired while the E3 ubiquitin ligase complex is functional. This would actually suggest that these would be gain-of function mutations as type1 VHL disease patients have no or a low risk for pheochromocytomas (Hoffman *et al.*, 2001).

Link between VHL and tumour growth and metastasis

pVHL has an effect on matrix metalloproteinases (MMPs) and their tissue inhibitors of matrix metalloproteinases (TIMPs), which is independent of the hypoxia-responsive pathway. Loss of VHL function regulated negatively TIMPs, such as TIMP2, while upregulating MMPs (2 and 9) (Koochekpour *et al.*, 1999). As MMPs are important in angiogenesis, morphogenesis and tissue remodelling and have been associated with cellular invasiveness (Lafleur *et al.*, 2003), the regulation by VHL attributes a role to VHL in tumour growth and metastasis. In addition lack of functional VHL has been associated with overproduction of carbonic anhydrases 9 and 12 (CA9 and CA12), which favour the

growth and invasive properties of tumour cells by their involvement in the acidification of the tissue microenvironment (Ivanov *et al.*, 1998).

Link between VHL and microtubules

VHL has been recently shown to bind to and stabilize microtubules (Hergovich *et al.*, 2003) and even more recently it has been proposed that VHL changes the behaviour of MTs dependent on their subcellular localization (Lolkema *et al.*, 2004). This implies a role for VHL in cellular processes such as migration, polarization, and cell-cell interactions.

1.4 mVHL-the mouse homologue of VHL

The VHL gene sequence has homologues in the nematode worm *C. elegans* (Woodward *et al.*, 2000) and in *Drosophila* (Adryan *et al.*, 2000; Aso *et al.*, 2000) and it is highly conserved in primates and rodents. Sequence conservation is particularly high across regions known to be involved in binding to other proteins or in maintaining the pVHL structure, and conservation of function has been confirmed in *Drosophila*.

The murine VHL gene also gives rise to two proteins, $pVHL_{25}$ and $pVHL_{21}$, which, in contrast to the human homologue, have only one acidic repeat within the N-terminal 19aa that distinguishes them (Gao *et al.*, 1995).

Several groups have attempted to develop a mouse model that mimics the phenotypic features of VHL disease. The complete VHL knockout published in 1997 revealed an essential role for pVHL in development as homozygous animals died between day E10.5-E12.5 due to vascular abnormalities in the placenta. Heterozygous mice on a C57BL/6 background though were phenotypically normal (Kleymenova *et al.*, 2004; Gnarra *et al.*, 1997). Heterozygous VHL mice on a BALB/c background were later shown to develop blood vessel tumours in the liver (hepatic hemangiomas) (Haase *et al.*, 2001) and this implies that the strain background must have an impact on the observed phenotypes. To avoid embryonic lethality Haase *et al.* utilized Cre/loxP site-specific recombination using an albumin promoter driven Cre recombinase to conditionally inactivate the VHL gene in the liver. They could confirm that homozygous deletion of VHL in the liver resulted in hepatic tumours leading to death at 6-12 weeks (Haase *et al.*, 2001). However no other organ was affected in this conditional VHL knockout model.

In another attempt to produce a VHL conditional knockout mouse model that more closely mimicked human VHL disease a human β–actin promoter-driven cre transgenic mouse that expresses cre in a mosaic pattern in multiple organs was utilized (Ma *et al.*, 2003).

In this case loss of pVHL resulted in an extensive abnormal vascular phenotype in multiple mouse organs, which appears consistent with the ability of pVHL to control the expression of genes whose product participate in angiogenesis, a crucial stage in tumour progression.

Recently it has been shown that VHL has a crucial role in endochondral bone development by conditional inactivation of murine VHL in all cartilaginous elements (Pfander *et al.*, 2004). The mice were viable, but grew slower than control littermates developing a severe dwarfism. VHL is therefore necessary for normal chondrocyte proliferation *in vivo*. This is in contrast to the idea that VHL actually helps cell cycle exit. However these findings are consistent with another report that lack of pVHL inhibits cell proliferation in a teratocarcinoma model (Mack *et al.*, 2003). It is therefore possible that pVHL actions on the cell cycle vary in different cell types.

In the thesis presented herein we first tried to create a conditional VHL mouse where exon 1 of VHL would have been flanked by loxP sites (see also chapter 3), a so-called floxed VHL mouse. Unfortunately in our case it didn't work out, but it was published at the same time by Haase *et al.*. The availability of these floxed VHL mice allowed us to create a conditional VHL knockout model in the brain with severe impacts on the brain development as shown in chapter 9.

Chapter 2

The Retina and Cerebellum

-A closer look at two tissues in the context of VHL disease-

VHL disease is characterized by a defined subset of tumours that can be found only in specific tissues (as presented in chapter 1). Given the fact that VHL is expressed in a multiplicity of tissues, a broad distribution of tumours arising from mutations in the VHL signalling axis would be expected. Nevertheless this is not the case with the retina and cerebellum being primarily affected in VHL patients. It is thus likely that the tissue context is a major factor dictating tumour formation driven by VHL inactivation.

To investigate in more detail the VHL protein expression pattern in specific tissues we decided to focus on the retina and the cerebellum, as both tissues can be affected by the same type of blood-vessel tumour, a so-called hemangioblastoma, and as this type of tumour is among the most common and widespread features of the VHL disease. We hoped to gain more insight into possibly tissue-specific expression and roles of VHL that would allow hypotheses about the origin of hemangioblastomas to be put forward, as this is still a matter of debate. The results of this expression study are presented in chapter **8**, whereas this chapter is meant to give a short overview of the retina and the cerebellum and their respective development, especially in the mouse.

2.1 The Retina

The retina is a thin sheet of neural tissue lining the back of the eye, which is involved in light detection (FIG. 9). It consists of seven major cell types, six types of neurons and one glial cell type, organized into three main cellular layers: the outer nuclear layer (ONL) comprising the nuclei of the rod and cone photoreceptor cells, the inner nuclear layer (INL) comprising the nuclei of interneurons (such as bipolar, horizontal and amacrine cells) and Müller glial cells, and the ganglion cell layer harboring the ganglion cells (GCL). The situation in the retina is even more complex than depicted here as all of the seven major cell types have in turn subtypes. So in the end mammalian retinas contain approximately 55 distinct cell types all serving unique roles in the intricate circuitry of the retina (Masland, 2001).

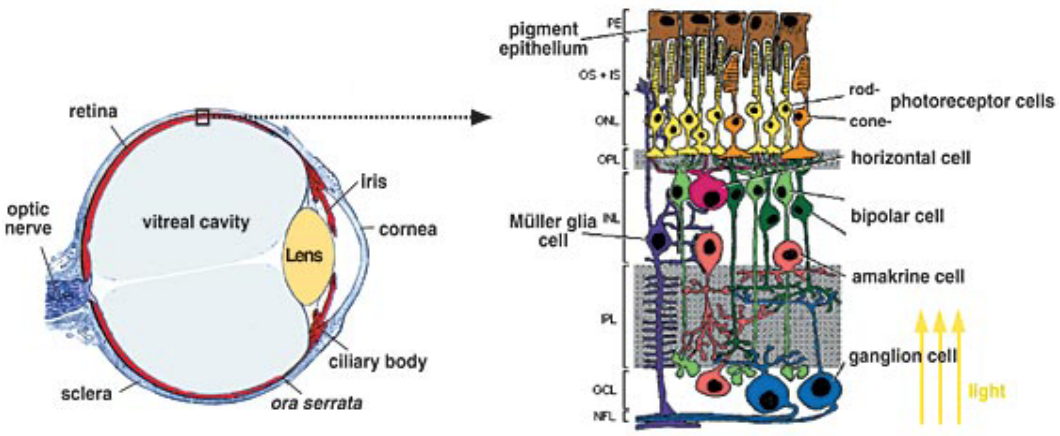

Figure 9. Overview of the morphology of the eye and focus on the retina. On the left a schematic sagittal section through an eye is depicted. From the top: the RPE is a non-neuronal cell layer whose apical processes surround the outer segments of the photoreceptor cells, namely rods and cones. Rods and cones stretch over three layers named the outer segment, the inner segment and the ONL. The outer segment herein contains stacks of membranous discs rich in the visual pigment rhodopsin, the inner segment contains the machinery of the cells (like the mitochondria, golgi apparatus and endoplasmic reticulum) and the ONL the nuclei. The OPL layer contains many axons of horizontal cells and the dendritic trees of bipolar cells, whose nuclei are found together with nuclei of the amacrine and Müller glial cells in the INL. Bipolar and amacrine cells extend their axons also into the IPL. In the GCL a second population of amacrine cells can be found together with the ganglion cells. And finally, the ONF consists of axons of the ganglion cell layer that make up the optic nerve and ultimately carry retinal signals into the brain.

The retina is able to receive a light signal that is focused on its surface and convert this signal to a neural message, which is then conducted to a cortical area of our brain responsible for sight. Light passing through the cornea is focused by the lens on the outer segments of the rod and cone photoreceptors in the ONL. After the absorption of various wavelengths of light by the photoreceptors, the information gets transmitted to the bipolar neurons found in the INL that integrate this information and transmit the signal to the ganglion cells, which in turn send the information through the optic nerve to the brain for higher order processing. The horizontal cells and the amacrine cells, which provide lateral connections in the INL, can modulate these direct signaling circuits.

The cone photoreceptor cells function in bright light amplitudes and are responsible for colour vision, whereas the rods are sensors of dim light and do not discern colour. Human vision relies heavily upon cones, of which there are three types-blue, green and red- and uses only one variety of rod photoreceptor. By contrast mice and rats rely almost entirely on rod-mediated vision. Approximately 76 % of all cells in the mouse retina are photoreceptors and about 97 % of these are rods. In addition mice also don't have the centrally localized cone-rich region named the fovea normally found in humans in the center of a yellowish spot called macula (Morrow *et al.*, 1998). Among the various cell types that can be found in the inner nuclear layer bipolar cells make up *ca.* 41 % of all cells in the layer, amacrine 39 %, Müller cells 16 % and horizontal cells 3 % (Jeon *et al.*, 1998).

The one non-neuronal cell type found in the retina, the Müller glial cell, plays very important roles in supporting neuronal survival and information processing and will be elucidated further in chapter 2.1.1.

2.1.1 Müller glial cell

The vertebrate retina contains a specialized and very unique type of glial cell, the Müller glia, which spans the entire thickness of the retina contacting every type of neuronal cell body and process (FIG. 10). As a reflection of this morphological relationship, the Müller glial cells play a crucial role in supporting neuronal survival and information processing (for reviews Newman & Reichenbach, 1996; Bringmann & Reichenbach, 2001).

Müller glial cells:

1) are responsible for the structural stabilization of the retina
2) regulate the extracellular homeostasis of relevant ions, including pH, and of the water content of the extracellular space
3) deliver trophic substances to neurons and remove metabolic end-products
4) metabolize glucose to lactose, which is preferentially taken up by photoreceptors as a source of energy for their oxidative metabolism
5) play a crucial role in the glutamate-glutamine cycle within the retina as glutamate is degraded in Müller glial cells leading to (among others) synthesis of glutamine by the glutamine synthetase and to synthesis of glutathione
6) act as intra-retinal modulators of immune and inflammatory responses
7) release VEGF in reponse to hypoxia and induce neovascularization of the retina (Eichler *et al.*, 2000)

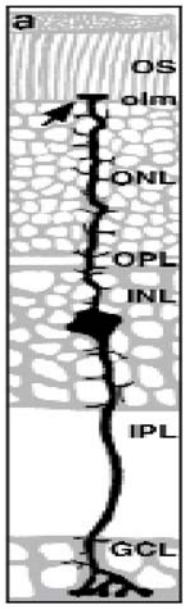

Figure 10. Drawing of a Müller glial cell depicting its positioning in the context of the retinal tissue.
Dyer & Cepko, 2000

Interestingly, virtually every alteration, injury or disease of the retina is associated with morphological, cellular and molecular changes of Müller glial cells, a process called reactive gliosis. This process is characterized by proliferation, changes in cell shape due to alteration in intermediate filament production, changes in ion transport properties and secretion of signaling molecules such as vascular endothelial growth factor (VEGF). In

response to experimental retinal injury, Müller cells have been shown to down-regulate their expression of the tumour suppressor protein $p27^{Kip1}$ (which is expressed exclusively in this retinal cell type after differentiation, see also chapter 2.1.2), resulting in Müller cell proliferation and suggesting that post-mitotic Müller glia have an intrinsic requirement for p27 in maintaining their differentiated state (Dyer and Cepko, 2000). The proliferation initiated by p27 downregulation is transient and reaches a maximum 24 hours after injury. Then proliferation ceases due to downregulation of cyclin D3, which is accompanied by upregulation of GFAP (glial fibrillary acidic protein). Gliosis is extremely important for the protection and repair of retinal neurons and Müller cells are also potential sources for neural regeneration within the postnatal retina (Fischer & Reh, 2003 and 2001) as they retain their capability to dedifferentiate and proliferate.

In contrast to the wealth of information available regarding Müller cell function, there are several areas where current knowledge of Müller cell biology is rudimentary as e.g. very little is known about the mechanisms concerned with Müller cell development and determination, or the actual role of Müller cells in retinal development. In addition there is also a scarcity of knowledge as to whether there is a direct involvement for Müller glial cells in retinal disorders.

2.1.2 Development of the retina

The retina develops as an outgrowth of the neural tube known as the optic vesicle and is accomplished by postnatal day P8 in the mouse. By E9.5 the fates of the inner and outer layers of the optic cup are clearly different. While the outer layer remains as a monolayer of cuboidal cells that will give rise to the pigment layer of the epithelium, those cells in all but the periphery rapidly multiply giving rise to multilayers of cells which differentiate to form the various components of the neural retina. Retinal progenitors are initially arranged as a pseudo-stratified neuroepithelium, whereby cells contact both surfaces of the optic cup. During mitosis cells forego these contacts and divide at the outer surface.

In the murine retina the diverse retinal cell types derive from a pool of proliferating pluripotent precursor cells and are generated by spatial and temporal differentiation during development in a characteristic order (Ahmad *et al.*, 1999; Turner & Cepko, 1987). Birth-dating studies have shown that retinal cell types are generated in overlapping but well-defined intervals with ganglion cells, cone photoreceptors, amacrine cells, and horizontal cells generated prior to birth and bipolar neurons and müller glia generated after birth (FIG. 11)

(Young *et al.*, 1985). The formation of rod photoreceptors occurs pre-and postnatally with a peak of genesis coincident with the day of birth in the mouse.

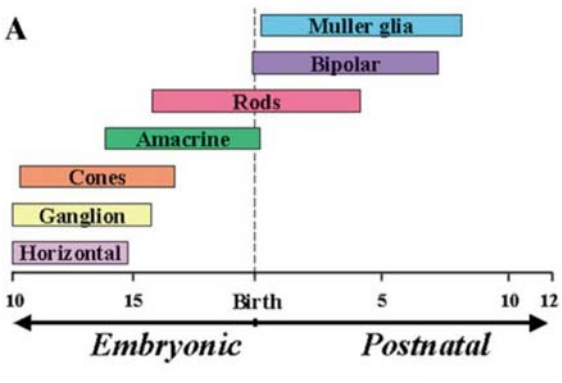

Figure 11 . The course of retinal histogenesis.

The "competence model" of retinal cell fate specification states that the instrinsic ability (the competency) of mitotic retinal progenitor cells to produce a particular cell fate in response to the retinal environment changes continuously throughout development (Livesey *et al.*, 2001; Cepko *et al.*, 1996). Once a cell passes through a particular developmental stage, it is only competent to become "later born" cells. In addition to the contribution of intrinsic determinants of cell fate specification extrinsic factors play also a major role.

Terminal cellular differentiation is thought to be associated with irreversible cell cycle exit. The proportion of cells that exit the cell cycle at each developmental stage must be regulated carefully, because if too many cells exit the cell cycle during early stages of development there might be an increase in the proportion of early-born cell types at the expenses of later-born cell types. The decision to divide or to exit the cell cycle occurs during the first gap phase of the cell cycle, G1, which is governed by cyclin-dependent kinases (CDKs), whose activity can be negatively regulated by so called cyclin-dependent kinase inhibitors (CDKI) (Sherr and Roberts, 1999). The cyclin-dependent kinase inhibitor protein, $p27^{Kip1}$, among other members of the Cip/Kip familiy of CDKIs such as $p57^{Kip2}$, has been shown to be expressed in the retina in a temporal pattern coincident with the onset of differentiation of most retinal cell types (Cunningham *et al.*, 2002; Dyer and Cepko, 2001; Levine *et al.*, 2000). In addition overexpression of $p27^{Kip1}$ has been shown to inhibit proliferation of progenitor cells.

Accompanying and following retinal cell differentiation, apoptosis can be observed in the retina (Voyvodic *et al.*, 1995). In this context, apoptosis presumably plays an important role in establishing the proper ratios of the cell types and in fine-tuning the retinal connections.

Little was known of the cell and molecular biology of progenitor cells, or of the transcriptional networks that define their intrinsic states that change during development. But detailed analysis of genes expressed in these cells and the identification of expression profiles characteristic for this cell type are currently emerging (Blackshaw *et al.*, 2004 and 2001;

Livesey *et al.*, 2004). As mentioned already above, the p27 and p57 CDKIs are e.g. expressed at different times during the cell cycle in the mouse retina suggesting that this reflects their different roles in regulating retinal progenitor cell cycle exit. In addition retinal cells use different components of the cell cycle machinery over the course of development, e.g. cyclin D1 during embryonic and perinatal stages, whereas cyclin D3 is expressed in a restricted population of progenitors towards the end of retinal histogenesis. A number of homeodomain transcription factors such as Chx10 and Six3 have also been identified shown to regulate the proliferation of retinal progenitor cells and the specification of cell fate (Dyer, 2003). Crx, an otx-like homeobox gene, has been shown to be expressed in photoreceptor and regulates photoreceptor differentiation (Furukawa *et al.*, 1997). And regarding gliogenesis, recent studies demonstrated that activation of the Notch signaling pathway can play a role in regulating Müller cell development (Furukawa *et al.*, 2000; Vetter & Moore, 2001). Furthermore p27, apart from regulating proliferation of Müller glia in response to stress or injury, can probably also promote their development, although there are some contrasting results from xenopus and mice (Vetter & Moore, 2001).

In summary, despite all these recent findings, there are still many open questions regarding the mechanism underlying the coordination of proliferation and cell fate specification to be addressed in order to attain a better understanding of retinal development.

2.2 The Cerebellum

The cerebellum is the primary center for fine motor control of movement and posture found in the central nervous system (CNS). It is a relatively simple CNS structure with well-defined anatomy and physiology and can be morphologically divided into a central vermis, which is flanked by lateral hemispheres (FIG. 12). Both the vermis and hemispheres are further subdivided by a series of parallel fissures defining a conserved pattern of folia.

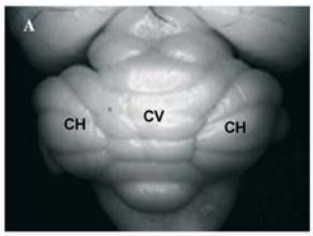

Figure 12. Dorsal view of an adult mouse cerebellum. The cerebellar vermis (CV) and the hemispheres (CH) are indicated.
Chizkov *et al.*, 2003

The mammalian cerebellum consists of deep centrally located neurons, referred to as the deep nuclei, and a peripheral cortex. This cortex contains two principal neuronal subtypes, the Purkinje cells, which are inhibitory, γ-aminobutyric acid (GABA) releasing neurons, and the cells of the internal granular layer (IGL), the glutamate-releasing, excitatory granule neurons. Each neuronal

cell type has a stereotypic and distinct morphology and is located in a discrete lamina within the cerebellum (FIG. 13).

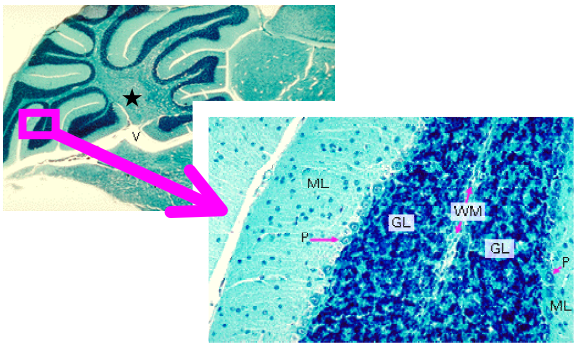

Figure 13. Sagittal section through a mouse cerebellum. The outer portion of the cerebellum is composed of grey matter in two layers: **the molecular layer** (ML; outer, lighter) and the **granular layer** (GL; inner, dark; also called internal granular layer to distinguish from the external granular layer present during development). The white matter is seen in the middle of the cerebellum (WM). Purkinje cells (PL) are large neuronal cells with numerous dendrites, which mainly form the border between the molecular layer and the internal granule cell layer. The star in the left picture marks cells of the deep cerebellar nuclei

The connections between the principal neurons are arranged in a stereotyped circuitry that is repeated throughout the cerebellum (FIG. 14): sensory information about movement and the position of the body is sent to the cerebellum via the so-called 'precerebellar system', a group of nuclei in the brainstem. These nuclei in turn project to granule cells, which communicate with the Purkinje cells. In parallel the inferior olivary nucleus from the brain stem projects directly to Purkinje cells. The Purkinje neurons then provide the primary output from the cerebellar cortex by projecting to the deep cerebellar nuclei, which then finally project to the cerebral cortex, mediating the fine control of motor movements and balance. In addition to the already-mentioned cerebellar neurons there are three additional classes: Golgi cells, which contain GABA and glycine and provide feedback inhibition to granule neurons, and the GABA-releasing stellate and basket cells, which modulate Purkinje cell output.

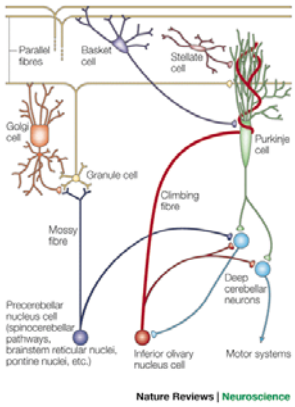

Figure 14. The circuitry of the cerebellum.
Wang & Zoghbi, 2001

The murine cerebellum contains *ca.* 10^8 granule cells, which control the activity of the Purkinje cells. These cells are critical for normal cerebellar function as mutant mice with a loss of granule cells suffer from severe ataxia (Hamre & Goldowitz, 1997).

2.2.1 Development of the cerebellum

Much of what is known about the cerebellum comes from information provided by investigations in mice, especially by using mutant mice. Given the high degree of

conservation of cerebellar anatomy and function between human and mouse, an understanding of mouse cerebellar development has provided insights into human cerebellar development.

The cerebellum develops from the dorsal region of the posterior neural tube and the neural populations of the cerebellum arise from at least two different germinal zones. While most of the cells, including the Purkinje cells, arise from the ventricular germinal matrix or zone (VZ), granule cell precursors come from a specialized germinal matrix called the rhombic lip. The proliferating cells of the rhombic lip, which are committed to become external granular layer (EGL) neurons, start by E13 to disperse rostrally over the surface of the cerebellar anlage, where they establish the EGL. The EGL contains dividing granule neuron progenitors and proliferation of precursors continues until P15, when the layer finally disappears. By E18.5 the EGL is normally about eight cells thick. Starting at birth and until day P20, when maturation of the cerebellum is complete, the post-mitotic granule cells leave the EGL to migrate inwards in order to form the internal granular layer (IGL). In the IGL the granule neurons then terminally differentiate. Migrating neurons are probably guided by Bergmann radial glia fibers through the molecular layer and, before reaching the IGL, they pass through the Purkinje neuron layer (PL) containing the cell bodies of Purkinje neurons and Bergmann glia. Purkinje cells appear at around E13, at which time they exit the cell cycle and migrate along the radial glial fibre system to the cerebellar anlage. The whole development is depicted as a schematic drawing in figure 15.

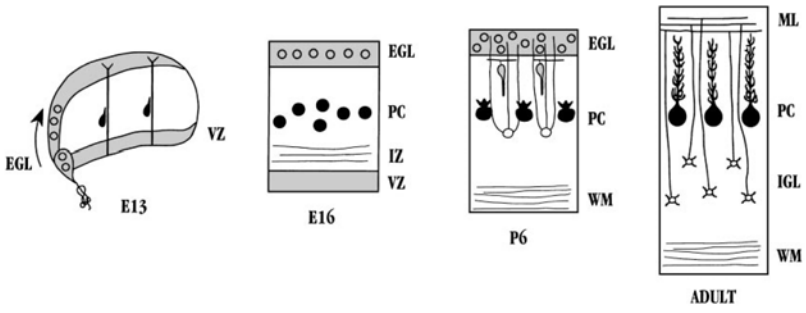

Figure 15. Schematic diagram of the developing cerebellum. During early developmental stages (*left, E13 and E16*), both of the principal neuron classes are specified. While Purkinje cells become postmitotic (*filled circles*) and migrate through the wall of the cerebellar anlage, precursors of the granule cell (*unfilled circles*) sweep across the roof in a morphogenetic movement. In the perinatal period (third panel from left, P6), granule cells become postmitotic and migrate inward, along the Bergmann glia, to assume a position deep below the Purkinje cell. In the adult (*right*), the pattern of connections of the granule neuron and the Purkinje cell (coronal plane) are established. Granule cells extend parallel fibers, which form synaptic connections with the dendrites of the Purkinje cells. **EGL**, External germinal layer; **PL**, Purkinje cell layer; **VZ,** ventricular zone; **WM**, white matter; **IZ**, intermediate zone: **IGL**, internal germinal layer.
Adapted from Hatten, 1999

The signals and the mechanism underlying control of granule cell proliferation and transition to terminal differentiation are starting to be uncovered and imply a variety of factors that are expressed at specific points either during proliferation, exit of cell-cycle, migration and terminal differentiation (reviews: Komuro & Yacubova, 2004; Sotelo 2004; Chizhikov & Millen, 2003; Kagami & Furuichi, 2001; Wang & Zoghbi, 2001; Hatten *et al.*, 1999; Goldowitz & Hamre, 1998). For example in the outer EGL, where only proliferating precursor cells can be found, there is a strong expression of a factor termed Math1, that has been shown to be required for the genesis of granule cells (Jensen *et al.*, 2004; Ben-Arie *et al.*, 1997). When granule neuron precursors then start exiting the cell cycle, becoming post-mitotic, they are in a state of pre-migration and can be found more in the inner EGL. The change from proliferating to post-mitotic state has been shown to be affected by the cyclin-dependent kinase inhibitor p27, which is expressed in the inner two third of the EGL, partly overlapping with the proliferating pool of granule cell precursors (Miyazawa *et al.*, 2000). Mice lacking p27 have an increased level of proliferation and therefore a larger cerebellum and this further emphasizes the need of p27 expression for granule cell precursors to start differentiating. In addition it has also been shown that mature granule cells in the inner granular layer express p27 again, whereas this expression cannot be detected during the migration of the postmitotic precursor cells through the molecular layer into the IGL.

But in addition to these intrinsic factors also extrinsic factors play a role. As an example, Sonic hedgehog (SHH) secreted by the Purkinje cells plays an important role in the development of granule cells (Lewis *et al.*, 2004; Dahmane & Altaba, 1999). Furthermore, CXCR4, a recently identified target gene of HIF, has been shown to be present on granule cell precursors where it plays a role together with its ligand, stromal-derived factor (SDF1) (expressed from pial cells) to enhance the SHH induced proliferation of granule cell precursors (Staller *et al.*, 2002; Klein *et al.*, 2001).

Chapter 3

Generation of mutant mouse strains by gene targeting

Gene targeting techniques have revolutionarized the field of mouse genetics and allowed the analysis of diverse aspects of gene function *in vivo* in the context of the whole animal. Defined as the targeted alteration of a specific DNA sequence in its genomic locus, 'gene targeting' occurs as a result of a process called 'homologous recombination' in which two DNA entities, with a high sequence homology, interact and recombine, i.e. exchange genetic information by adding or replacing their sequence elements. Gene targeting by homologous recombination can lead to inactivation or alteration of gene expression ("*knock-out" /loss of function* **or** "*knock-in" /gain of function* mutation respectively). By this means it has therefore become possible to engineer mice with specific genetic alterations that have become an invaluable new tool to produce mouse models of human inherited diseases (for reviews Mueller, 1999).

Nowadays, a routinely used technique to modify the mouse genome at any chosen locus employs homologous recombination in embryonic stem (ES) cells (Capecchi, 1989; Evans and Kaufmann, 1981; Martin, 1981). ES cells are derived from pluripotent, uncommitted cells of the inner cell mass (ICM) of a pre-implantation embryo, called a blastocyst, collected from a donor mouse 3.5-days p.c. (post coitum; after fertilization) (FIG. 16). These cells behave like ordinary somatic cells when cultured *in vitro* and prevented from differentiating by culturing on an irradiated feeder layer of fibroblasts, which secret Leukemia Inhibitory factor (LIF). LIF is very often also supplemented additionally with the medium.

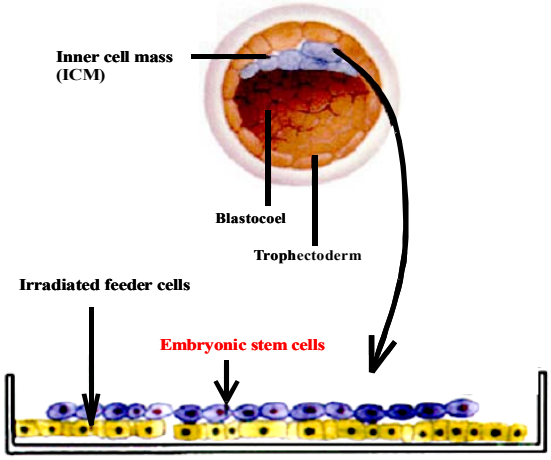

Figure 16. Establishment of pluripotent Embryonic Stem (ES) cells. A blastocyst is placed on a feeder cell layer, which provides a matrix for attachment and prevents ES cell differentiation. As the blastocyst is cultured, the outer layer of differentiated cells (trophectoderm) attaches and spreads, exposing the inner pluripotent cells (inner cell mass or ICM). The ICM is then extracted, mechanically dissociated, and the resulting cell clumps transferred onto fresh feeder cells. After culture, colonies, which exhibit appropriate morphology, are separated, dissociated into single cells, and seeded onto a feeder layer. Those cells that form ES colonies are further passaged to obtain permanent cell lines

Drawing adapted from cba.musc.edu/COBRE/ CORE-B/Resources-B.html
Text adapted from "Manipulating the mouse embryo-A laboratory manual", Hogan et al., 1994

Upon injection into a normal blastocyst though, ES cells retain their full developmental potential, contributing efficiently to both somatic and germ-line tissues (Bradley, 1984).

A common strategy used nowadays to generate mutant mice strains involves the following steps, which will be subsequently discussed more in detail (FIG. 17):

1. Construction of a **targeting vector** containing regions of identity with the mouse chromosome (homology arms), one or two selectable markers [generally a cassette that confers neomycin (G418) resistance] and planned modifications that ablate or alter the expression of the targeted gene.

2. Introduction of the linearized targeting vector into mouse **ES cells**, derived from *mouse strain A with coat color* **A** **[usually 129, therefore white or agouti (brown)]**, by electroporation (Thomas & Capecchi, 1987).

3. Selection and screening by PCR and Southern for those rare targeted ES clones that have integrated the planned modifications by homologous recombination.

4. Microinjection of targeted ES cells into host **blastocysts** obtained from *mouse strain B with coat color* **B** **(e.g. C57BL/6, therefore black)**. The blastocysts then get re-implanted into the genital tract of a pseudopregnant mother and are allowed to grow to term.

5. Among the offspring there will be so called **chimeras**, mice containing two populations of cells, namely those derived from the blastocyst (**B**) and those derived from the ES cells (**A**) and which can be easily spotted by the coat color as this will be a mixture of **A** and **B**.

6. Crossing the chimeric mice with wild-type animals, and subsequent intercrossing of the heterozygous animals in the F1 generation finally leads to the generation of homozygous animals carrying the desired mutation in their genome. But this only happens in case the *in vitro* modified ES cells contributed to the germ-line of the chimeric animals.

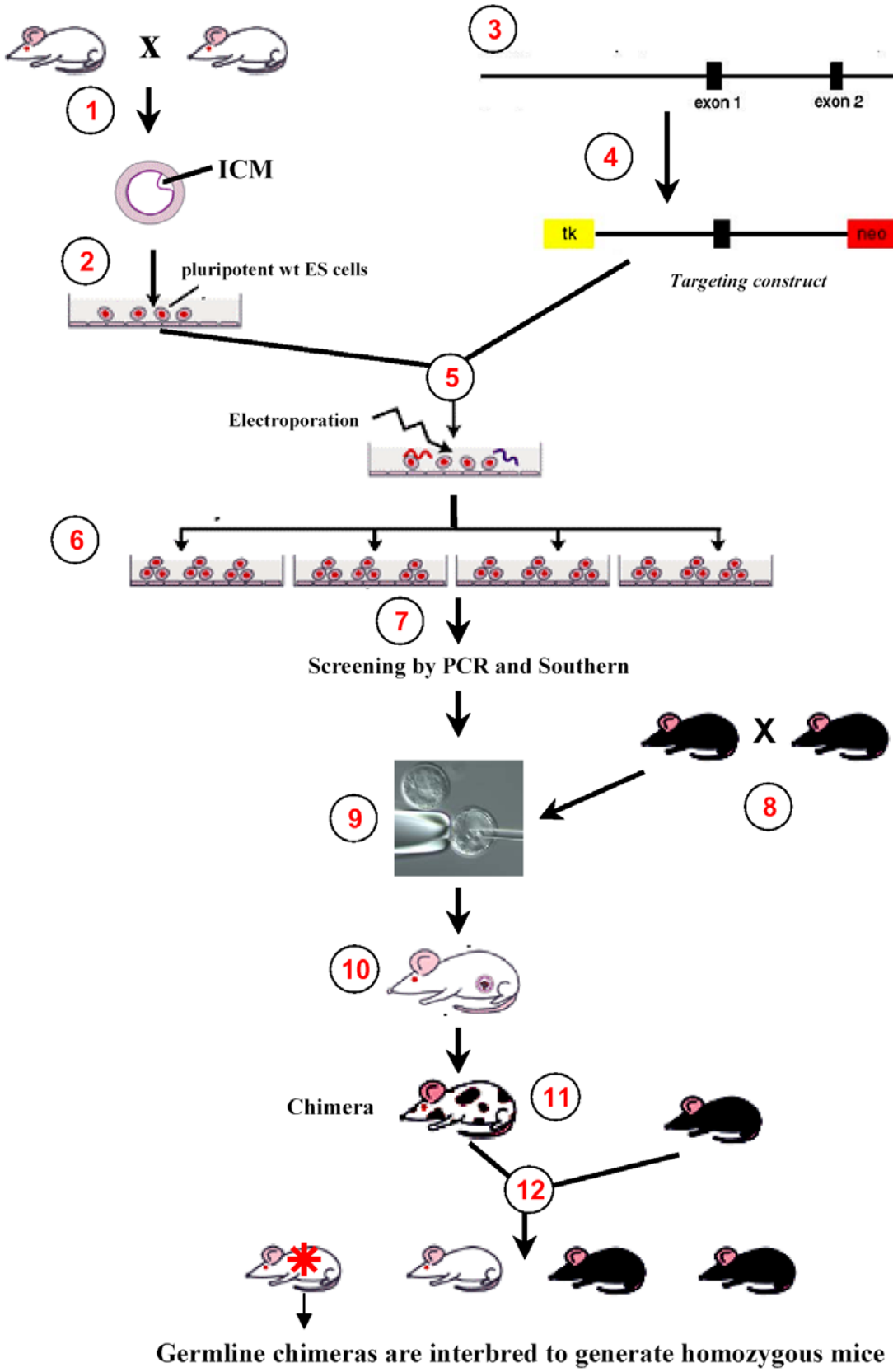

Figure 17. Text on the following page.

1. Wild-type mice (+/+), having a coat colour referred to as coat colour A, are mated and the female will be the donor of the pre-implantation embryo 3.5 days after fertilization. In the example depicted here the coat colour is white as e.g. from 129 mice.

2. Embryonic stem (ES) cells are obtained from 3.5 day pre-implantation embryos (blastocysts) collected form donor mice.

3. Isolation and Characterization of a genomic clone harboring the gene of interest that is going to be mutated.

4. Construction of the TARGETING VECTOR- a piece of DNA that carries a gene or DNA sequence of interest which has been modified and has integrated a positive (neo) and a negative (tk) selection marker. In this case the positive selection marker has substituted exon 2. More about selection markers see chapter 3.1.

5. The linearized targeting construct is introduced into wild-type ES cells by electro-poration, a process that delivers an electric pulse to the cells and enhances absorption of the construct across the cell membrane. Once inside ES cells, the construct can undergo recombination with the intact genome, exchanging the construct's DNA for that of the native DNA in a specific region.

6. ES cells that successfully incorporated the construct are selected for with antibiotic treatment, e.g. with G418 (neo) or gancyclovir (tk).

7. By extensive screening by PCR and/or Southern blotting the ES cell clones, in which homologous recombination has taken place, are identified and the clones expanded.

8. Wild-type animals (+/+) from another strain than the donor mice for ES cells are mated to obtain blastocysts. In this case animals with black coat colour (referred to as coat colour B) could be used, like e.g. C57 BL/6 mice.

9. Injection of the targeted ES cells into the host blastocyst. In the illustration the blastocyst is immobilized on a holding pipette (on the left) so that the inner cell mass (ICM) is positioned on the far left-hand side of the embryo. The injection needle on the right side is releasing the cells slowly into the blastocoel cavity.

10. Implantation of the blastocysts into a pseudopregnant foster mother.

11. Among the offspring, chimeric animals are identified by coat colour, which will be a mixture of the ES cell donors with coat colour A and blastocyst donors with coat colour B. The mouse depicted here is strongly chimeric as most of its skin tissue is derived from coat colour A.

12. Chimeric mice, confirmed also as such by PCR and Southern, are crossed back to wildtype mice. The offspring will be composed of mice having the same coat colour as the ES cell donor (A) and mice having the same colour as the blastocyst donor (B). 50 % of the animals with colour A will be heterozygous for the mutated allele. These germline chimeras are then interbred to generate homozygous mice (25 % of offspring)

3.1 Design of targeting vectors

As the substrate for homologous recombination in a gene targeting experiment, a targeting vector should be designed in such a way that it recombines with a specific chromosomal locus in order to mutate it. Targeting vectors can be classified as replacement or insertion vectors, depending on their linearization and on the subsequent end result occurring by homologous recombination leading either to the replacement of the chromosomal target sequences with the vector sequences or to the duplication of the genomic sequences (FIG. 18). The most frequently employed vector type to date, especially for the generation of null mutants, has been the replacement vector.

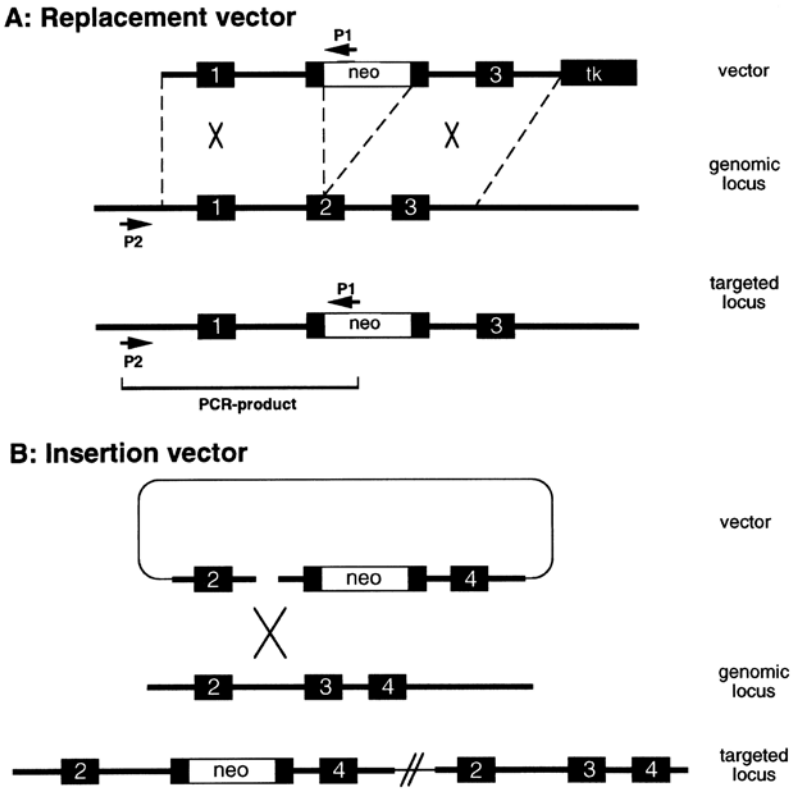

Figure 18. Classification of targeting vectors. (A) Replacement type vector. In this example the targeting vector is designed so that the second exon of a target gene is disrupted by a positive selection cassette harbouring a neomycin resistance gene and a HSV thymidine kinase gene (tk) is positioned outside the area of homology. After homologous recombination (HR) with the linearized vector the tk is lost and in the targeted locus exon 2 has been replaced with neo. PCR primers P1 and P2 can be used to screen for HR. (B) Insertion type vector. The vector is linearized within th region of homology between exon2 and exon3 that carries a neo insertion as positive selection marker. HR leads to integration of vector sequences and partial duplication of genomic sequences. Thin lines represent plasmid backbone sequences; the exons are numbered; stippled lines indicate regions of homology.

When designing a targeting vector, the following factors are essential to allow homologous recombination to occur with a specific chromosomal locus and to enable facilitated localization of the rare recombinant ES cell clones:

1) **arms of homology**: these are sequences having the same nucleotide sequence as the desired chromosomal integration site. Targeting vectors generally contain a so-called *short* and a *long arm of homology* flanking the mutated region. In general, recombination rates increase with the length of total homology to about 10 kb, the minimum length of the short arm of homology being about 0.5 kb (Deng and Capecchi, 1992).

2) **Selectable marker:** Most integrations of transfected DNA molecules into genomic DNA occur at a low frequency rate and will normally be random (illegitimate recombination). As only a small portion of these integration events (0,1-10 %) may occur by homologous recombination at the desired chromosomal locus, in order to maximize selection for these homologously recombined ES cell clones, the targeting vectors should include positive and negative selection markers (Mansour *et al.*, 1988). Selectable markers require a promoter that is active in ES cells and relatively position-independent.

POSITIVE SELECTABLE MARKERS	*selectable with*
Neomycin aminoglycoside phosphotransferase (neo)	G418 (geneticin)
puromycin (puro)	puromycin
Hygromycin B phosphotransferase (hyg)	hygromycin B

The most commonly used positive selection markers mentioned above are encoded by bacterial genes and confer resistance to drugs, therefore allowing a facilitated selection for ES cell clones that have stably incorporated the targeting vector DNA, though irrespective of its integration site. In addition, the introduction of the hypoxanthin-phosphoribosyltransferase (HPRT) gene in ES cells deficient for HRPT can also be used as a positive selection marker and in this case transfectants then need to be screened in HAT-medium (Matzuk *et al.*, 1992).

NEGATIVE SELECTABLE MARKERS	*selectable with*
HSV-ThymidineKinase (TK)	FIAU, gancyclovir
diphteria toxin A (DT-A)	-

While positive selection markers are normally inserted in the targeting vector in between the two arms of homology, negative expression cassettes are mostly positioned at one or both ends of the vector. The main difference between these two selection types lies in the fact that a positive marker, when expressed, simply confers drug resistance, whereas the expression of a negative marker leads to cell death and its presence is therefore not wanted in the final homologous recombined ES cell. Cells expressing e.g. HSV-TK in presence of the nucleoside analogue gancyclovir {or FIAU=[1-(2-deoxy-2-fluoro-b-D-arabino-furanosyl)-5-iodouracil]} phosphorylate the latter and convert it into a toxic derivative, which finally kills the cells. The combined positive-negative selection, combining the ability to both positively select for stable transfectants as well as negatively select against random integrants can enrich for targeted events by up to 10-fold. The selection marker cassette should be removed after homologous recombination because of possible interference with the expression of neighbouring genes.

3) **Sequence identity** should be maintained since it has been reported that recombination rates increase with usage of isogenic vector DNA (te Riele *et al.*, 1992). This means that the targeting vector should be constructed from a genomic clone of the same genetic background as the ES cells to be used. The genetic background of the majority of available ES cell lines is 129.

4) **Linearization of the targeting construct** is important for obtaining homologous recombinants. A single cutting site should therefore be available or made available at a site in the backbone of the plasmid, not within the homologous region or area of interest.

Typically the creation of a targeting vector nowadays requires screening of a genomic library to obtain the gene of interest followed by restriction mapping. To design a cloning strategy the restriction mapping is necessary, also if the sequence is already available, to confirm the size of restriction fragments that will be needed for the subsequent cloning and for finding a possible unique site that will be needed for the linearization of the vector prior to transfection into ES cells. The cloning strategy normally involves numerous cloning and subcloning steps (e.g. see chapter 7, FIG. 28.).

Recently a new method for a much more rapid generation of gene-targeting vectors was reported (Cotta-de-Almeida *et al.*, 2003). The basis of this technology is to utilize strains of

E.coli that can efficiently carry out homologous recombination between short terminal homology regions on a linear PCR-derived fragment and sequences on a recipient plasmid. This strategy has been referred to as recombineering (for recombinogenic engineering). It involves identification of the genomic gene sequence of interest from publicly available databases and purchasing of an *E.coli* clone containing a BAC encompassing these sequences. Then, with the appropriately constructed template vector and the essential recombination machinery, the use of homologous recombination in *E.coli* can be used to manipulate directly the gene of interest in the BAC, avoiding numerous subcloning steps. The manipulated sequence within the BAC is then finally removed by identifying flanking restriction sites from the published sequence and under antibiotic selection the targeting vector is generated.

3.2 The Cre/loxP recombination system

The Cre/loxP recombination system originates form the bacteriophage P1 and provides nowadays the basis for the most versatile and widely applied strategy to introduce non-selectable mutations. The 38 kDa enzyme Cre (**c**auses **re**combination) catalyses the site-specific recombination between 34 bp sequences referred to as loxP (**l**ocus **o**f crossover (**x**) in **P**1). The loxP sequence consists of two 13 bp inverted repeats interrupted by an 8 bp nonpalindromic sequence, the so-called spacer, which dictates the orientation of the overall sequence (FIG. 19A). When two lox P sites are placed in the same orientation, and at least 82 bp apart, Cre excises the so called 'floxed' sequence placed between them, leaving one loxP site within the genome whereas the second loxP is found on the excised circularised

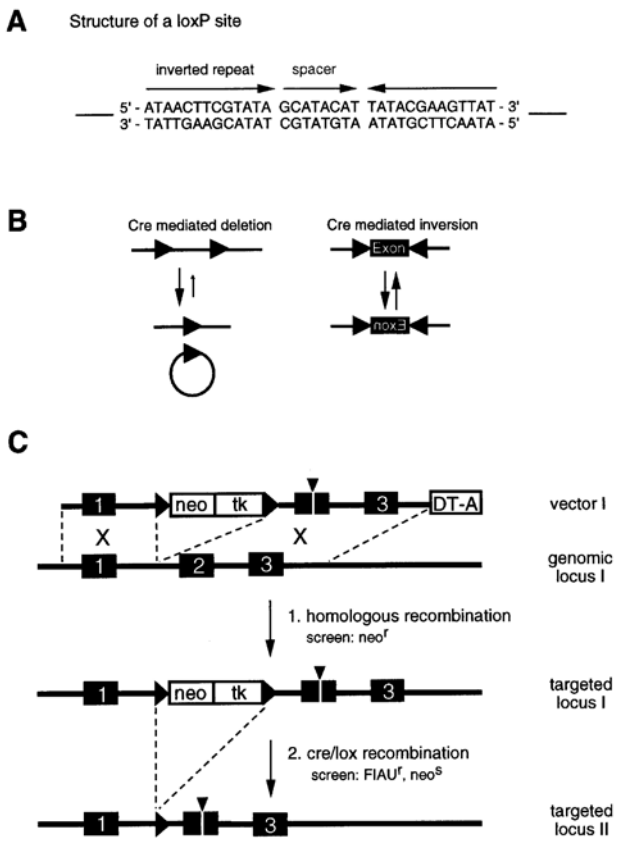

Figure 19. The Cre/laxP recombination system and making subtle mutations. (A) Structure of a loxP site (B) Cre-mediated recombination reactions (C) Example of an introduction of a point mutation and removal of selection markers by Cre mediated recombination. Firstly, a replacement type targeting vector is used to introduce a point mutation into exon 2 (white line and filled triangle).

fragment. If the two sites are oppositely orientated, inversion of the intervening DNA occurs (19B). To catalyse a recombination, Cre itself is sufficient and does not require additional co-factors. Cre has been shown to work in vitro as well as in various cells and as Cre does not have any endogenous target sequences it is more than suitable to be used in other species. In FIG. 19C an introduction of a point mutation is depicted. First, a replacement type targeting vector (exlained in FIG. 18A) is designed and used to introduce a point mutation into exon 2 (point mutation characterized by a fine white line within the exon marked from above with a little black triangle). As negative and positive selection cassettes the Diphtheria toxin A fragment (DT-A) and a neo-tk cassette are used respectively. Upon homologous recombination the DT-A fragment is lost in those cells that have integrated the vector in the right position, whereas if it was randomly inserted the DT-A will kill the cells. Secondly, selection markers flanked by loxP sites are removed by Cre mediated recombination in ES cells leaving one loxP site in the genome, clones that lost the TK gene can be enriched by their resistance to FIAU.

An alternative recombination system used, though with lower efficiencies, is the Flp/Frt recombination system from yeast, which is essentially the eukaryotic homolog of the Cre/loxP system (Dymecki, 1996; Meyers *et al.*, 1998). Flp, a 423 amino acid monomeric peptide is very similar to Cre in that it requires no cofactors, uses a phosphotyrosine intermediate for energy, and is relatively stable. FRT is also similar to loxP in that it is composed of three 13 bp repeats surrounding an 8 bp asymmetric spacer region. The asymmetric region dictates whether excision (same orientation) or inversion (inverted orientation) of an intervening DNA sequence occurs after recombination.

3.3 Screening and isolation of recombinant ES cells

Following linearization of the targeting vector and transfection into ES cells, e.g. by electroporation, ES cell clones that survive positive (and negative) selection are identified, their DNA isolated, and investigated for the presence of a specific recombined allele. Verification of correct targeting is done either by polymerase chain reaction (PCR) and Southern blotting or by Southern blotting alone. The PCR analysis has the advantage that it can be done with minimal expansion of clones saving culture time/resources and helping to preserve the totipotency of the ES cells. It is therefore much quicker and provides results faster. In addition screening by PCR narrows down the number of putative positive clones

that then subsequently should still be confirmed by Southern in order to rule out the possibility of aberrant recombination products.

If one wants to employ a PCR/Southern screening, the targeting vector will need to contain a short and a long arm of homology. A short arm of homology is generally in the range of 0.5-2 kb in size in order to be still amplifiable by PCR and detectable on agarose gels, whereas the long arm is generally in the range of 4-8 kb depending on a number of variables such as e.g. availability of sequence. A PCR screen ideally employs a primer adjacent to the region of homology (outside the short arm) and a second within the novel sequence within the targeting construct, e.g. the selectable marker as the positive selection marker is generally inserted at an asymmetric location near the short arm of homology. In this way only in the case that the two primer sites are juxtaposed by homologous recombination the correctly sized PCR product will be generated.

Southern blotting analysis of the structure of the locus usually employs probes inside (internal, e.g. in the selection cassette) and outside (external 5' and 3' primers to check that precise recombination has occurred in both arms) of the targeting vector to exclude clones with aberrant recombination products. Appropriate restriction digests have therefore to be performed that should lead to the generation of diagnostic restriction fragments created by homologous recombination that can be easily distinguished from the endogenous copies.

If one decides to use only Southern blotting for screening, the homologous DNA should be more equally distributed among the two vector arms as aberrant recombination products are found more frequently using short arms.

3.4 Production of chimeric mice

Following the identification of the correctly mutated, *in vitro* manipulated ES clone, the latter gets amplified/expanded and then injected into the blastocoel of 3,5-days old mouse-embryos called blastocysts. Approximately 10-20 ES cells are injected per blastocyst. The manipulated blastocysts are then in turn implanted into the uterine horns of day-3 pseudopregnant recipient foster mothers, which have been obtained by mating females with vasectomized males. Ideally *ca.*12-16 blastocysts are transferred to a single foster mother meaning 6-8 per uterine horn.

Following blastocyst injection, ES cells become incorporated within the developing inner cell mass (ICM) of the host embryo and contribute to the development of the different embryonic lineages in competition with the host cells. Some ES cells will migrate

to the genital ridge and become germ cells. And as germ cells are derived from the same cell lineage that gives rise to the skin (primitive ectoderm), ES cells that have become germ cells will also contribute to the coat colour. Therefore to identify easily animals that harbour both host and ES cell contributions (so-called chimeras) blastocysts and ES cells from different mouse strain background are used. For example: ES cell contribution from the commonly used agouti (brown) 129 strain is readily detected in chimeras on the black background of C57BL/6 because these animals are patchy with black and brown areas. And the probability of germ cells originating from the implanted ES cells can be roughly equated with the degree of chimerism, meaning that in the above mentioned example a chimera with a high proportion of brown fur will have a high probability of transmitting the targeted gene to its offspring.

Alternatively to blastocyst injection in order to generate ES cell/embryo chimeras, ES cells can also be injected into morula-stage (8 cell stage; 3 day old) embryos, or aggregated with morulae after removing the zona pellucida. In addition also tetraploid embryos may be used for injection or aggregation to make ES cell derived foetuses (Plagge et al).

Most of the 129 derived ES cell lines are male and therefore germ-line transmission is usually through male chimeras. To establish a new mouse strain with ES-cell genotype, male chimeric animals are bred with wild-type females. As the chimeric animal will have a similar degree of chimerism in every tissue including the gonads, two types of progeny will be generated, e.g. in the example mentioned above the mating of the chimera with a BL6 wild-type mouse will give black animals with BL6 phenotype and agouti (brown) animals with the 129 component. 50 % of these agouti animals will carry the mutation (only one allele was targeted) that was originally generated in the ES cells and therefore serve as heterozygous founders for a new mouse line. Agoutis with one targeted allele (+/-) should be identified by PCR (tail biopsy) and mated with each other to produce wild-type (+/+), heterozygous (+/-) and homozygous (-/-) animals for initial phenotyping. 25 % of the offspring will finally be homozygous harbouring the desired mutation on both alleles.

3.5 Conditional Gene Targeting

In contrast to the “conventional” gene targeting, that leads to inactivation or modification of a gene in all tissues of the body from onset of development throughout the whole lifespan, the “conditional” gene targeting is a restricted gene modification in the mouse, which is limited to either certain cell types (tissue-specific), to only a portion of its lifetime

(temporally-specific) or both. Conditional gene targeting approaches are particularly useful in cases where complete gene inactivation has been shown to lead to a lethal or otherwise adverse phenotype that therefore impedes a detailed analysis. Moreover, tissue specific gene inactivation may define physiological roles of the gene product of a widely expressed gene in certain tissues, without compromising other functions in the organism.

The currently favoured method for conditional gene targeting in mice is operating with the Cre/loxP system (FIG. 20). The Flp/FRT would be an alternative to this recombinase system, but as its temperature optimum is *ca.* 28 °C whereas the mouse body temperature lies around 39 °C, Cre recombinase with a temperature optimum of 37 °C is much more suitable and efficient.

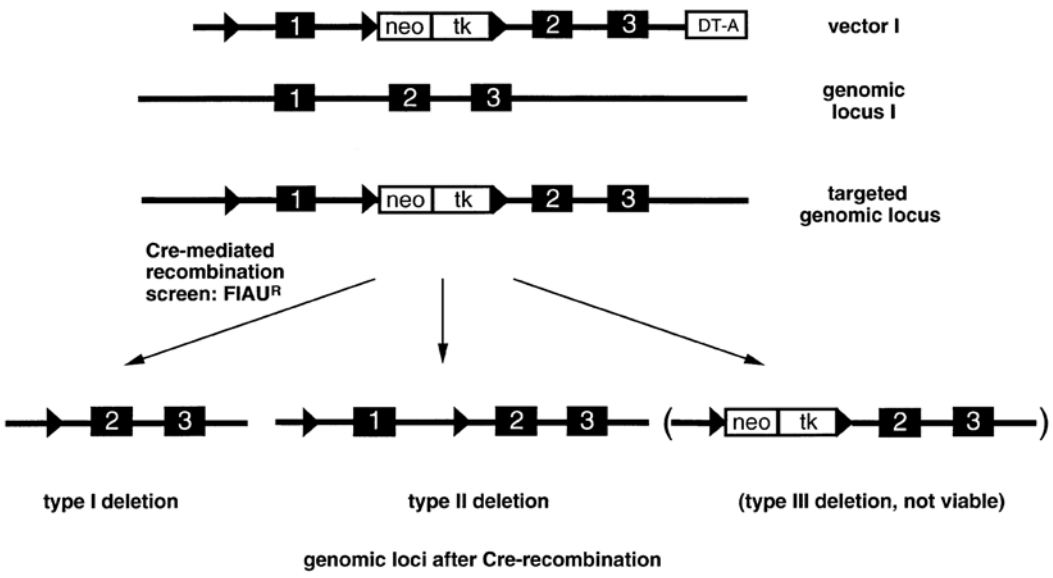

Figure 20. Conditional knockout strategies: generation of targeted mice. In the first step, three loxP sites are introduced by HR into silent regions (e.g. introns) of a target gene (in this case two loxP sites flank the neo-tk selection cassette, the third one is upstream of exon 1). Upon Cre-mediated recombination in ES cells and FIAU selection, two different genomic deletions (type I and II, ***type III is not viable in FIAU***) are obtained, depending on the loxP sites used. Type I deletions may represent non-functional alleles, whereas mice solely harboring two loxP sites in silent regions (type II deletion) should display no phenotype. These mice may then be crossed to Cre transgenic mice and double transgenic mice will undergo Cre-mediated recombination.

Utilization of the Cre/loxP system for conditional gene inactivation or modification *in vivo* involves two lines of mice:

1) A mouse line that has been generated using ES cell technology and that should give mice with so-called floxed alleles in all cells (FIG. 20). These mice should be phenotypically normal because the loxP sites were initially inserted into introns where they theoretically shouldn't affect gene function.

2) The second line of transgenic mice is normally generated by standard oocyte injection techniques. These mice express Cre under the control of a transgenic promoter.

Mating these two mouse lines should result in Cre-mediated gene disruption only in those cells in which the promoter is active (FIG. 21).

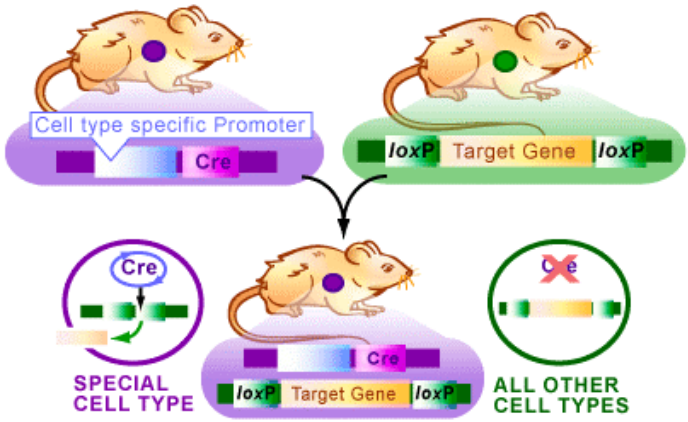

Figure 21. Cre/*lox* Mouse Breeding. Mice with the Cre protein expressing in a specific cell type are bred with mice that contain a target gene surrounded by *loxP* sites. When the mice are bred, the cells carrying Cre will cause those cells to lose the target gene.

Alternatively to the use of Cre transgenic mice the Cre gene has recently been delivered to somatic tissues by using Cre expressing adenoviral vectors or in even more recent times by lentivirus.

Chapter 4

Materials

4.1 General Chemicals

Reagent	*Supplier*
Acetic acid	Merck
Activated CH Sepharose 4B	Pharmacia
Acrylamide	Bio-Rad
Agar	Gibco BRL
Agarose	Progen
Ammonium acetate	Fluka
Ampicillin	Fisons
Aprotinin	Boehringer
Blocking Buffer	Roche
Boric acid	Fluka
Bromophenol blue	Ajax
BSA (bovine serum albumin)	Fluka
Centricon	Millipore
Chloroform	Fluka
Colcemid	Gibco BRL
L-cysteine	Sigma
DAPI (4'6'-diamidine-2'-phenylindole dihydrochloride)	Boehringer
DMEM (Dulbecco's Modified Eagle Medium)	Gibco BRL
DMSO (dimethylsulfoxide)	Fluka
DTT (dithiothreitol)	Promega
DNA Ladder:	
Marker II, Marker V and Marker VI	Roche
ECL (enhanced chemiluminescence)	Amersham
EDTA (ethylenediamine tetra-acetic acid)	Boehringer
EtOH (ethanol)	Fluka
Ethidiumbromide	Sigma
FCS (fetal calf serum)	Gibco BRL
Formalin (10%)	Merck
Formaldehyde	Fluka
Formamide	Merck
G418	Gibco BRL
L-Glutamine	Trace
Glycerol	Fluka

Reagent	*Supplier*
HBSS	Gibco BRL
HCL (hydrochloric acid)	Fluka
HEPES (N-2-hydroxyethylpiperazine-N'-2-ethanesulfonic acid)	Boehringer
H_2O_2 (Hydrogen peroxide)	Sigma
Isopropanol	Merck
KAc (potassium acetate)	Fluka
Kanamycin (for BAC clones)	Sigma
KCL (potassium chloride)	Sigma
Klenow enzyme	Boehringer
KLH (keyhole limpet hemocyanin)	Calbiochem
N-Laurylsarcosyl	Roche
β-Mercaptoethanol	Sigma
Methanol	BDH
$MgCl_2$ (magnesium chloride)	Sigma
Milk powder	Migros
Mowiol	Calbiochem
NaAc (sodium acetate)	Merck
NaCl (sodium chloride)	Merck
Na_2HPO_4 (Sodium hydrogen phosphate)	Fluka
NaH_2PO_4 (Sodium dihydrogen orthophosphate)	Fluka
NaOH (sodium hydroxide)	Merck
Nonidet P-40	Sigma
Normal Goat Serum	Vector Lab
Papain	Sigma
Paraformaldehyde	Fluka
Paraffin	Fluka
PBS (phosphate buffered saline)	Trace
Penicillin	Trace
Phenol	GibcoBRL
PMSF (phenyl-methyl-sulfonyl-fluoride)	Boehringer
Poly-L-Lysine solution	Sigma
Proteinase K	Gibco BRL
SDS (sodium dodecyl sulfate)	Eurobio
Taq DNA polymerase	Invitrogene
TEMED (N,N,N',N'-Tetramethylethylenediamine)	Bio-Rad
Tris (Tris (hydroxymethyl) aminomethane)	Sigma
Triton X-100	Fluka
Trypsin EDTA	Gibco BRL
Tween-20	Sigma
Vectashield	Vector Lab

If chemicals are not listed here the supplier is probably already named in the methods part.

4.2 Radiochemicals

[α-^{32}P]dCTP (~3000 Ci/mmol) was obtained from Amersham as 10mCi/mL solutions.

4.3 Restriction enzymes

Restriction enzymes were purchased from Boehringer, New England Biolaboratories or Promega and used with supplied buffers according to recommended protocols.

4.4 Bacterial strains and buffers

Plasmid DNA was grown in the bacterial strain DH5α (Life Technologies).

DIG-Buffer	0.1 M Maleic acid (Fluka) 0.15 M NaCl pH 7.5
10x DNA Loading buffer	250 mg bromophenol blue (Roche) in 33 ml 150 mM Tris pH 7.6 Add 60 ml glycerol and 7 ml H_2O
HTB (competent cells)	10 mM HEPES 0.477g 15 mM $CaCl_2$ (Fluka) 0.441g 250 mM KCl 3.728g dissolved in 150ml H2O and pH adjusted to 6.7 with KOH (4M). Then MnCl2 was added and dissolved 55mM MnCl2 1.384g volume adjusted to 200ml, filter-sterilized through a 0.45µm filter stored at 4°C
LB-Medium	1 % (w/v) Bacto-tryptone (BD) 0.5 % (w/v) Bacto-Yeast extract (BD) 1% (w/v) NaCl pH 7.0
LB-Agar	LB-Medium + 20 /l agar
PBS	bought as a ready to make mix, needed only resolving in water and autoclaving.

SDS-PAGE running buffer	10 g SDS 30.3 g Tris 144.1 g glycin in 800ml H_2O adjust to 1 l
SOB (competent cells)	20 g Bacto tryptone, (BD) 5 g Bacto yeast extract (BD) 0.5 g NaCl dissolved in 950 ml H_2O and 10ml 250mM KCl were added. pH was made up with NaOH to 7 and the volume adjusted to 1l. The medium was then aliquoted, autoclaved and cooled to 60°C before adding 5ml sterile 2M $MgCl_2$
20x SSC	3 M NaCl 0.3M Na-citrate pH 7.0
TBE buffer	89mM Tris 89 mM Boric acid 2 mM EDTA pH 8.0

4.5 Oligonucleotides

T7 primer	TAATACGACTCACTATAGGG
T3 primer	ATTAACCCTCACTAAAG
SP6 primer	GATTTAGGTGACACTATAG

mVHL primer

cDNA primer 1 -5'
5′– ACC CGG ATC CAC CAT GCC CCG GAA GGC AGC CAG TCC AG –3′

cDNA primer 2 –3'
5′– TCC AGA ATT CAC CTC AAG GCT CCT CTT CCA GGT GCT GA –3′

short form mVHL-5'
5′– CGG TGG ATC CAC CAT GGA GGC TGG GCG GCC GCG GCC GG –3′

Exon 1
5' primer 5′– AAT GCC CCG GAA GGC AGC CAG TCC –3′
3' primer 5′– CTC GGT AGC TGT GGA TGC GGC GGC –3′

Exon 2
5' primer 5′– CGA GGT CAT CTT TGG CTC TTC AGG –3′
3' primer 5′– ATA CAC TGG CAA TGT GAT GTT GGC –3′

Exon 3

5' primer 5′– TGT ATA CCC TGA AAG AGC GGT GCC –3′
3' primer 5′– GGA CTC CTT CAA GGC TCC TCT TCC –3′

KNOCKOUT PROJECT

For sequencing the *BAMHI*-fragments containing the VHL exons:

T7 term	GCT AGT TAT TGC TCA GCG G
Cl 17 v/n NdeI	GTA CTA TCA GGT ATG TGT GG
5-BAC	GTA CAT GAG TAC ACT TTA GT
11Ex2	AAG GTG TGC ACC ACC ACA GC
Ex1-4A	AGG TAG GTG GCT CGC GTG TC
Ex1-4B	TCG CAA GCT GGA CGT GGG CG
41103793	GAT GGG CTC TAT TAA TAA CG
41017635	TTC ACC GAG CGC AGC ACC GG
Ex2-5′	AGG ATG GAA TAA ACT GAT GC
Ex2-3′	GGG CAA CGG CAC TCC TCT GG
vEx3	TCA TAG TTT ACC CTC CAG TG
nEx3	GGC TGA AGA GAC TGT AAA GG

loxP oligos for designing of the 3rd loxP site:

loxPfor primer 5′-GAT CTA TAA CTT CGT ATA ATG TAT GCT ATA CGA AGT TAT ATC AAG CTT ATC GC-3′

loxPback primer 5′-GGC CGC GAT AAG CTT GAT ATA ACT TCG TAT AGC ATA CAT TAT ACG AAG TTA TA

Nde-site (neo-tk cassette)

5′-Nde site primer 5′–TCG AGG TCG ACC ATA TGT GGC CGA G –3′
3′-Nde site primer 5′–CGC TCG GCC ACA TAT GGT CGA CC –3′

Exon 2- orientation

Orient-5 primer 5′–TCT CAG TAC CCA GGT CAG GC –3′
Orient-3′primer 5′–CGA GTC GCC ACC GTC GTC GG –3′

To check loxP orientation (in pET-17b-N/B-loxP)

vHind-loxP primer 5′–GGC CGA AAA CAA GTG AGT AT –3′
nHind-loxP primer 5′–CCT GGG GAT TGT ACA CCT GA –3′

neo-tk primer (for sequencing)

neo-tk middle primer 5′–GGC CGC GAG AAC GCG CAG CC –3′

neo-tk3-A primer 5′– CAT AGC CAG GTC AAG CCG CT –3′
neo-tk3-B primer 5′– ACG GTA TCG CCG CTC CCG AT –3′

neo-tk2-A primer 5′– CCA TGG GGG ACC CCG TCC CT –3′
neo-tk2-B primer 5′– GCC CGC CGT GTT CCG GCT GT –3′

southern testing

5′-PROBE
primer 5′.1 5′–CAT CTC ATG TTC TCA TGG GC–3′
primer 5′.5 5′–GCA TTC AGG TAT AAT CCA CC–3′
3′-PROBE
primer 3′.4 5′–GTG CCA CTG CGT CTG CCC–3′
primer 3′.6 5′–AGC ATC CAA TGG TTT CTT CG–3′

Primer PCR

Nestin:

Cre-primer1 5′– GCG GTC TGG CAG TAA AAA CTA TC –3′
Cre-primer2 5′– GTG AAA CAG CAT TGC TGT CAC TT –3′

Il-2 primer1 5′– CTA GGC CAC AGA ATT GAA AGA TCT –3′
Il-2 primer2 5′– GTA GGT GGA AAT TCT AGC ATC ATC C –3′

VHLflox:

C1 primer 5′– CAT GTG CCT GCA GAG ACC AG –3′
C2 primer 5′– CAC GCA TCC ACA TCA GGT G –3′

D3 primer 5′– GGA GTA GGA TAA GTC AGC TG –3′
B2 primer 5′– GTA CAC CTG AGA GCG GCT TC –3′

Chapter 5

Methods

5.1 Plasmid DNA purification from bacteria

The isolation of plasmid DNA from bacteria was performed using the NucleoBond PC Kit from Macherey-Nagel, according to manufacturer's instructions:
A bacterial culture was set up by inoculating 50 ml of LB medium (plus antibiotic) with a single colony from a freshly streaked plate or from a glycerol stock. After overnight shaking at 37 °C the saturated culture was centrifuged at 6.000 x g for 15 min at 4 °C. After discarding the supernatant the pellet was re-suspended in 4 ml buffer S1 (50 mM Tris-HCl, 10 mM EDTA; pH 8.0) containing 100 µg/ml RNase A. 4 ml Buffer S2 (200 mM NaOH, 1% SDS) were then added to the suspension to denature both the chromosomal and plasmid DNA. Following a short incubation of max. 5 minutes at room temperature (RT) addition of 4 ml buffer S3 (2.8 mM KAc, pH 5.1) neutralized the lysate and caused the formation of a precipitate containing chromosomal DNA and other cellular components. This incubation was carried out for 5 minutes on ice. The suspension was then filtered through NucleoBond filters pre-wetted with sterile deionized H_2O and the cleared lysate applied onto an equilibrated column (equilibrated with 2.5 ml buffer N2 (100 mM Tris, 15% EtOH, 900 mM KCl, 0,15% Triton X-100, pH 6.3)). Following washing of the column with 10 ml buffer N3 (100 mM Tris, 15% EtOH, 1.15 M KCl, pH 6.3) the plasmid DNA bound to the anion exchange resin was eventually eluted with 5 ml buffer N5 (100 mM Tris, 15% EtOH, 1 M KCl, pH 8.5). 3.5 ml Isopropanol precipitated the eluted plasmid DNA and after 30 minutes centrifugation at 15000 g at 4 °C the supernatant was discarded and the DNA pellet washed carefully with 70% EtOH. The pellet was then dried at room temperature and finally dissolved in 50 µl sterile deionized H_2O.

5.2 Enzymatic treatment of DNA

Restriction digest: The typical restriction digest was performed in a final volume of 20 µl. The following volumes of reagents would be added to the reaction tube: 1 µg DNA (usually 1-5 µl), 1 µl 10x Restriction enzyme buffer, 1 µl restriction enzyme and sterile deionized H_2O was used to fill up until 20 µl.

Dephosphorylation of 5´ends: In a total volume of 50 µl 44 µl DNA were supplemented with 5 µl 10x One-Phor-All-Plus Buffer (Pharmacia) and 1 µl of a 1:20 dilution of Alkaline Phosphatase (Calf Intestine Mucosa; Pharmacia). The reaction mix was incubated at 37 °C for 30 minutes, followed by an incubation to stop the enzymatic activity at 85 °C for 20 minutes. The reaction mix was then filled up to 100 µl with sterile H_2Odest and extracted with Phenol/Chloroform and once chloroform. Addition of 1/10 Vol. NaAc and 2 Vol EtOH and centrifugation at 14.000 rpm for 30 minutes at 4 °C precipitated the DNA that was then re-suspended in 20 µl H_2O.

Ligation: The ligation of DNA fragments was performed using the Rapid DNA Ligation Kit from Roche. The vector DNA and insert DNA was dissolved in thoroughly mixed and diluted 1x conc. DNA Dilution Buffer to a final volume of 10 µl. 10 µl T4 DNA Ligation buffer was added to the reaction vial and mixed thoroughly. Finally 1 µl of T4 DNA-Ligase was added to the tube and after mixing the reaction was allowed to incubate for 5 minutes at RT. The ligation mix was then used directly for the transformation of competent cells.

5.3 Isolation of DNA from agarose gels

DNA was isolated from agarose gels by use of the QIAquick Gel Extraction kit from Qiagen according to manufacturer's instructions.

5.4 Polymerase chain reaction (PCR)

PCR's were mostly carried out using the Taq polymerase and additional buffers from Invitrogen. Each PCR reaction amounting up to a total volume of 20 µl contained: 1 µl each of the forward and the reverse primers (both 10 pmol; final conc. 0.5 µM), 2 µl 10x PCR buffer (200 mM Tris-HCl (pH 8.4), 500 mM KCl), 0.6 µl 50 mM $MgCl_2$ (final conc. 1.5 mM), 1 µl 1% W-1 to improve thermo-stability), 0.4 µl 10 mM dNTP mixture (final conc. 0.2 mM each), 0.2 µl of 5 units/µl Taq DNA Polymerase and 12,8 µl sterile ultra-pure water to increase the reaction volume to 19 µl. 1 µl of DNA was pipetted to a PCR tube and the 19 µl mix added. After short mixing the amplification reactions were performed in a thermocycler. Negative controls in which H_2Odest replaced the DNA were included in every series of reactions as well as positive controls as a guideline for the migration of the expected bands. Thermal cycling conditions were 94 °C for 3 minutes, 35 cycles of 94° C for 20 seconds, primer annealing for 30 seconds at the described

temperatures, 72 °C for and a final 72 °C incubation for 10 minutes. PCR reactions were subsequently analyzed by agarose gel electrophoresis (different agarose concentrations (depending on expected product size) containing 0.5 g/ml ethidium bromide). Inclusion of appropriate molecular weight standards DNA Markers enabled sizing of PCR products.

5.5 Reverse Transcriptase-PCR (RT-PCR)

First strand cDNA synthesis was performed using SUPERSCRIPT II RNase H^- Reverse Transcriptase from GibcoBRL for the RT-PCR. Reaction was set up following manufacturers instructions.

5.6 DNA sequencing

Initial sequencing was carried out at the FMI internal facility utilizing an ABI PRISM 377 DNA sequencer. Microsynth, a company providing sequencing services, then carried on the sequencing.

5.7 Construction of VHL-knockout-construct

Generation of VHL construct

The VHL targeting vector was designed with the aim of flanking exon 1 of the VHL gene with two loxP sites in order to create a 'floxed' VHL mouse strain in which exon 1 could be deleted by crossing this strain with a tissue-specific Cre-mouse. The targeting construct was composed of: a neo-IRES-tk selection cassette flanked by loxP sites, allowing positive and negative selection, two arms of homology (homologous to the targeted chromosomal VHL locus) and a single 3rd lox P inserted 3' of exon 1.

Generation of the backbone vector of the targeting construct containing the 5' arm of homology: The 5 kb-*BamHI* fragment, containing exon 1 of VHL, was excised from pBS and ligated into the pET-16b vector digested with *BamHI* and *Bgl II* in order to delete one BamHI site. The clone confirmed to have the insert in the right orientation (as depicted in the scheme) was digested with *Nde I* and *BamHI* and the obtained fragment was ligated into a pET-17b vector in order to have a unique *Hind III* restriction site in the insert and not present in the vector any more (b). The pET-16b vector containing the short fragment of the *BamHI/BglII-NdeI* fragment was going to be the backbone in which the whole targeting construct would be constructed in in the end and provided the shorter arm of homology (a).

3rd lox P site: By oligo annealing the 3rd lox P site was created flanked by a *BglII* and a *NotI* site and containing a *HindIII* site. This fragment was subcloned into pBSKS and excised again by digestion with Hind III (c).

Insertion of the 3rd loxP site: Fragment (c) was cloned into the unique *HindIII* site of plasmid (b) and thereby the 3rd loxP site was introduced 3' of exon 1 (d). By NdeI and *BamHI* digestion the *NdeI-BamHI* fragment, which now contained the additional loxP site, was reinserted into the original pET-16b construct (a) from where it hade been excised in the first place (e).

Insertion of the 3 kb BamHI fragment creating the second arm of homology 3' of the 3rd loxP site. Into this plasmid (e) the *BamHI* fragment harboring exon 2 was cloned (from pBS) (f).

Insertion of the neo-tk selection cassette: The neo-tk cassette was excised from pBS, (this construct was a kind gift from Ulrich Mueller) flanked with *NdeI* sites, by oligo insertion and cloning into pET-28a (*XhoI* and *NotI*), and was then introduced into the unique *NdeI* site of (f) completing the targeting vector construct.

The plasmid maps can be found in the appendix and the sequences of the inserted oligos under material-oligonucleotides.

Mouse VHL full-length construct: Full length mVHL-cDNA was created by RT-PCR on RNA samples kindly provided by Anne-Isabelle Michou. The primers used for this purpose were cDNA primer 1 -5' and cDNA primer 2 –3' (see primer list in materials).

5.8 Isolation of genomic DNA from ES cell clones

Medium was aspirated from each tissue culture well of 24-well plates containing ES colonies grown to confluency. After washing once with PBS, 400 µl Lysis buffer (100 mM Tris pH 8.5, 5 mM EDTA, 0.2 % SDS, 200 mM NaCl) including 50 µg/ml Proteinase K were added to each well and the plates were then incubated in a 37 °C incubator over night. The cell-lysate of each well was then carefully transferred into eppendorff-tubes and extracted with 400 µl of a 1:1 mixture of Phenol/Chloroform. After mixing and centrifugation at 14000 rpm for 2 minutes the upper phase was transferred into a new tube and extracted with 400 µl Chloroform. After mixing and centrifugation at 14000 rpm for 10 minutes the upper phase was again transferred into a new tube and 1 ml of 100 % EtOH was added. The DNA precipitated as a white pellet that after an additional centrifugation at 14000 rpm for 10 minutes was washed once with 70 % EtOH, centrifuged again and then

left to dry for at least 5 hours to get rid of all the Ethanol. Subsequently the pellet was re-suspended in 50 µl H_2O and agitated on a shaker at 30 °C for 24 hours to help re-dissolving. 20 µl (approximately 10 µg) of this DNA were then used for the digest.

5.9 Isolation of genomic DNA from mouse tails

DNA for PCR:

0,5-1 cm of the tail of a mouse were cut and lysed immediately or frozen at –20 °C. To each tail tip 500 µl of DNA digestion buffer (50 mM Tris-HCl pH 8.0, 100 mM EDTA pH 8.0, 100 mM NaCl, 1% SDS), supplemented with proteinase K at a final concentration of 0.2 mg/ml, were added and the lysis was allowed to occur at 55 °C for 6-24 hours with gentle shaking. After a short centrifugation the supernatant was transferred into new tubes, diluted 1:50 with H_2Odest and 1 µl was used in a PCR reaction.

5.10 Southern blot analysis

5.10.1 DOT-BLOT and radioactive Southern Blot

Dot-Blot: After subcloning the *BamHI*-fragments of the BAC clones into the pBSKS-vector, the colonies obtained after over night incubation at 37 ^{o}C on an agar plate with ampicillin (amp) selection, were striked onto two fresh agar-(amp)plates. One of them had a Hybond nylon membrane on top of it soaked onto the agar and the other one served as 'master plate' allowing the further usage of the later identified positive clones (and was kept at 4 ^{o}C after appropriate expansion of the colonies). After allowing the clones to grow overnight at 37 ^{o}C, the nylon membrane was carefully removed from the agar plate and incubated for 7 minutes in the denaturing solution (0.5 M NaOH, 1.5 M NaCl), followed by 2x 3 minute-incubations in the neutralizing solution (0.5 M Tris pH 8.0, 1.5 M NaCl). After 5 minutes washing in 2x SSC the membrane was dried in 3MM paper (whatman) for 10 minutes and UV-crosslinked with the stratagene transilluminator.

BAC-clone Southern Blot: The DNA of the BAC clones was digested with the appropriate restriction enzyme(s) over night (where the enzyme was added at least twice as 1 µl) and loaded on a 0.8 % agarose-gel. Following migration, the gel was stained subsequently with ethidiumbromide (0.5 µg/ µl) for 30 minutes and a picture was taken to asses proper digestion of the DNA. The DNA on the gel was then denatured by incubation of the gel for 45 minutes in denaturing solution (1.5 M NaCl, 0.5 M NaOH) under constant

gentle agitation. After shortly rinsing the gel in H_2O, it was incubated for 2x 15 minutes in neutralizing buffer (1 M Tris pH 7.4, 1.5 M NaCl) and the incubated in 10x SSC for 30 minutes, as was a nylon membrane. Capillary transfer of the DNA from the agarose gen onto the nylon membrane was allowed for at least 24 hours. Following transfer the membrane was marked and then washed in 5x SSC for 15 minutes before being subjected to UV-crosslinking by the stratagene transilluminator.

Generation of Southern Probes – radioactive labeling: The probes utilized for screening the BAC-clones for the presence of the VHL gene were labeled with the random primed Megaprime DNA labeling kit: The DNA was denatured for 10 minutes at 100 ^oC and then cooled on ice. In a microfuge tube to 25 ng of this denatured DNA 3 µl of unlabeled dNTPs, 2 µl of the 10x reaction buffer and 5 µl of α^{32}P-dCTP (= 50 µCi) were added and the reaction volume was increased to 19 µl by addition of H_2O. Then 1 µl of Klenow enzyme was added and the whole reaction mixture was incubated for 10 minutes at 37 ^oC. The reaction was stopped by addition of 2 µl 2 M EDTA (pH 8.0) and additional heating to 65 ^oC for 10 minutes. The specific activity of the probe was determined, and the probe was then subjected to a Nick-spin sepharose G-50 column (Pharmacia-Biotech) to eliminate unincorporated nucleotides. The specific activity was reassessed, to ensure that it didn't get lost on the column, and if it didn't drop below 10^6cpm, the probe was stored at –20 ^oC until further usage.

Pre-hybridisation: The membrane was incubated for 4 hours in 65^oC pre-warmed Church & Gilbert (C&G) Hybridisation buffer (0.25 M Na_2HPO_4 pH 7.3, 1 % BSA, 1 mM EDTA pH 8.0, 7 % SDS – all sterile filtered).

Hybridisation: 100µl of salmon sperm DNA (10mg/ml) and probe were both denatured by heating to 95 ^oC for 5 minutes before being mixed. This DNA-mixture was then added to 15 ml of C&G buffer and incubated with the membrane at 65^oC overnight. The membrane was then washed 4x 30 minutes at 65 ^oC with washing buffer (20 mM Na_2HPO_4 pH 7.3, 1 mM EDTA pH 8.0, 1 % SDS) and then dried slightly between two whatman papers. Finally the membrane was then exposed to film for at least over night at –80 ^oC.

5.10.2 Non-radioactive Southern Blot for genomic DNA (ES-cells or mouse tail)

Generation of Southern Probes – DIG labeling: For the creation of a 5`-probe to test for homologous recombination primers 5`.1 and 5`.5 were used in a PCR reaction utilizing genomic wild-type DNA as template whereas for the creation of a 3´-probe primers 3.`4 and 3.`6 were used. The bands corresponding the expected sizes were then isolated from an agarose gel and the purified DNA subjected to another PCR using the DIG labeling Kit from Roche. The 50 µl reaction contained 1x PCR buffer, 2 mM $MgCl_2$, 2 µl primer.
The following program was used: denaturation at 94 °C for 3 minutes, 35 cycles of denaturation at 95 °C for 20 seconds, annealing at 57 °C for 30 seconds and elongation at 72 °C for 45 seconds. This was followed by incubation at 72 °C for 10 minutes. From the 50 µl starting volume 5 µl were loaded on an agarose gel to check for PCR efficiency and 3 µl were dissolved in 20 µl H_2O, denatured for 5 minutes in a boiling water bath and placed on ice for 5 minutes before being added to 15 ml pre-warmed Pre-hybridisation (Pre-hyb) buffer.

DNA-gel blot analysis: DNA was digested with the appropriate restriction enzymes in a reaction volume of 30 µl containing 3 µl buffer and 1 µl enzyme. The restriction digest was allowed to take place at 37 °C over a period of ca. 24 hours, during which two more additions of enzyme occurred. 5 µl loading dye were then added to the reactions and the DNA was resolved on 0.8 % agarose gels, which were run overnight at 40 V. A DIG-labelled Marker II was used to enable sizing of the DNA fragments.
The gels were then incubated in an ethidium bromide “bath” (0.5 µg/ml) with gentle agitation for half an hour, washed in H_2Odest for 5-10 minutes and a picture was taken to see whether the digest had been successful. If so, the gels were incubated for 20 minutes in Denaturing buffer (1.5 M NaCl, 0.5 M NaOH) at RT and constant gentle agitation, followed by two 20 minutes-incubations in Neutralizing buffer (87.6 g NaCl, 60.8 g Tris, 33 ml 37% HCl in 1 l H_2O). DNA was then capillary transferred in 20x SSC to Zeta-Probe GT positively charged nylon membranes (Bio-Rad) and fixed by UV-crosslinking.

Pre-hybridization was performed for 2 hours in 15 ml Pre-Hyb-buffer (for 30 ml: 15 ml Formamid, 7.5 ml 10x Blocking buffer (50 g powder in 500 ml DIG-Buffer), 7.5 ml 20x SSC, 300 µl 10 % N-Laurylsarcosyl, 60 µl 10 % SDS and 1 ml sonicated salmon sperm DNA (10 mg/ml)) at 42 °C. After addition of the denatured probe, **hybridisation** was performed overnight under the same conditions. The membranes were washed

consecutively in 2x SSC/0.1 % SDS (5 minutes, RT), in 0.5x SSC / 0.1 % SDS (20 minutes, 68 °C) followed by 20 minutes at 68 °C in 0.1x SSC / 0.1 % SDS. Finally the blots were subjected to immunological detection using an anti-DIG antibody conjugated to alkaline phosphatase and the CDP-star kit from Roche Diagnostic, according to manufacturer's instructions.

5.11 Preparation of competent cells

A 200 ml SOB medium culture inoculated with about ten large colonies from a freshly grown plate of DH5alpha was left to grow at 26 °C with vigorous shaking until reaching an OD_{600} of 0.45. The culture was then split into sterile centrifuge tubes (4x 50ml falcon tubes) and placed on ice for 10 minutes. After spinning for 15 minutes at 2500 g, the supernatant was discarded, the pellet re-suspended in 64 ml HTB (4x 16ml) and placed on ice for 10 minutes. After spinning and discarding the supernatant again the pellet was re-suspended in 16 ml HTB (each pellet in 4 ml and then pooled). 1.2 ml filter-sterilized DMSO were added slowly while gently swirling the cell suspension and the cells were then immediately aliquoted into convenient aliquots (200 µl, 500 µl) and quick frozen by throwing into liquid nitrogen. Storage of competent cells occurred at –80 °C.
In some exceptional cases XL10-Gold Ultracompetent cells from Stratagene were used according to the manufacturers transformation protocol.

5.12 Transformation of E.coli

100 µl of cold bacteria competent cells were added to the ligation mix or DNA and the whole reaction was incubated for 30 minutes on ice. After heat-shock for 2 minutes at 42 °C, followed by 5 minutes incubation on ice, the transformed cells were spread on LB-Agar plates containing the appropriate antibiotic.

5.13 ES cell karyotype analysis

ES cells were split onto a gelatine coated 10 cm dish the day before the analysis to ensure actively dividing cells. Fresh ES-medium was added 3 hours prior application of colcemid (10 µg/ ml; Gibco). After four to six hours incubation at 37 ˚C, the cells were washed once with PBS and trypsinized with 0.1 % trypsin for 3 minutes at 37 ˚C. 5 ml ES-medium were added to stop the reaction, followed by centrifugation at 900 rpm for 5 minutes. The

supernatant was removed and the cells were resuspended in 1 ml PBS. Cells were pelleted by centrifugation at 2000 rpm for 2 minutes. After removal of the supernatant the cells were carefully resuspended in 1 ml 0.56 % KCl and left standing at room temperature for 10 minutes. After centrifugation at 2000 rpm for 2 minutes the pellet was resuspended slowly in ice-cold and freshly made fixative (methanol/ acetic acid 3:1). After incubation on ice for 10 minutes and short centrifugation the last step was repeated and the cells were let sit overnight at 4 ˚C. The next day after short centrifugation, the cells were resuspended again in 0.5 ml fixative. With the help of a Pasteur pipette the cells were dropped onto a clean microscopic slide from about 0.5-1 meter above and dried on a tray on top of a 37 ˚C water bath. The next day the cells were stained for 20-30 minutes in 3% Giemsa (in GuRR buffer) at room temperature. The slides were then washed briefly in water, air-dried at room temperature and coverslipped in entellan. The solutions like Giemsa, ES-medium and entellan were provided by the transgenic facility at the FMI.

5.14 Primary antibodies

The rabbit polyclonal antibody α-pVHL$_{Mm}$ (CT) was raised against the synthetic peptide RKDIQRLSQEHLESQHLEEEP that corresponds to the carboxyl terminal amino acid sequence of the murine VHL protein. The peptide was coupled to keyhole limpet haemocyanin (KLH) (Pierce) by Glutaraldehyde (Serva, Heidelberg) coupling and injected into rabbits. Antiserum was obtained from Eurogentec (Bruxelles) and affinity purified over a column generated by coupling 10 μg of the peptide to 1 g of activated CH-Sepharose 4B (Pharmacia) according to manufacturer's protocol.

Other antibodies used in the expression study were: rabbit polyclonal α-calbindin D-28k (Swant, Bellinzona, CH), mouse monoclonal α-Rho4D2 (kindly provided by Robert Molday, Vancouver, Canada), rabbit polyclonal α-p27 (C19) (Santa Cruz), rabbit polyclonal α-CRALBP (kindly provided by John Saari, Seattle, WA), mouse monoclonal α-GS (Chemicon, Temecula, CA), mouse monoclonal α-Vimentin (Chemicon, Temecula, CA) and rabbit polyclonal anti-RPE65 (kindly provided by Andreas Wenzel, Zürich, CH). The secondary antibodies were α-rabbit-Cy5, α -rabbit-FITC, α -mouse-Cy5 and α -mouse-FITC (Dianova).

5.15 Cell culture

Mouse NIH3T3 cells were maintained in Dulbecco´s modified Eagle´s Medium (DMEM, Invitrogene) supplemented with 5 % bovine calf serum (BCS), whereas the murine kidney tumor cell line RENCA was cultured in DMEM supplemented with 10 % fetal calf serum (FCS). Cultures were maintained at 37 °C in a humidified 95 % air and 5 % CO_2 atmosphere.

5.16 Western Blot analysis

For immunoblot analysis either postnatal P2 eyes from euthanized C57BL/6J mice were isolated, enucleated and the neural retina separated from the retinal pigment epithelium or alternatively NIH3T3 and Renca cells were harvested after being rinsed with phosphate buffered saline (PBS, Biochrom AG). Retinas or cells were homogenized through a G25 syringe in lysis buffer (20 mM HEPES, 0.4 M NaCl, 25 % glycerol, 1 mM EDTA, 5 mM sodiumfluoride, 0.1 % Nonidet P-40, 100 µg/ml phenylmethylsulfonyl fluoride, 100 µg/ml aprotinin, 1 mM Dithiothreitol). After standing on ice for 30 minutes the cell lysates were cleared by centrifugation at 14.000 rpm at 4 °C for 10 minutes. Protein concentrations were measured using the BioRad Protein Assay (Bio-Rad Laboratories) and cell lysates containing equal amount of protein were resolved by electrophoresis on a 12 % polyacrylamide-SDS gel and electroblotted onto nitrocellulose membrane (Optitran BA-S83, Schleicher&Schuell). After blocking in TBST buffer (50 mM Tris-HCl buffer, pH 8.0, containing 150 mM sodium chloride, 0.1 % Tween 20) with 5 % (w/v) nonfat dry milk, the membrane was incubated over night at 4 °C with α-$pVHL_{Mm}$ (CT) diluted 1:500 in TBST + 5 % milk. Washing of the membrane for 30 minutes at room temperature in TBST was followed by incubation with horseradish peroxidase-conjugated secondary antibody. The antigen-antibody complexes were detected using a chemiluminescence reagent kit (ECL Kit, Amersham Biosciences) according to manufacturer's instructions.

5.17 Preparation of murine tissues for immunohistochemical staining

C57BL/6J mice were obtained from Charles River Laboratoires France. Experimental procedures were designed to conform to the cantonal guidelines.

Eyes and cerebellum from euthanized C57BL/6J mice at various stages of development were used for immunohistochemical studies. Embryonic day E 0.5 was determined by the presence of a vaginal plug and the day of birth was designated as postnatal day P0. Tissues

were fixed overnight at 4 °C in 10 % formalin, embedded in Paraffin and sectioned at 5-20 µm.

5.18 Immunohistochemical studies

Paraffin sections were subjected to de-paraffinization in xylene and subsequently ethanol series. After incubation in PBS (+ 0.3 % Triton X-100) for 20 minutes, sections were subjected for 10 minutes to 97 °C in 10 mM Citrate Buffer pH 6.0 for antigen retrieval and slides were then left to cool down by standing for at least 20 minutes at room temperature. Short incubation in PBS at RT was followed by incubation for 30 minutes in 3% H_2O_2 / 10 % methanol to block endogenous peroxidases. After short washes in PBS sections were pre-incubated with 10 % normal goat serum (NGS; Vector Laboratories) in PBS (+ 0.3 % Triton X-100) for 30 minutes. Incubation with primary antibody was allowed over night at 4 °C or for 2 hours at RT. For ABC stainings the α-pVHL$_{Mm}$ (CT) antibody was diluted 1:200, whereas for immunofluorescent studies all primary antibodies were diluted 1:50 in 10 % NGS in PBS (+ 0.3 % Triton X-100), except α-Rho4D2 and α-calbindin that were diluted 1:100.

a) ABC staining:

   After 3 washes of 5 minutes in PBS (+ 0.3 % Triton X-100) sections were incubated with biotinylated goat α-rabbit diluted 1:200 in 10 % NGS in PBS. Colometric detection using the ABC Elite Kit (Vector Laboratories) was performed according to manufacturer's instructions. Slides were counterstained with hematoxylin and finally mounted using Mowiol.

b) Immunofluorescent staining

   Sections were washed in PBS (+ 0.3 % Triton) and incubated for 1 hour at room temperature with FITC- or Cy5-labeled secondary antibodies. After shortly rinsing the slides in H_2O, sections were coverslipped with Vectashield (Vector Laboratories).

c) Immunofluorescent staining using TSA kit

   If two rabbit polyclonal antibodies were to be used in a co-staining experiment the Tyramide Signal Amplification Kit (TSA; Perkin Elmer) was used according to manufacturer's protocol.

We used either conventional or confocal fluorescence microscopy to view the slides.

5.19 BrdU labelling

P7 mice were injected intraperitoneally with 100 µg BrdU / g body weight. Mice were sacrificed 2 hours later, their brains dissected, fixed in 10 % formalin and processed for paraffin sectioning. The in situ cell proliferation KIT, FLUOS (Roche) was used according to manufacturer's protocol.

5.20 Retinal Tissue dissociation

To dissociate retinal tissue a protocol by Wahlin *et al.*, 2004 was followed. In short: After euthanization of BL6 mice their eyes were enucleated and the neural retinae were isolated from the retinal pigment epithelium (RPE) in PBS without Ca^{2+} and Mg^{2+} at RT. The retinae were cut into smaller pieces and incubated in HBSS containing 1 mM EDTA and 5 U / ml Papain, pre-activated with the reducing agent L-cysteine (2.7 mM) for 30 minutes at 37 °C. For Müller glia cell isolation retinas were incubated for 15 minutes at room temperature followed by at least two washes with DMEM containing 10 % FCS. Dissociation of the tissue occurred by sequential trituration with Pasteur pipettes and the dissociated cells were then pelletted and resuspended in DMEM / 10% FCS. Dissociated cells were dropped onto polylysine-coated slides and incubated for a couple of minutes to allow attachment. Subsequently the cells were fixed with 4 % paraformaldehyde for 5 minutes, gently washed in PBS and permeabilized for 20 minutes in PBS containing 0.3 % Triton X-100. After blocking with 10 % Normal Goat Serum in 0.3 % Triton X-100 in PBS incubation with the primary antibody was carried out overnight at 4 °C. Antibody dilutions were: anti-CRALBP 1:50, anti-calbindin 1:50, anti-Rho4D2, anti vimentin 1:50. After short washes in PBS secondary antibody incubation was allowed for 45 minutes at RT. The slides were then shortly rinsed and mounted with Vectashield.

Aim of this thesis

The aim of this thesis was to obtain a detailed picture of VHL protein expression in primary VHL-disease target tissues, such as the retina and the cerebellum, in order to use this information to model VHL disease in mice and consequently attain a better understanding of its pathophysiology.

Chapter 7

Results

-Part One-

Generation of a "floxed" VHL allele in ES cells by Cre-mediated recombination

-towards the development of a conditional vhl knockout-

Homozygous disruption of VHL in mice resulted in embryonic lethality by embryonic day E 10.5-E 12.5 due to the absence of placental embryonic vasculogenesis and subsequent hemorrhage and necrosis (Gnarra *et al.*, 1997). As this precluded the investigation of VHL function in the adult, we decided to use conditional gene targeting technology based on the Cre/loxP recombination system (see introduction chapter 3) to generate a conditional VHL knockout, a "floxed" VHL-mouse (overview FIG. 22). VHL could then be inactivated tissue-specifically by crosses of these floxed mice with Cre-mice.

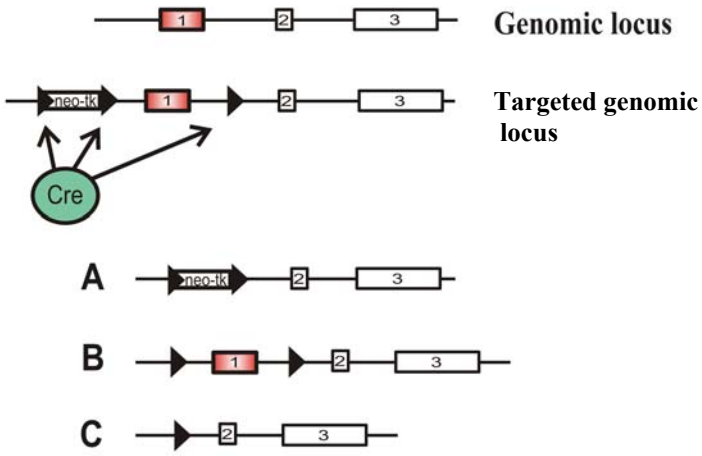

Figure 22. Overview of the strategy to produce a floxed VHL mouse or a complete VHL knockout. From the top: The genomic locus illustrates the genomic organisation of the VHL gene to be floxed or deleted (in red exon 1). Below, the targeted genomic locus is depicted. In case of a homologous recombination event taking place the recombined targeted allele/locus will have the same structure as the targeting vector. The population of ES cells deriving from a clone harbouring a wt allele and a recombined allele, will then be transiently transfected with a Cre-expressing plasmid and clones will be selected with G418 and/or gancyclovir. The transfection will lead to three types of site-specific recombination. A) In this case exon 1 has been deleted but the selection cassette is still present. The ES cells containing this construct are not very useful as the selection cassette should be removed prior blastocyst injection, especially as the tk has been reported to cause male sterility if expressed in mice. B) This represents the 'floxed' allele or also called 2-lox allele as two lox P sites are still present, flanking exon1. This is the recombination event we were primarily interested in as mice homozygous for this allele could be crossed to tissue-specific Cre mice allowing the creation of a conditional VHL knockout. Therefore ES cells containing this allele would be used for blastocyst injection. C) ES cells containing the complete knockout, where the first exon has been deleted and the selection cassette is not present any longer would be suitable to create a complete knockout. The complete knockout, although already published, was still of interest to be created in a different strain background, as it has been shown that different mice strain backgrounds affect heavily the phenotype observed in knockout mice.

1) Targeting vector design and cloning

In order to design the cloning strategy for the creation of the VHL targeting vector the first step consisted in finding a genomic clone containing the whole gene of interest. Based on the information given about the mouse exon sequences of VHL (Gao *et al.*, 1995; Gnarra *et al.*, 1997), primer pairs specific for exon 1 (oligos *exon1-5'* and *exon1-3'*), exon 2 (oligos *exon2-5'* and *exon2-3'*) or exon 3 (oligos *exon3-5'* and *exon3-3'*) were ordered and tested for their efficiency to amplify the corresponding exon fragment from wild-type genomic DNA by polymerase chain reaction (PCR) (FIG. 23).

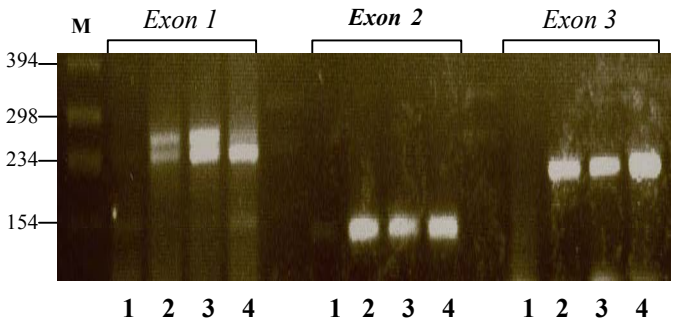

Figure 23. Testing PCR primers for specific amplification of the three VHL exons. Primers specific for exon 1, 2 or 3 of VHL were tested. Lane **1** always shows the negative control, where no template DNA was added to the PCR reaction, whereas in lanes **2**, **3** and **4** genomic DNA from different sources (129, C57BL/6 and 129 derived mouse strain respectively) was utilized. Marker VI (**M**) was used as a size reference. For exon 1 a fragment of 238 bp, for exon 2 123 bp and for exon 3 201 bp were expected. The primer pair for exon 1 always amplified two fragments, whereas the primer pairs for exon 2 and 3 specifically amplified the corresponding exon band, although for the exon 3 primers occasionally also another band appeared (not shown).

After identification of the exon 2-primer-pair as being the most efficient and specific one in amplifying the expected band of 123 bp, the primer pair together with the PCR protocol/conditions were sent to the company Incyte Genomics. There, this primer-pair was utilized for a PCR screening of a 129 mouse-derived genomic library with the goal of identifying specific BAC (bacterial artificial chromosome) clones that harboured the complete VHL gene. As the VHL gene lies within a stretch of genomic DNA smaller than 12 kB, it was enough to screen with only one primer-pair assuming that in the case of a positive hit, the positive BAC clone, normally enclosing 120 kB of genomic sequence, would harbour the whole gene including also exons 1 and 3.

In total three clones were obtained from the PCR screening and these were labelled with the numbers **361**, **383** and **422** respectively. The next step comprised characterizing these clones and scanning them for the presence of the VHL gene. PCR analysis of the three BAC clones with the original primers used to amplify the three exons of VHL revealed the presence of all 3 exons within all three BAC clones (FIG. 24).

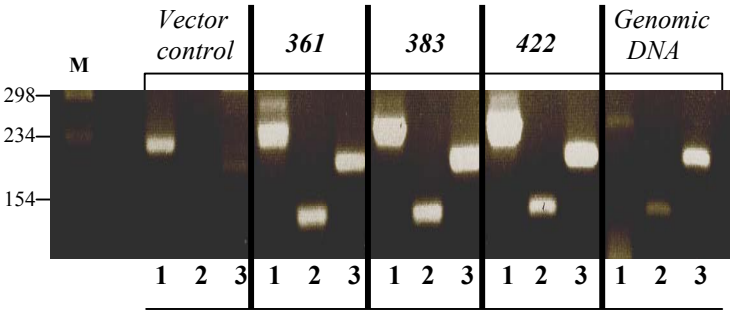

Figure 24. Confirmation by PCR of VHL exon presence within BAC-clones. The vector control, BAC clones 361, 383 and 422 and genomic DNA, as a positive control, were tested for the presence of the VHL exons. Lanes 1, 2 and 3 represent PCRs with primer-pairs specific for VHL exon 1, 2 and 3 respectively. In the genomic DNA control as well as in all three BAC clones the presence of all three exons of VHL was confirmed. In the vector control a band for the exon 1 primer-pair was detected that was though lower than the expected size.

Physical mapping studies performed on the genomic clones obtained in the paper published by Gnarra in 1997 had shown that a digestion of these clones with *BamHI* gave

restriction fragments of 5 kb, 6 kb and 4 kb containing exons 1, 2 and 3, respectively. In addition a unique *HindIII* restriction site within the 6 kb-*BamHI* fragment of exon 2 was identified, whereas there were no *HindIII* sites within the other two *BamHI*-fragments containing either exon 1 or exon 3.

In order to confirm the presence of these fragments in our case, the genomic DNAs of all three BAC clones were digested with *BamHI* alone or with *BamHI* and *HindIII,* and then subjected to Southern Blotting analysis by hybridization with a full-length mVHL-cDNA-probe randomly labelled with α-^{32}P-dCTP. As depicted in figure 25, the genomic BAC DNA, when digested using the *BamHI* restriction enzyme and hybridised with a full-length mVHL-probe yielded 3 fragments/bands of 3, 4 and 5 kb instead of the expected 4, 5 and 6 kb. When comparing the *BamHI*-restricted with the *BamHI/HindIII* restricted DNA the only striking difference was the disappearance of the 5 kb-band (9.6 kb band in case of clone 383) and the, as an alternative appearing smaller fragment of *ca.* 3.7 kb, which led to the assumption, always based on Gnarra's paper, that the 5 kb-fragment could be the one containing exon 2.

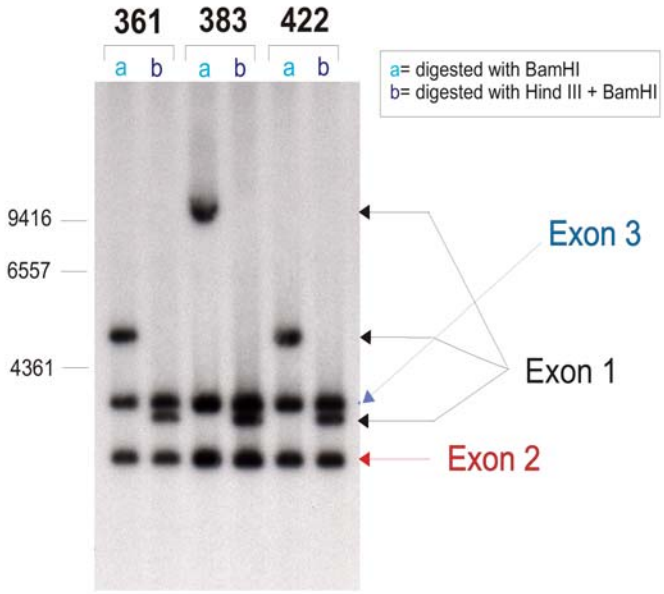

Figure 25. Southern Blot of BAC-clones confirming the presence of VHL exons and defining their *BamHI*-fragment distribution. Screening of a 129 mouse-derived genomic library for BAC-clones harbouring the VHL gene yielded the identification of three clones: n. 361, 383 and 422. To confirm the presence of the three VHL exons within these clones their DNA was digested with *BamHI* (lanes a) and *BamHI / HindIII* (lanes b) and subjected to Southern Blot analysis with a full-length mVHL cDNA probe (positive probe was on the same gel, but not shown as fragment run much lower). All three clones contained 3 *BamHI*-fragments of *ca*. 5, 4 and 3 kb (except clone 383 that instead of the 5 kb fragment had a much bigger sized fragment). Additional *HindIII*-digestion only resulted in disappearance of the 5 kb-*BamHI*-fragment (or of the *ca.* 9.6 kb band for clone 383) and in the appearance of a *ca.* 3.7 kb band. Subsequent labelling with an exon1-, exon2- or exon3-probe allowed the association of the *BamHI*-fragments with the corresponding VHL-exons harboured within (Data not shown, result just indicated by arrows).

In order to link the three *BamHI*-fragments to the corresponding exon contained within, the southern blot was hybridised with specific probes for exon 1, exon 2 and eventually exon 3 (the probes were created by PCR on genomic DNA using the before mentioned specific primer-pairs) and the fragments were therefore identified as following: the **5kb**-fragment contained **exon 1**, the **3kb**-fragment **exon 2** and the **4kb**-fragment contained **exon 3.** The *HindIII*-site predicted to be in the *BamHI*-fragment containing exon

2 was not confirmed by our result, instead it was rather the *BamHI*-fragment harbouring exon 1 that had to contain such a restriction site.

The BAC clone **361** was chosen to be digested with *BamHI*, the fragments between 2,5-5,5 kb were extracted from the gel and subcloned into the Bluescript vector pBSKS. Single colonies were plated on a fresh plate and a Dot Blot was performed using the exon 1- or exon 2-specific probes to identify which clones had inserted the right fragments (FIG. 26).

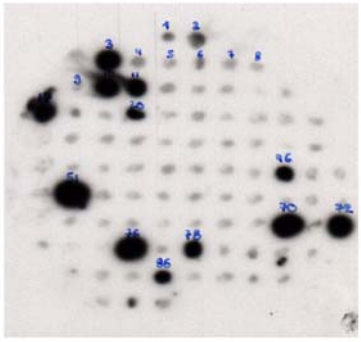

Figure 26. Example of a dot blot. After sub-cloning the 5 and the 4 kb *BamHI*-fragments into pBS, the colonies surviving ampicillin selection were plated on a nylon membrane and this one hybridized with probes specific for exon 1, 2 or 3 in order to find positive clones harbouring the different fragments.

With this strategy we obtained 3 clones harbouring exon 1 in the Bluescript (pBSKS) vector, 3 clones harbouring exon 3 and finally 2 clones harbouring exon 2 in the pBS-vector. All clones were confirmed by sequencing.

In order to design the VHL targeting vector we had to first assemble the sequence of the VHL gene. As the whole sequence was not yet available, the clones had to be sequenced through completely to obtain all the information needed to design the cloning strategy (primers for sequencing see materials, chapter 4). In addition *in silico* analysis of the already known parts of the VHL gene locus was undertaken and compared with the sequenced DNA. When finally the whole sequence was deciphered, and all the possibly interesting restriction sites found, the design and subsequent cloning of the vector was initiated.

For the VHL targeting vector only the two *BamHI*-fragments containing exon 1 (5 kb fragment) and exon 2 (3 kb fragment) were utilized (FIG. 27). A targeting cassette flanked by loxP sites, containing both a positive (neo) and a negative (tk) selection marker, was inserted into a unique *NdeI*-site approximately 2.6 kb upstream of exon 1. A third, single loxP element was inserted into a *HindIII*-site lying downstream of exon 1. In order to

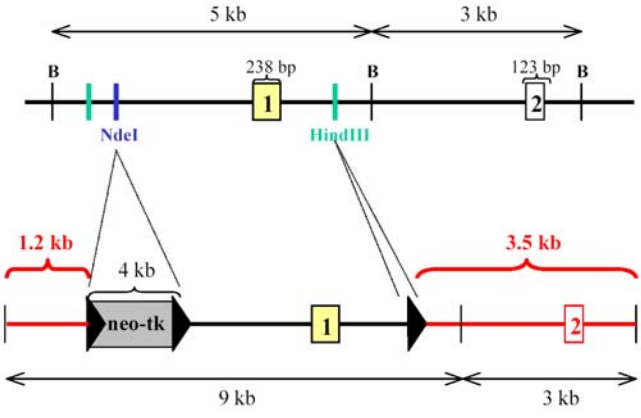

Figure 27. Design of the targeting vector (below) in comparison to the genomic locus of the VHL gene (top). In red are the two arms of homology. B= BamHI restriction site. Further details see text

favour the homologous recombination event in the mouse, two arms of homology had to be present in the targeting vector. A shorter arm of homology of *ca.* 1.2 kb was provided nearby the positive/negative selection marker cassette and a longer arm of homology of *ca.* 3.5 kb, containing also exon 2, was provided 3' of the 3rd loxP site. The whole cloning strategy is depicted in figure 28 and is explained in more detail in the methods section in chapter 5.7. The final construct was confirmed by sequencing especially for checking the correct orientation of all loxP elements.

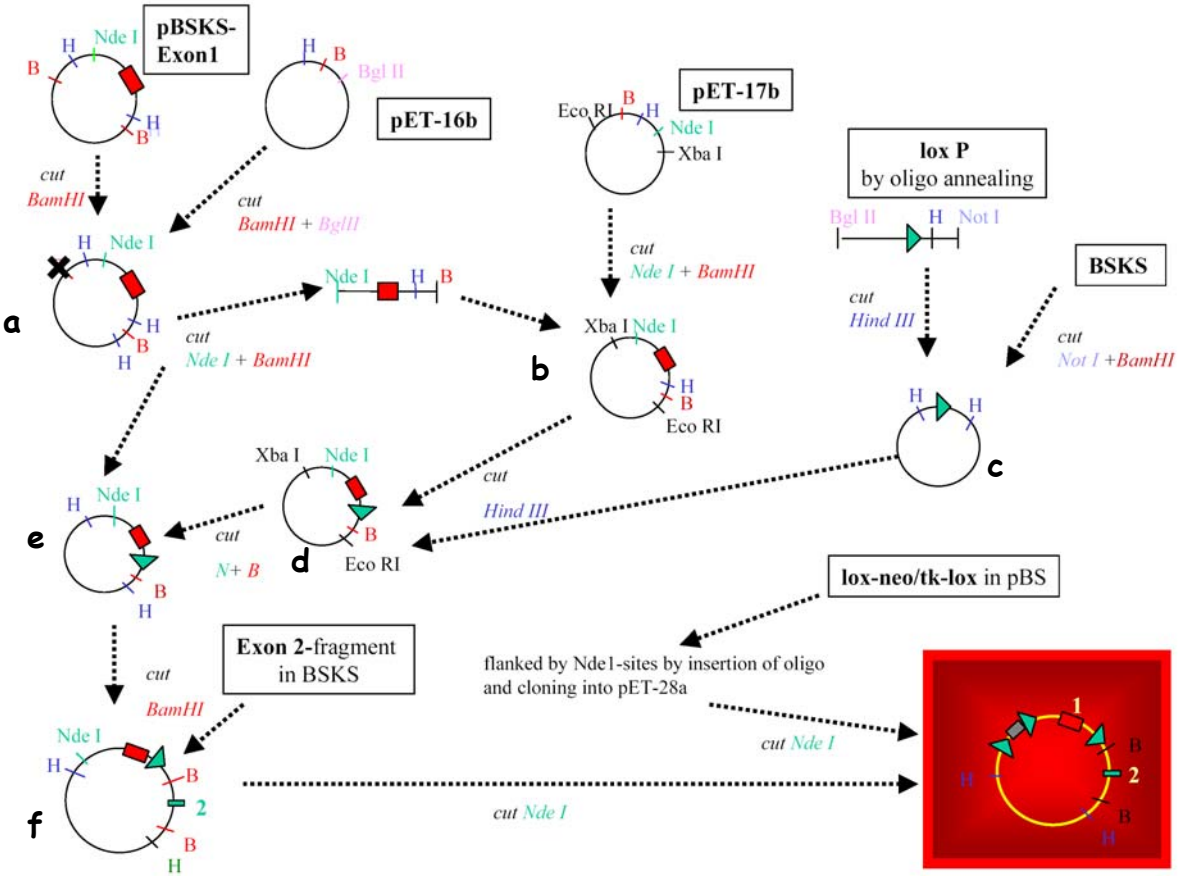

Figure 28. Schematic overview of the cloning steps involved for the creation of the VHL targeting vector. Details about the cloning are found in chapter 5.7.

2) Electroporation of the targeting vector in ES cells and subsequent screening

Prior transfection into embryonic stem (ES) cells, the vector was linearized by digesting the targeting vector (inside the pET-16b plasmid backbone) with the restriction enzyme *ClaI*, which only cut once, outside the construct, in the vector. ES cells were then electroporated to incorporate the targeting vector into the ES cell genome. The ES cell line used was

derived from a 129 mouse strain, which is characterized by the dominant brown (agouti) colour.

The transfection of the targeting vector into ES cells and the subsequent selection with G418 (250 µg/ml) for ES-clones containing the neomycin-resistance gene were performed by Patrick Koop in the transgenic facility at the Friedrich Miescher Institute in Basel. G418 resistant clones were then picked and expanded to isolate enough genomic DNA to perform Southern analysis.

With the aim of identifying the correctly recombined clones, three probes, which had been tested for their efficiency on wild-type genomic DNA before, were employed: two external, 5' and 3', probes and an internal neo-probe (kindly provided by Christiane Wirbelauer). The 3'-probe was used to confirm the proper insertion of the 3rd single loxP site by digestion of genomic DNA with *NdeI* and *EcoRV*, while the 5' probe and the neo-probe could both be employed on *BclI* digested DNA to screen for the presence of the selection cassette. As illustrated in figure 29 restriction digests of genomic DNA with *EcoRV* and *NdeI* and hybridisation with the 3'-probe were expected to generate a band of 9.1 kb for the wild-type allele and a 5.9 kb band for the targeted allele.

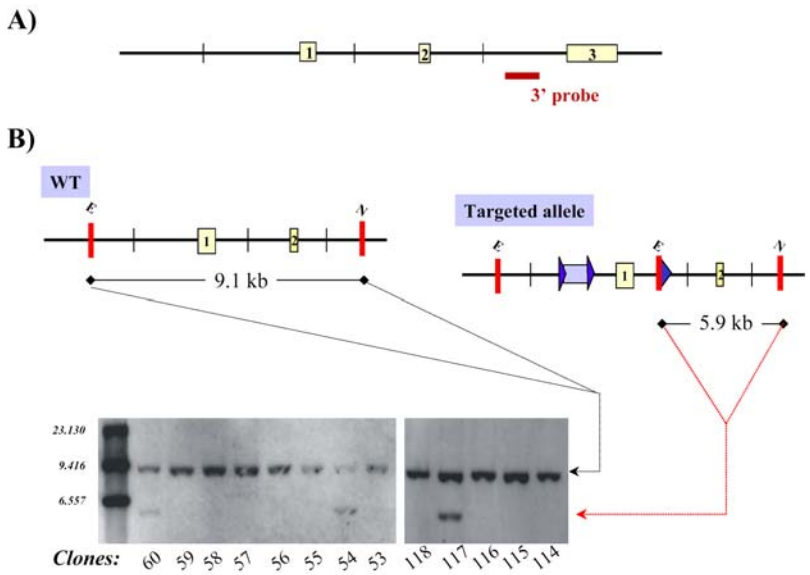

Figure 29. Southern Blot with the 3`-probe. A) Schematic diagram of the genomic locus of VHL and the relative position of the 3'-probe herein, depicted with red bar. B) The genomic VHL wt DNA, when restricted using *EcoRV* (E) and *NdeI* (N), was expected to generate a 9.1 kb fragment, whereas the targeted allele would in that case generate a 5.9 kb fragment due to an additional *EcoRV* restriction site that had been introduced together with the 3rd loxP site. The restriction sites are shown as vertical red lines and the loxP sites as blue arrowheads. The neo-tk selection cassette is shown as a light blue box flanked by loxP sites (blue arrowheads). In the depicted examples of southern blots all tested clones contained the wt fragment, but only 3 clones were positive for the targeted allele fragment of 5.9 kb (clones 54, 60 and 117).

168 clones were digested with *EcoRV* and *NdeI* and hybridised with the 3' probe. Among these, 4 clones, numbers 54, 60, 107 and 117, proved to have the right insertion of the 3rd single lox P in one of their two alleles. Only these four clones were expanded again and DNA was isolated in order to perform another southern to check with the 5' and the neo-probe for proper insertion of the other elements of the targeting vector.

Genomic DNA of the four clones that tested positive for the proper insertion of the 3rd single loxP site was digested with *BclI* and subjected to southern blot analysis using first the 5'-probe and then the neo-probe. As depicted in figure 30 digest with *BclI* was expected to produce a 6 kb fragment for the wild-type allele and a 10 kb fragment for the recombined allele due to the inserted neo-tk cassette, which is about 4 kb in length.

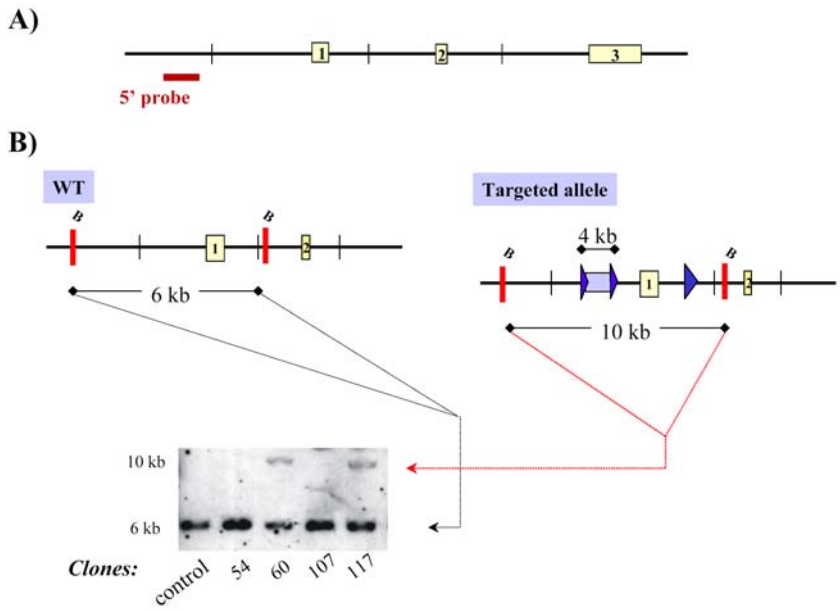

**Figure 30. Southern Blot with the 5`-probe.** A) Schematic diagram of the genomic locus of VHL and the relative position of the 5`-probe herein, depicted as red bar. B) The genomic VHL wt DNA, when restricted using *BclI* (B) was expected to generate a 6 kb fragment, whereas the targeted allele would in that case generate a 10 kb fragment due to the insertion of the neo-tk selection cassette of about 4 kb in size. The restriction sites are shown as vertical red lines and the loxP sites as blue arrowheads. The neo-tk selection cassette is shown as a light blue box flanked by loxP sites (blue arrowheads). In the depicted southern blot of the four clones, which had been positive for the insertion of the 3rd single lox P site, only two clones gave the expected fragment of the targeted allele (clones 60 and 117; control represents genomic wt DNA). Strangely enough as this blot was hybridized with a neo-probe all four clones confirmed the presence of the neo-tk selection cassette as a 10 kb fragment (Data not shown).

But in this case only two out of the four clones previously shown to be positive for the 3rd loxP site demonstrated the expected band of 10 kb. As the same blot could be hybridised with a neo-probe designed against the neomycin resistance gene in the neo-tk cassette, the presence of the selection cassette was though confirmed in all four clones with

this probe. These contrasting results made us chose clone 117 for further experiments, as this was one of the two clones that had shown the expected fragment patterns in all southern blot proving that homologous recombination had occurred in this case. In addition the band detected by the neo-probe for the other positive clone, clone 60, had been much fainter, so that clone 117 in the end seemed to be the only appropriate one to pick as the basis for the next transfection round.

The karyotype of the 117 ES cell clone population was investigated prior its utilization for the 2nd transfection as it is known that with time in culture abnormal variant cell clones can arise in ES cell populations. Among these some variants have an abnormal phenotype and may therefore be unable to contribute to germline transmission of genetic traits.

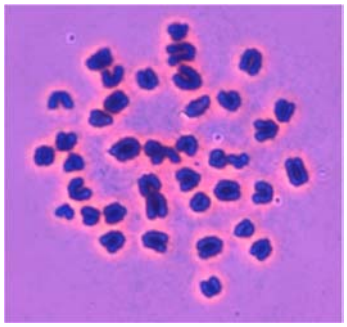

Figure 31. Karyotype of 117 ES cell clone.

The karyotype in this case was though proven to be acceptable, as 75 % out of 50 counted spreads didn`t show any karyotypic abnormalities.

3) Transfection of the positive clone from 1. Electroporation with a Cre-expressing plasmid and screening

After expansion of clone 117, this ES-cell population was transiently transfected with a cytomegalovirus promoter-driven Cre recombinase plasmid (performed again by Patrick Koop at the Friedrich Miescher Institute). This time negative selection was provided by the presence of gancyclovir (2 μM) in the medium and cells expressing the thymidinkinase gene (present in the cassette together with the neomycin resistant gene) normally convert this nucleoside analog into a toxic derivative leading to their own death, therefore enriching for clones that have lost the selection cassette due to excision by Cre action.

In total 168 surviving clones were picked and expanded, but unfortunately the DNA gained from the ES cells was not enough to perform southern blot analysis. Therefore a PCR screening strategy was utilized with the aim of identifying the putative positive clones, which would then have been subsequently re-grown in order to be confirmed by southern.

The PCR screen employed the primers schematically depicted in figure 32.

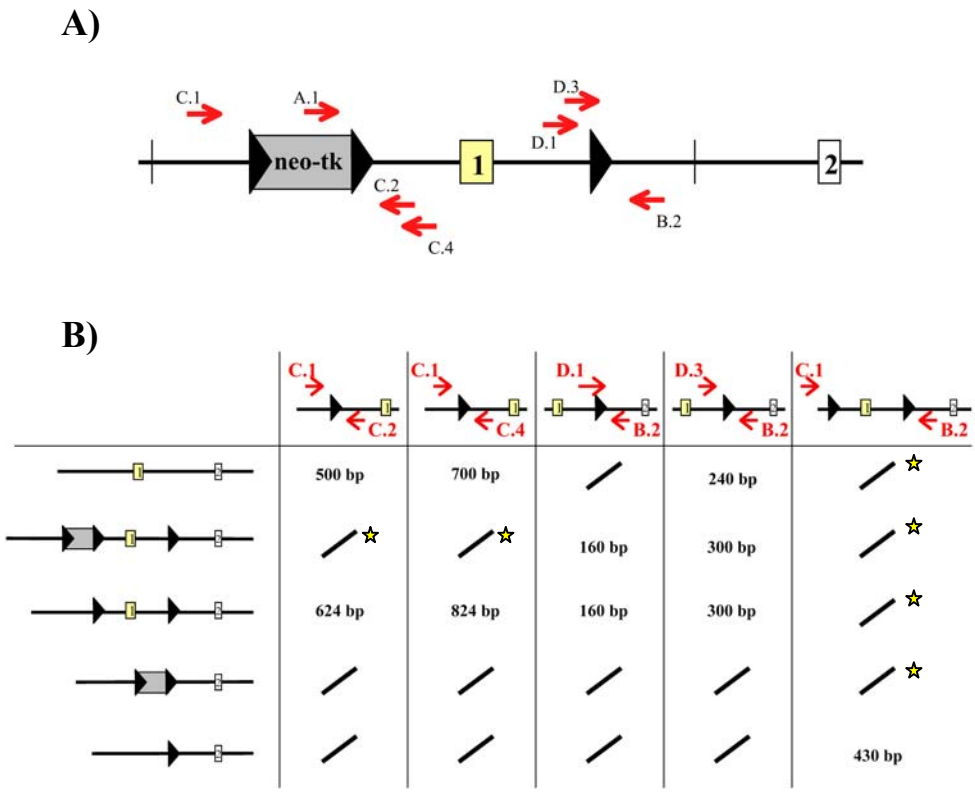

Figure 32. PCR screening strategy employed to identify clones containing either a floxed VHL allele or a VHL null allele. A) Schematic diagram of the targeted allele and the relative position of the employed primers (depicted as arrows) showing the orientation of the primers. B) The primer combination A.1 and C.2 depicted only in A) was used to select for clones that did not contain the neo-tk cassette any longer and where therefore no band was detectable by PCR. These clones were subsequently tested with all the primer sets listed in the table. On the left of the table the possible allele structures are depicted (although the second and fourth from the top should in theory not be present any more due to the selection with the A.1 and C.2 primer in the beginning that was thought to ensure the absence of the selection cassette). The fragment sizes expected with the primer pairs depicted on top of the table are shown for every possible allele structure. Little stars mark the cases where the primers would have recognized the corresponding DNA, but where the fragments were too big to be synthesized by PCR.

All the clones were first tested for the presence of the neo-tk cassette with the primer pair **A.1** and **C.2** that could only give a band in case the cassette was still in one of the two alleles. With this screening approach out of the 168 screened clones the following numbers did not test positive and were therefore likely to have lost the selection cassette: n. 4, 7, 8, 9, 18, 23, 29, 30, 31, 43, 47, 63, 85, 92, 121, 124, 137, 144 and 166. The high number of clones that still seemed to contain the neo-tk cassette led to the assumption that the gancyclovir selection hadn't been very efficient, nevertheless we continued screening the above-mentioned clones for both the floxed and the complete knockout on one allele.

Before screening these clones though, clone 117 was re-tested with this PCR screening also to ensure the usefulness of the strategy. As shown in figure 33 clone 117, the clone that was chosen from the 1st transfection to be transfected with the Cre-plasmid, when compared to genomic wild-type DNA and screened with different primer sets confirmed the presence of the neo-tk cassette and the 3rd lox P site.

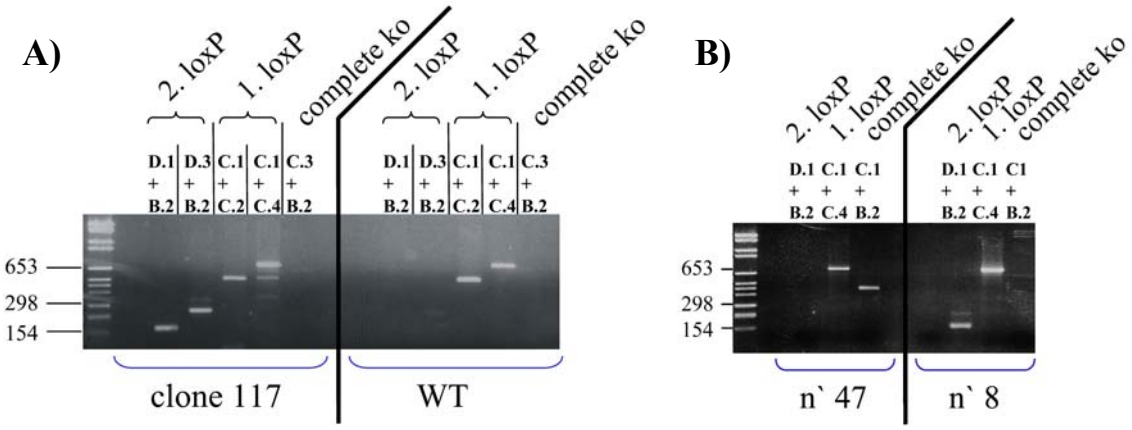

Figure 33. PCR screening strategy employed to identify clones containing either a floxed VHL allele or a VHL null allele. A) ES cell clone 117 (from first transfection) was tested with different primer combinations for the Presence of the neo-tk cassette and the 3rd lox P site (defined here as 2. loxP. The two loxPs refer to the floxed allele that we wanted to screen for, therefore the primer pairs were utilized to screen for the presence of the first (1. loxP) or the second loxP (2. loxP)). As control wt genomic DNA was utilized to prove efficiency of the selected primers. Clone 117 showed all the expected fragment sizes (the lower and fainted band in the C.1 + C.4 lane was not reproducible in other experiments and is therefore neglected) and was therefore re-confirmed as a clone in which homologous recombination had taken place. B) Clone n. 47 showed the fragments or absence of fragments defining it as a possible candidate for a complete knockout, where VHL exon 1 had been excised leaving only a single loxP. Clone 8 is depicted as an example of many clones that didn't show any clear result as they had been negative for the presence of the neo-tk cassette but for the rest behaved as if they contained the selection cassette.

Among the clones obtained from the 2nd transfection there were four clones (n. 47, 121, 137 and 166) that seemed to have a complete knockout (where exon 1 was excised and only a single lox P site left) on one allele (always remember that only one allele is recombined or 'targeted', while the other one remains WT). Unfortunately no clear "conditional " clones, containing a floxed and a wt allele, could be identified, as the remaining clones showed abnormal PCR patterns.

Nevertheless 12 clones of the originally 168 were re-grown and subjected to southern blot analysis. The DNA was digested with *EcoRV* and then hybridised with the 5'-probe already used for the screening of the first transfection. Figure 34 illustrates the possible results.

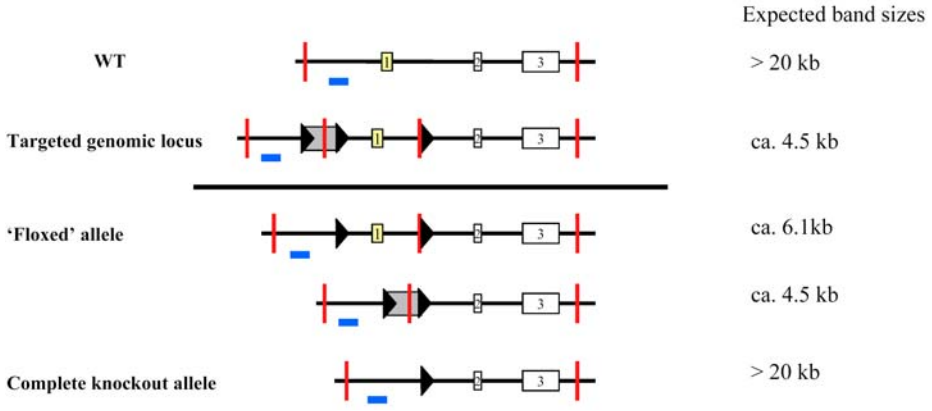

Figure 34. Southern Blot strategy testing the outcome of the 2nd transfection. The *EcoRV* restriction sites are depicted as vertical red lines and the 5'-probe is depicted as a blue bar.

The Southern Blot didn't give any 6.1 kb band expected in the case of a recombined 'floxed' allele, but the wild-type band expected to run above 20 kb could be seen for all clones confirming that the southern blot per se had worked. This result excluded the possibility of a floxed VHL gene within the selected clones, but didn't eliminate the possibility of a complete knockout, where exon 1 had been deleted.

In order to screen for a complete knockout, the DNA was digested with the *BclI* restriction enzyme and a VHL exon1-specific probe (used for screening the BAC clones in the beginning of this study) was utilized. As depicted in figure 35, digestion with *BclI* was expected to generate a fragment of 6 kb for the wild-type allele and a 3.3 kb fragment for the complete knockout allele. The result of the southern blot confirmed the presence of three clones that had excised exon 1 and that were therefore complete knockouts (heterozygous though).

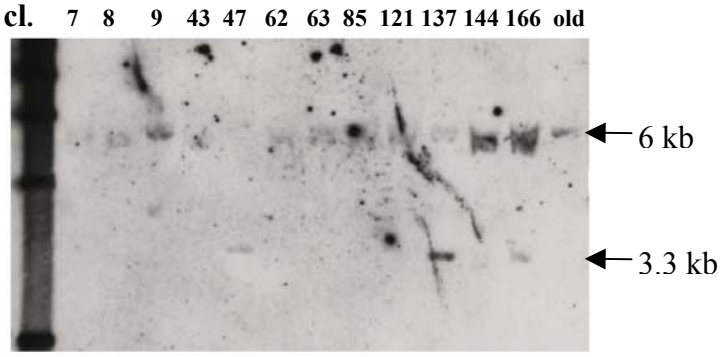

Figure 35. Southern Blot testing for complete knockout ES cell clones. The digest with *BclI* was expected to create a 6 kb fragment for the wt allele (see also figure 30). In the case of a VHL knockout allele, where exon 1 had been excised by Cre, a 3.3 kb fragment was expected. Among the 12 tested clones (cl.) three showed a strong (cl. 137) or faint (cl. 47 and 166) 3.3 kb band in addition to the wt allele band.

The main aim of this project had been to create a conditional knockout as it had been shown that the complete knockout was lethal. Although it would have been interesting to knock out VHL in another mouse strain due to the fact that it is known that the background affects the different outcome of a knockout, it was still more interesting and challenging to create a conditional knockout, so another attempt was undertaken.

4) Re-Transfection of the positive clone from 1. Electroporation with a Cre expressing plasmid and screening

After expansion of clone 117, that had been tested positive for the homologous recombination event in the first place (see 3)), another transfection with the Cre-plasmid was carried out. This time instead of gancyclovir selection, that hadn't seemed to be very efficient in the first try, selection was carried out with G418. As opposed to the screening after the 1st transfection (of the targeting vector into the ES cells) in this case cells that

were dying were screened, as these had lost the selection cassette and were therefore the interesting ones.

67 clones died during G418 selection and, as it was not possible to re-grow all of them, only 12 clones were chosen to be re-grown and tested by Southern.

The southern strategy was the same one already explained before under point 4) and as a control DNA from clone 117 was utilized (FIG. 36).

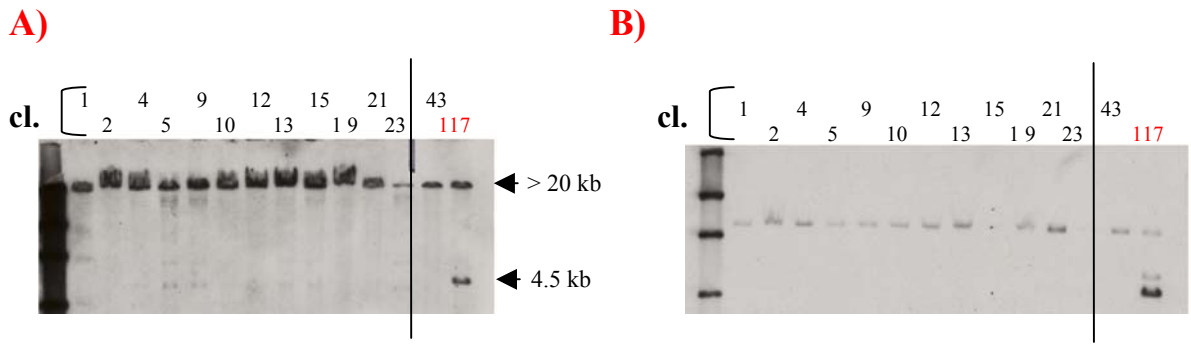

Figure 36. Southern Blots of 12 clones that were supposed to have lost the neo-tk cassette. A) Southern blot with the 5'-probe following *EcoRV* digestion was expected to give a 20 kb fragment for the wt allele and a 6.1 kb fragment for the floxed VHL allele. The 117 ES cell clone (in red) was utilized as negative control, as this still retained the neo-tk cassette and gave a 4.5 kb fragment (see also figure 34). Clone 43 came from the previous transfection round which had given only complete knockout clones. None of the tested clones showed a fragment of 6.1 kb. B) The same blot was tested for the presence of the neo-tk cassette with a neo-probe. Although the clones had been selected for their inability to survive selection with G418 the hybridization with the neo-probe revealed that all clones except one (cl.23) gave bands of a specific size. In addition clone 117, on which the 2nd transfection was based on, gave multiple bands that were not explicable.

As shown in figure 36A the wt band of >20 kb could be seen for all twelve clones, whereas there was no clone that showed a fragment of 6.1 kb. While clone 117 contained a second fragment of the expected size of 4.5 kb, some of the other clones showed multiple faint bands. Testing of these clones for the neo-probe gave even more incomprehensible bands (FIG. 36B). In addition also clone 117, on which this second transfection was based on, started to show a strange band pattern putting everything in question that had been done until that moment. As, on top of everything, the conditonal knockout had been published in the meantime, this project was stopped.

Chapter 8

Results

-Part Two-

pVHL-expression study in the murine retina and cerebellum

VHL gene expression studies on human fetal and adult tissues showed VHL mRNA to be ubiquitously detectable. Expression was not restricted to specific areas known to undergo abnormal differentiation as part of the VHL syndrome such as kidney, cerebellum and pancreas, but it was also present, among others, in the heart, lung and prostate. In addition VHL gene expression was evident in all derivatives of the three germ cell layers also during mouse embryogenesis, being most prominent in epithelial components of the lung, kidney and eye (Richards *et al.*, 1996; Kessler *et al.*, 1995).

Expression studies of the VHL protein (pVHL) utilizing poly- and monoclonal antibodies against human VHL revealed wide cytoplasmic expression in human adult tissues (Sakashita *et al.*, 1999; Corless *et al.*, 1997; Los *et al.*, 1995). However, despite the emergence of data on overall *Vhl* gene expression and elucidation of VHL function, little was known about the detailed VHL protein expression in the retina and cerebellum.

To investigate pVHL expression during murine development and adulthood a mouse pVHL-specific antibody was raised and utilized in a detailed immunohistochemical study focusing on the development of two tissues that play a very important role in the course of VHL disease, namely the retina and cerebellum.

1) Characterization of the α-pVHL$_{Mm}$ (CT) – antibody

Polyclonal rabbit serum was raised against the synthetic 21mer peptide corresponding to the C-terminus of murine pVHL. In order to test for the specificity of this antibody, defined as α-pVHL$_{Mm}$ (CT), cell lysates of mouse NIH3T3 and Renca cells were prepared, loaded onto a 12% SDS-gel and subjected to immunoblotting. As illustrated in figure 37A the affinity-purified α-pVHL$_{Mm}$ (CT) antibody recognized exclusively two endogenous proteins of expected molecular weights, 21 and 25kD. The abundance of the endogenously detected proteins was significantly increased in whole cell lysates prepared from cells previously transfected with a mammalian expression plasmid encoding either the long or the short form of pVhl$_{Mm}$. Thus the migration of the endogenous proteins is consistent with the one of over-expressed proteins (data not shown) and the antibody proves to be specific for murine Vhl.

As in human, the mouse *Vhl* gene also encodes two proteins, termed pVHL$_{21}$ and pVHL$_{25}$, arising from two alternative start codons. The primary sequence in this case only differs by the additional presence of a single acidic repeat unique to the longer VHL protein, pVHL$_{25}$. The mouse pVHL shares high homology with the human pVHL, sharing a 90% identity in the amino acid sequence in the middle part harboring the most important

sites. As the α-pVHL$_{Mm}$ (CT) antibody recognizes both forms equally, no distinction between the forms will be made and both forms will be subsumed under the term "pVHL".

To study pVHL expression during development mouse embryos were euthanized, fixed in 10% formalin and embedded into paraffin. Sections were then stained with the α-pVHL$_{Mm}$ (CT)-antibody. Immunohistochemical staining of murine tissues from E17.5 using α-pVHL$_{Mm}$ (CT) revealed strong VHL expression in a variety of tissues. Representative examples of pVHL staining in tissues such as pancreas, lung and ear as well as in the retina are illustrated in figure 37B (a,d,g) and Fig. 37C (left panel). These findings correlate with the impressive Vhl expression pattern noted in Kesslers paper where e.g. at E16.5 the inner and outer neuroblastic layers of the retina revealed strong VHL mRNA expression activity. Moreover as shown previously for VHL mRNA, pVHL expression was not exclusively present in tissues known to be at risk in VHL disease development, but also in tissues not connected to the known VHL phenotypes.

To document the specificity of the Vhl staining, the antibody was pre-incubated with an excess of peptide before use in immunostaining. As illustrated in Figure 37B (b,e,h) and 37C (right panel) the pre-incubation with the CT-peptide, which was originally used to create the antibody, reduced the staining dramatically whereas incubation with a control peptide mimicking the N-terminus of Vhl didn't affect the staining at all (Fig 37B right panels).

pVHL expression in the retina was additionally confirmed by western blot. Whole cell extracts of retinas from P2 mice were resolved by electrophoresis on a 12 % polyacrylamide-SDS gel and electroblotted onto nitrocellulose membrane. Incubation of the membrane with α-pVHL$_{Mm}$ (CT) revealed exclusively two bands migrating at the same size of the above characterized pVHL bands in NIH3T3 whole cell extracts. In this experiment expression of the longer pVHL form, pVHL$_{25}$ seemed to be more prominent than the expression of the so-called shorter form, pVHL$_{21}$. This difference in expression levels has been seen reproducible and will be interesting to be investigated in more detail in future.

In conclusion these data show that α-pVHL$_{Mm}$ (CT) is a highly specific antibody recognizing both forms of pVhl in mouse.

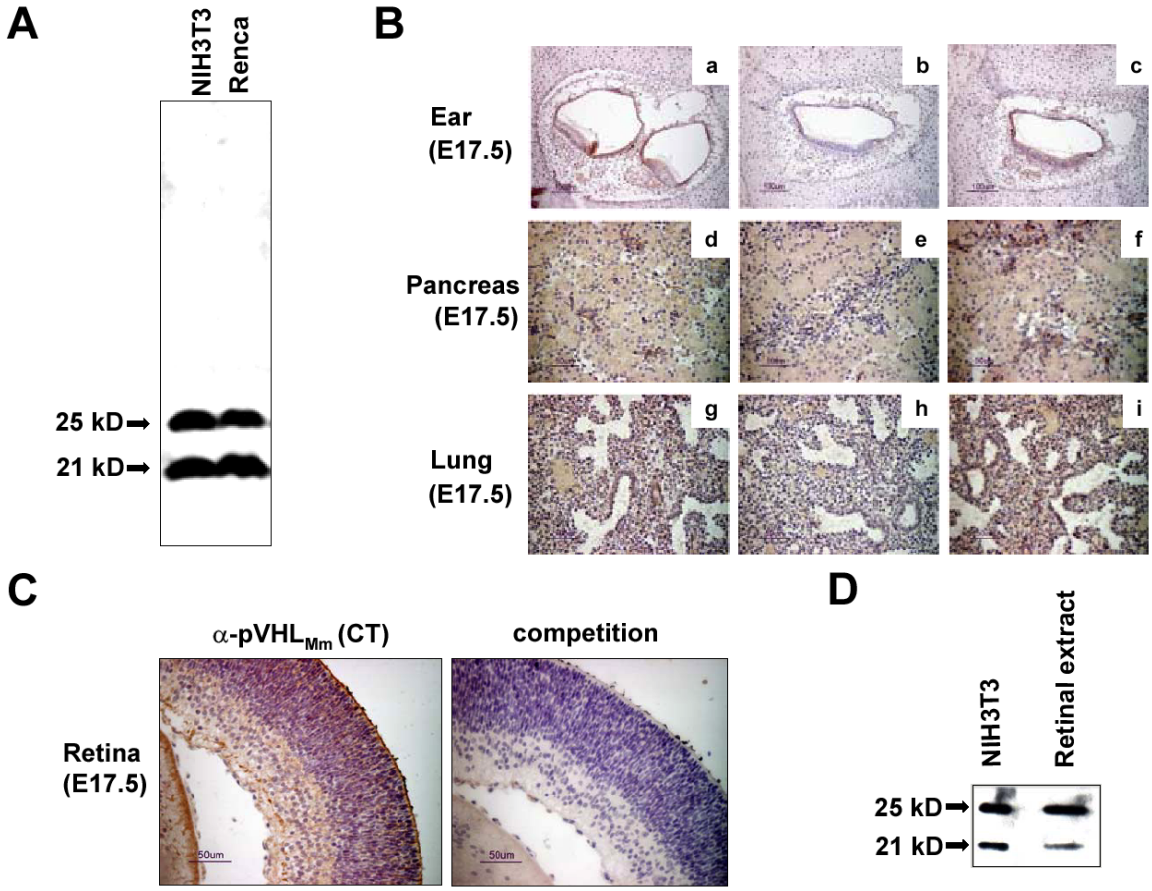

Figure 37. Antibody characterization of the α-pVHL$_{Mm}$ (CT) antibody.
(A) Whole cell lysates of NIH3T3 (lane 1) and Renca (lane 2) cells were subjected to immunoblotting utilizing the α-VHL$_{Mm}$ (CT) antibody. In both mouse cell lines the antibody specifically recognized the endogenous expression of two pVHL (Mm) forms defined as pVHL21 and pVHL25 (indicated by arrows). The migration of the detected endogenous bands was confirmed by overexpression of the Vhl proteins in transfection experiments (data not shown).
(B) At E17.5 pVHL expression was detectable among others in the ear, pancreas and lung (a, d, g). Pre-absorption of the α-pVHL$_{Mm}$ (CT) antibody with the CT-peptide (1mg/ml), which was originally used to create this antibody, showed strong competition of the signal (b, e and h), whereas pre-absorption with an NT-peptide as a negative control showed no competition (c, f and i).
(C) Strong pVHL expression at E17.5 was also detectable in the retina (left panel), where the signal could be abolished completely by pre-absorption of the antibody with the CT-peptide (1mg/ml) (right panel).
(D) pVHL expression in the retina was further confirmed by western blot in retinal whole cell extracts (lane 2). The shorter pVHL form (21kD) seemed less abundant than the longer form (25kD) in comparison to NIH3T3 whole cell extracts (lane 1).

2) Localization of VHL expression during murine developmental and adult retina

To determine pVhl expression at specific developmental stages during murine retinal development retinae from E10.5, E12.5, E14.5, E17.5, P0, P4, P8, P11, P16, P18 and adult animals were isolated, fixed in 10 % formalin, embedded in paraffin and sectioned at 12µm. Postnatal stages P0, P4, P11, P16 and adult are represented in figure 38. In the left panels negative controls omitting the primary antibody are shown, whereas on the right side sections stained with α-pVHL$_{Mm}$ (CT) can be seen.

pVHL expression was detectable throughout development, from early embryonic stages on until adulthood. During postnatal development the overall pVHL-staining in the retina started to delineate a more pronounced pattern that could be already noticed by P4. In adult animals pVHL localized to a defined specific structure.

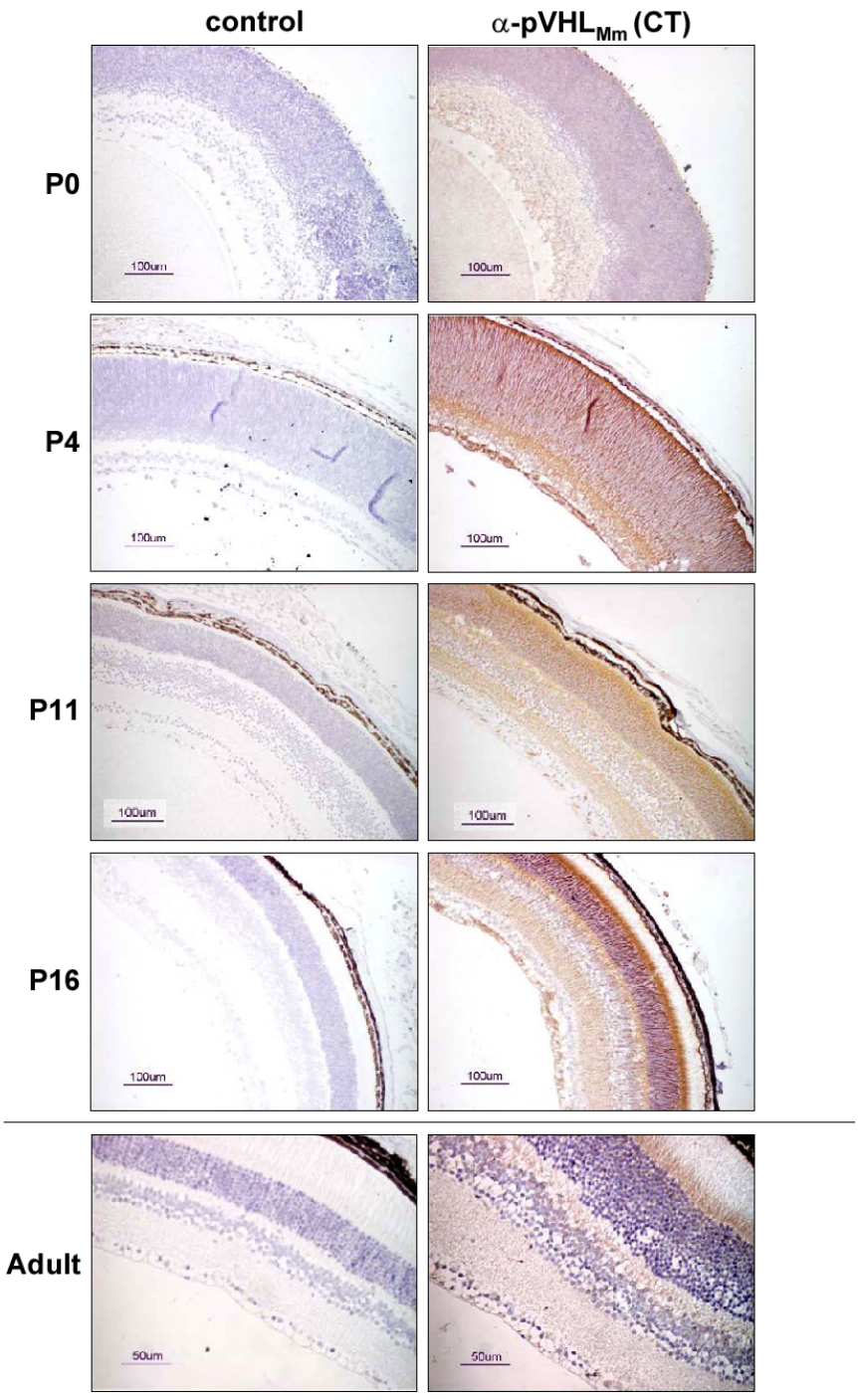

Figure 38. Localization of pVHL expression in the developing mouse retina. Mouse retina sections of different developmental time points (P0, P4, P11, P16 and adult) were counterstained with hematoxylin in the presence (right panels, right row) or absence (left panels, left row; CONTROL) of the primary α-pVHL$_{Mm}$ (CT) antibody. A strong VHL signal was detected throughout development and in adulthood. Scale bars are indicated.

To find out which specific cells towards the end of retinal development were expressing pVHL to such a high level, we performed immunofluorescence stainings on paraffin sections utilizing cell-specific markers (FIG. 39). At first strong pVhl expression was re-confirmed throughout development as shown at E17.5 (b) and P16 (c) [negative control with no primary antibody seen in (a)]. Utilizing a Rod specific marker, α-Rho4D2 (e), did not show any co-localization with the α-pVHL$_{Mm}$ (CT) (d) to the same set of cells (f) as did not markers for retinal pigment epithelium, amacrine cells, horizontal cells and bipolar cell (data not shown). Strong co-localization was though found with a monoclonal antibody against Glutamine synthetase, α-GS, a known marker for müller glial cells (g-i) and even further confirmed with another müller glia cell marker, namely α-CRALBP (k), that also co-localized with α-pVHL$_{Mm}$ (CT)(j) to the same cells (l).

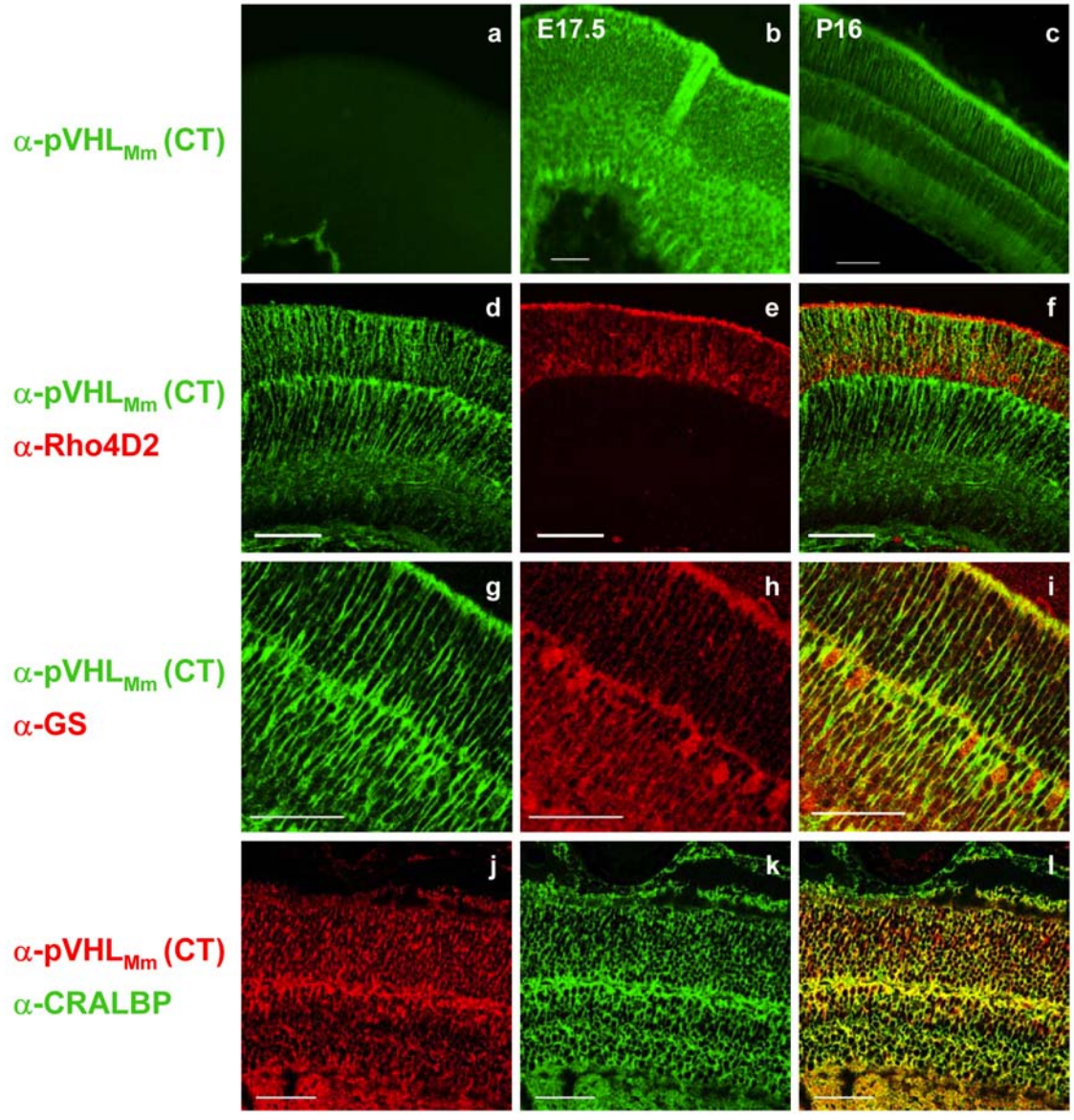

Figure 39. Immunofluorescent analysis of pVHL expression in the mouse retina by use of cell-specific markers.

Mouse retina sections were stained with α-pVHL$_{Mm}$ (CT) antibody and cell specific marker antibodies. (a- c) Immunostaining utilizing a FITC-conjugated secondary antibody in the presence or absence (a) of α-pVHL$_{Mm}$ (CT) as primary antibody confirmed strong pVhl expression in the retina as shown at E17.5 (b) and at P16 (c). (d-f) Co-staining of P9 retinae with α-pVHL$_{Mm}$ (CT) (d) and α-Rho4D2, a rod-specific marker (e) revealed no colocalization (f). (g-h) Co-staining of P7 retinae with α-pVHL$_{Mm}$ (CT) (g) and α-GS, a Müller glial cell-specific marker (h) revealed strong co-localization (i). (j-l) Vhl immunostaining at P12 (j) also coincides with another Müller glial cell marker, namely α-CRALBP(k), and confirms herewith its localization to this specific cell type. For all the shown stainings FITC- (GREEN) or Cy5-(RED) coupled secondary antibodies were used. Scale bar represents 50µm.

To confirm and further analyze the subcellular distribution of pVHL localization to Müller glial cells and to investigate whether additional cells also expressed pVHL, we isolated retinal cells from adult mice and stained the dissociated cells with α-pVHL$_{Mm}$ (CT) (FIG. 40). Also in this case strong pVHL expression could be noticed in specific cells (a,c,h) identifiable as Müller glia both by morphology (b,f) and by the use of two marker antibodies, α-GS (d) and α-Vimentin (i) that co-localized with α-pVHL$_{Mm}$ (CT) (e and j respectively). Strikingly among these dissociated retinal cells another cell type was stained with α-pVHL$_{Mm}$ (CT) (k,m) that did not stain for the Müller glial cell marker vimentin (l,,m)

.

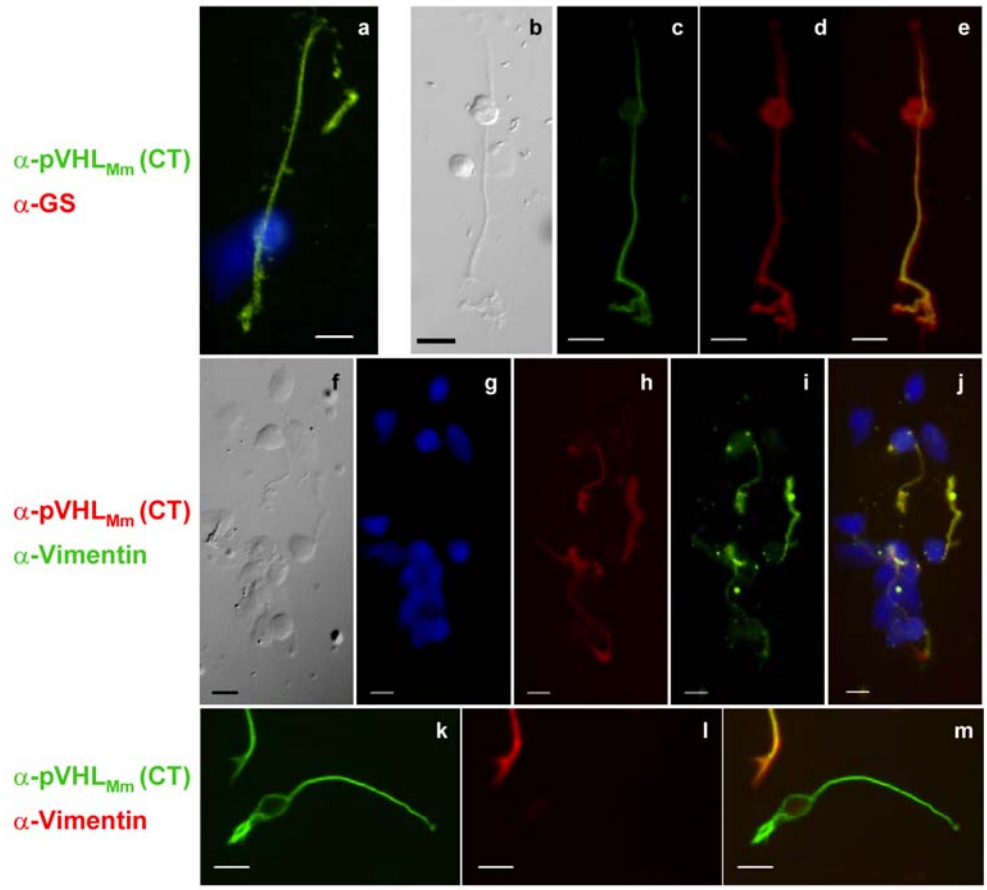

Figure 40. **pVHL is expressed predominantly in Müller glial cells, but also in another cell type.** Dissociated retinal cells from adult mice were stained with α-pVHL$_{Mm}$ (CT) and cell type specific markers. For all the shown stainings FITC- (GREEN) and/or Cy5-(RED) coupled secondary antibodies were used. pVhl expression localizes to specific cells (a,c,h) identifiable as Müller glia both by morphology (b,f) and by the use of two marker antibodies, α-GS (d) and α-Vimentin (i) that co-localize with α-pVHL$_{Mm}$ (CT) (e and j respectively) to the same cell. In addition another cell type stained for α-pVHL$_{Mm}$ (CT) (k,m) that did not stain for the Müller glial cell marker vimentin (l,m). Sections were counterstained with DAPI, shown in dark blue, to highlight position of nuclei. Scale bar represents 10 µm.

We conclude that pVhl is expressed in the murine retina throughout development and that at the later stages of development it localizes predominantly to Müller glial cells and to another yet-to-be-identified cell type. In addition we observed that pVHL expression in these cell types appears to be exclusively cytoplasmic.

3) Localization of VHL expression during murine cerebellar development

To investigate pVhl expression during murine cerebellar development, cerebella (FIG. 41) from P0, P7, P12, P16, P18, P21 and adult animals were isolated, fixed in 10 % formalin, embedded in paraffin, sectioned at 12 µm, stained with α-pVHL$_{Mm}$ (CT) and analyzed both by immunofluorescence utilizing FITC-conjugated secondary antibodies as well as by DAB staining. Postnatal development of the murine cerebellum revealed a particular pVHL expression that was confined predominantly to the outer parts of the cerebellar cortex (FIG.42, see white arrows).

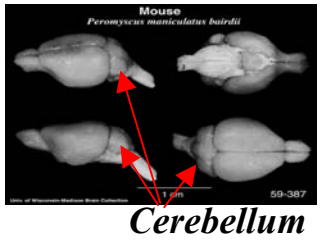

Figure 41. Position of the cerebellum.

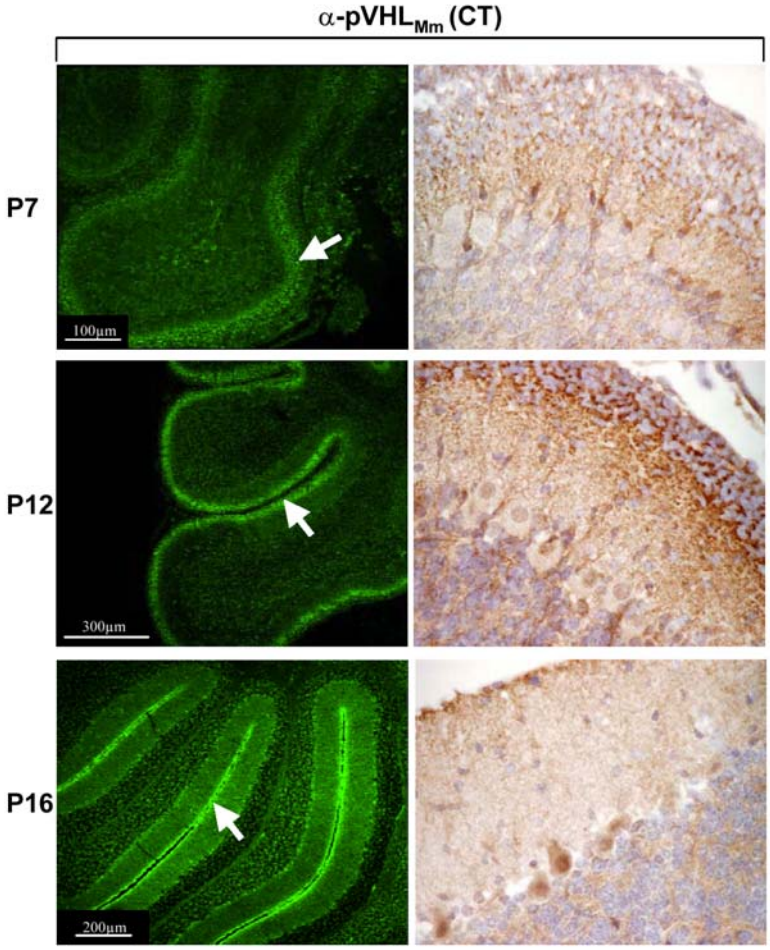

Figure 42. Localization of Vhl protein during postnatal development of the cerebellum. 12 µm thick sagittal sections of murine cerebella from P7, P12 and P16 were stained with α-pVHL$_{Mm}$ (CT) and analyzed both by immunofluorescence utilizing FITC-conjugated secondary antibodies (left panels) as well as by DAB staining counterstained with hematoxylin (high magnification view, right side). pVHL expression was confined predominantly to the outer parts of the cerebellar cortex (see white arrows).

The adult peripheral cerebellar cortex contains two principal neuronal subtypes, namely the Purkinje cells and the granule cells constituting the internal granular cell layer (IGL). The granule cells are derived from peripherally located mitotic or "cycling" cells in the external germinal layer (EGL) which after birth exit cell cycle, start differentiating and migrating along radial glia across the Purkinje cell layer to then settle and constitute the IGL. The inward migration of EGL cells continues approximately until P15 when the EGL disappears. The observed pVHL expression was localized to the molecular layer area and the EGL throughout development as specifically noticeable by P16 when only a thin stretch of VHL staining can be noticed on the very edge of the cerebellar foliae coinciding with the fact that by this developmental stage the EGL disappears.

The fact that pVHL has been shown to be expressed in CNS neuronal cell precursors and the specific change in position of Vhl expressing cells during cerebellar development made an involvement of progenitor cells likely. In order to identify the VHL-expressing cells immunofluorescent double-staining experiments were performed (FIG. 43).

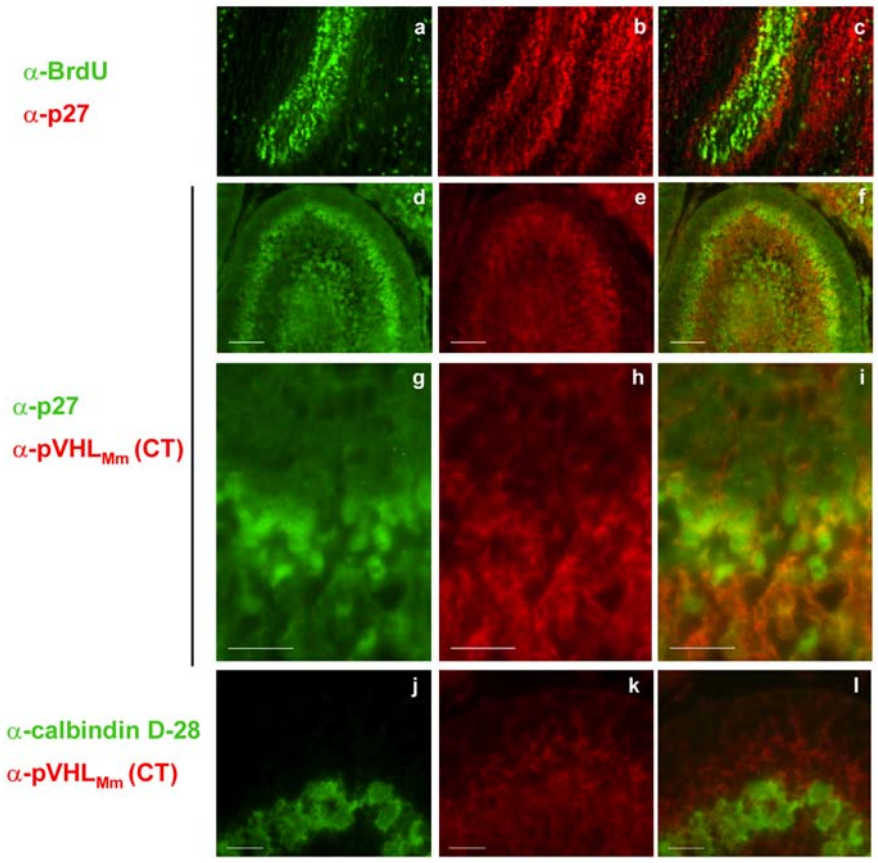

Figure 43. pVHL expression in the External Granular layer (EGL). Sagittal cerebellar sections were stained with α-pVHL$_{Mm}$ (CT) and markers of the cerebellar cortex. Proliferating GCP cells at P7 were highlighted by BrdU injection and subsequent staining for an BrdU antibody (a). Additional staining with α-p27 (b) confines p27 expression, as already shown, to postmitotic GCP and not colocalising with the BrdU signal (c). Staining P4 sagittal cerebellar section with α−p27 (d) and α-pVHL$_{Mm}$ (CT) (e) revealed pVHL expression in the same subset of cells in the EGL as α−p27 (f) as well as probably in adult granule cells (higher magnification view seen in g,h and i respectively). Staining sections with the Purkinje cell marker α-calbindin (j) and α- pVHL$_{Mm}$ (CT) (k) revealed no colocalization to the same cell (l) excluding VHL expression in Purkinje cells at this stage. Scale bar represents 50 µm (d-f) and 20 µm (g-l).

By marking mitotic cells at P7 in the EGL with BrdU (a) and staining additionally with p27 (b) we confirmed the well-documented fact that p27 is expressed in cells that have become postmitotic and therefore no colocalization could be seen (c). Staining P4 sagittal cerebellar section with α–p27 (d,g) and α-$pVHL_{Mm}$ (CT) (e,h) revealed that pVHL seems to be expressed in the same subset of cells in the EGL as p27 (f,i) as well as probably in adult granule cells. Staining sections with the Purkinje cell marker α-calbindin (j) and α- $pVHL_{Mm}$ (CT) (k) revealed no colocalization to the same cell (l) excluding VHL expression in Purkinje cells at this stage.

In summary we could show that pVHL expression during cerebellar development seems to be localized to a specific subset of granule cell precursors that have exited the cell cycle and are about to migrate. Whether Vhl expression persists in the migrating cells will have to be investigated further.

Chapter 9

Results

-Part Three-

Conditional inactivation of VHL in the mouse brain

-work in progress-

Based on the new finding, that VHL protein expression was strongly detectable during cerebellar and retinal development (chapter 8), and on the already proposed role for VHL in neuronal differentiation (Kanno *et al.*, 2000), we decided to investigate the role of the VHL tumour suppressor gene in neuronal precursor cells in the context of the CNS development.

In order to do so we took advantage of two already established mouse strains: the **VHL floxed/floxed (VHL$^{fl/fl}$)** mice (Haase *et al.*, 2001), which we had also tried to create (as shown in chapter 7), and transgenic mice that express the Cre recombinase under the control of the neuron-specific nestin promoter (***nes*-Cre**) (Tronche *et al.*, 1999). Nestin is an intermediate filament protein expressed predominantly in the neural progenitor cells during murine CNS development (Lendahl *et al.*, 1990) and in skeletal muscle. But in addition it can also be detected in the developing (neuro) retina around E12.5 (Yang *et al.*, 2000).

The VHL$^{fl/fl}$ mice contain on both alleles a loxP-flanked (floxed) exon 1, whereas the *nes*-Cre mice express Cre under the control of the rat nestin (*nes*) promoter and enhancer (FIG. 44)

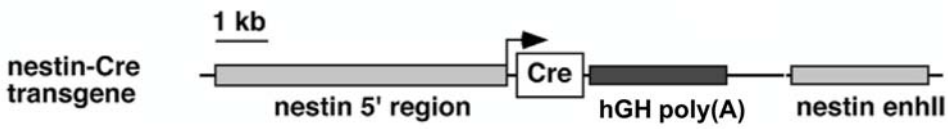

Figure 44. Structure of the nestin-Cre transgene. Cre recombinase was expressed under the control of the promoter and the nervous system-specific enhancer present in the second intron of the rat nestin gene. hGH poly(A), human growth hormone polyadenylation signal.

From Tronche *et al.*, 1999

Both mice strains had been shown to be viable and healthy and had been previously utilized in different conditional knockout experiments (Pfander *et al.*, 2004, Graus-Porta *et al.*, 2001; Haase *et al.*, 2001, Tronche *et al.*, 1999). In addition, the *nes*-Cre mice had been characterized by crossing them with a reporter mouse line that carries a Rosa26lacZ-loxP gene (where lacZ expression is induced by Cre-mediated recombination) showing efficient and widespread recombination in precursors of neurons and glia starting around embryonic day E 10.5 (Blaess *et al.*, 2004; Graus-Porta *et al.*, 2001).

1) Generation of nes-Cre; VHL$^{flox/flox}$ mutant mice

In a first breeding step VHL$^{fl/fl}$ mice were bred with *nes*-Cre mice in order to generate **nes-Cre; VHL$^{fl/+}$** mice (FIG. 45A). These mice were then bred again with VHL$^{fl/fl}$ and the offspring screened for the appearance of the nes-Cre; VHL$^{fl/fl}$ genotype (FIG. 45B). This genotype was then expected to lead to the excision of the floxed exon 1 of VHL only in

tissues where nestin was expressed. The genotype was determined by PCR on tail biopsies and the VHL status was assessed in addition by southern blot analysis (data not shown).

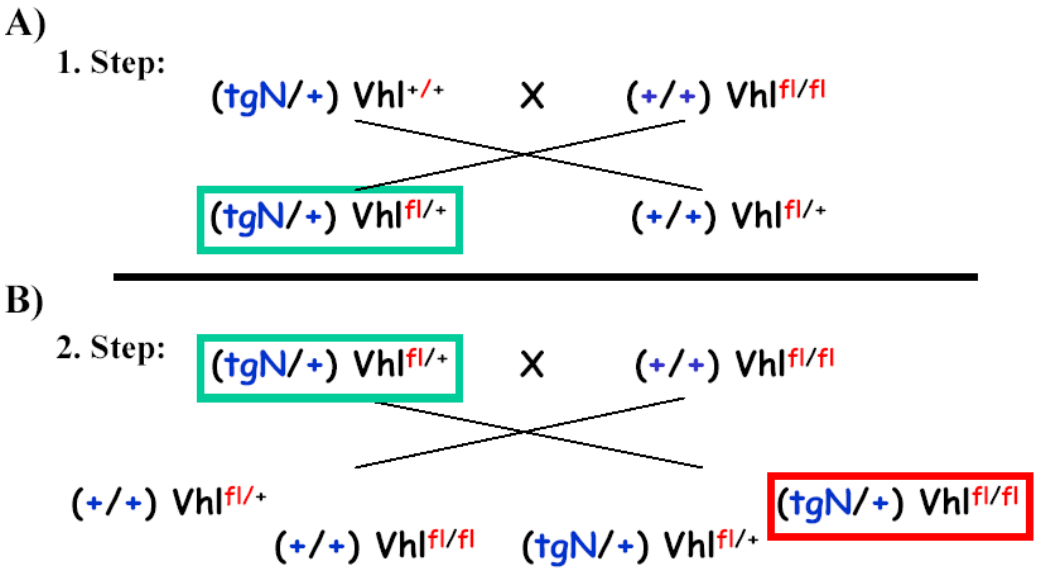

Figure 45. Schematic representation of the two breeding steps needed to obtain the *nes*-Cre; VHL$^{fl/fl}$ mouse. A) The *nes*-Cre mice are heterozygous, therefore the genotype is depicked as **tgN** (transgene Nestin) / + (for wildtype). By crossing a *nes*-Cre mouse with a VHL$^{fl/fl}$ mouse both **nes-Cre; VHL$^{fl/+}$** and **VHL$^{fl/+}$** mice were born at the expected mendelian frequency (1:1). **B)** By crossing the **nes-Cre; VHL$^{fl/+}$**, obtained in the first step, with **VHL$^{fl/fl}$** mice the conditional VHL knockout **nes-Cre;VHL$^{fl/fl}$** was obtained at a ratio of 1:4.

2) Mice that lack VHL in the nervous system show severe defects in brain development and die within a few hours after birth

As expected one out of four pups from a cross between nes-Cre; VHL$^{fl/+}$ and VHL$^{fl/fl}$ (FIG. 45B) had the genotype **nes-Cre;VHL$^{fl/fl}$** and the deletion of VHL in the nervous system led to death of newborn pups within a day after birth. The screening of the mice was performed by PCR analysis and an example is depicted in figure 46.

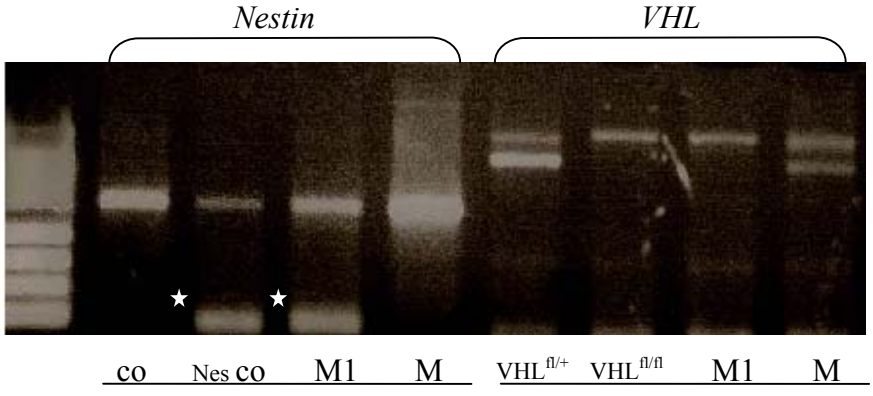

Figure 46. PCR analysis for VHL and Nestin status of mice. In this example (co) stands for genomic wt DNA, (Nes co) for a nes-Cre mouse DNA, (M1) was a dying mouse at PO, whereas (M2) was a mouse picked as a control within the same litter as M1. VHL$^{fl/fl}$ and VHL$^{fl/+}$ genomic DNA was used as control for the PCR investigating the VHL status. Stars represent the band of 100 bp for the nestin transgene. Concerning VHL the higher band of ? bp represents the floxed VHL DNA, whereas the smaller fragment of 500 bp comes from wt DNA. As can be clearly seen M1 is positive for the nestin transgene and in addition only shows the upper band for VHL, meaning that it is homozygous floxed. The expression of the transgene in a mouse with a floxed VHL gene leads to conditional inactivation of VHL in neuronal precursors. This though cannot be monitored by a PCR on tail biopsies, as there nestin will not be expressed.

To confirm that VHL expression had been really abolished in the brain of conditional knockouts, a Western Blot analysis on whole brain extracts was performed utilizing the α-$pVHL_{Mm}$ (CT) antibody, characterized in chapter 8. Different brain regions were in the first place examined for their normal VHL expression and were also compared to the VHL expression in the cerebellum and the forebrain of two mice which had been shown previously by PCR to be **nes-Cre;$VHL^{fl/fl}$** (FIG. 47).

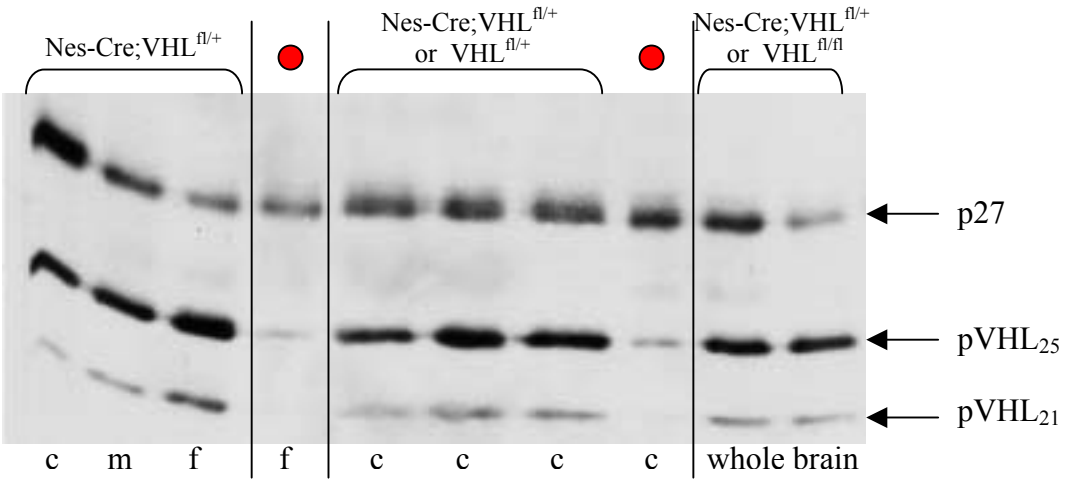

Figure 47. Western Blot analysis assessing pVHL expression in different brain compartments and comparing wildtype to mutant brains. 130µg whole cell extract were loaded onto a 12 %-SDS gel and subjected to immunoblotting with the α-$pVHL_{Mm}$ (CT) polyclonal antibody. The expression of both forms of VHL, $pVHL_{25}$ and $pVHL_{21}$, was detectable in all brain compartments of mice used as control (Nes-Cre;$VHL^{fl/+}$,$VHL^{fl/+}$ and $VHL^{fl/fl}$) . Overall the longer form, $pVHL_{25}$, seemed to be more abundant than the shorter form, $pVHL_{21}$. The VHL expression was dramatically reduced in parts of brains extracted from nes-Cre; $VHL^{fl/fl}$ mice (●). A faint band that is still detectable for the longer VHL form might arise from contamination from other tissue parts during preparation or from the fact that VHL might be expressed in other cell types that are not affected by nestin expression. p27-expression was tested as this has been shown to be present in differentiating granular precursors cells apparently co-localizing with pVHL expression. But no clear difference in the expression could be detected. F= forebrain, m=midbrain, c=cerebellum.

The expression of VHL was significantly reduced in the cerebellum and the forebrain of the two nes-Cre;$VHL^{fl/fl}$ mice tested, leading to the assumption that it was indeed the loss of VHL that caused the severe phenotype.

In order to investigate in more detail the brains of nes-Cre; $VHL^{fl/fl}$ mice whole brains were carefully removed from the scull the day of birth (P0) of the animals and the appearance of these "mutant" brains was compared to brains at P0 of wild-type C57BL/6, nes-Cre;$VHL^{fl/+}$ and $VHL^{fl/fl}$ mice (FIG. 48). Subsequently the brains were fixed in 10 % formalin and embedded in paraffin. 12 µm sections were cut and stained by immunofluorescence utilizing the α-$pVHL_{Mm}$ (CT) (FIG. 49) the HIF-1α or VEGF antibody (data not shown) or by simply staining with hematoxylin and eosin (FIG. 50).

When comparing the exterior appearance of the PO brains there were no phenotypic abnormalities noticeable in the whole structure (FIG. 48). However, the brains of nes-Cre;VHL$^{fl/fl}$ mice appeared slightly smaller and more vascularized as can be seen in figure 48B and 48C. It is nevertheless not clear whether this red colour and the vessels were not enhanced due to the stress of the death process that was ongoing in the moment the animals were euthanized

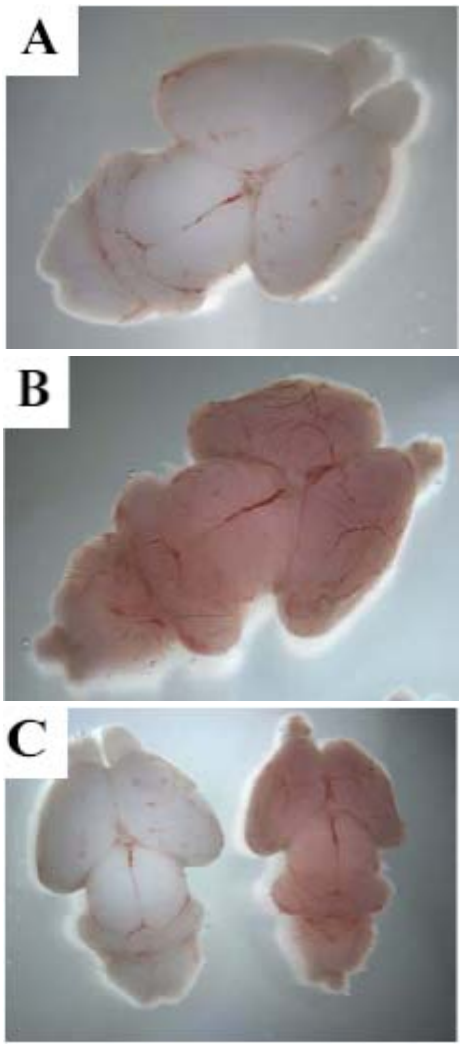

Figure 48. Comparison of wt brains at P0 with the conditional inactivated nes-Cre;VHL$^{fl/fl}$ **mice.** A) The brain of a wt mouse (or **nes-Cre;VHL$^{fl/+}$, VHL$^{fl/+}$ or VHL$^{fl/fl}$ mouse)** at PO appears whitish and some vessels can be distinguished. B) The brain of a nes-Cre;VHL$^{fl/fl}$ at PO presents itself as much more red in colour with strong highlighting of small vessels all over the brain. Besides the colour and the highlighted vessels the phenotypic appearance is though normal. C) When comparing directly a wt mouse with a nes-Cre;VHL$^{fl/fl}$ mouse the only noticeable additional difference, apart from the colour, is the size that seems to be slightly reduced in case of the nes-Cre;VHL$^{fl/fl}$ mice.

Before looking at the expression pattern of the VHL protein (pVHL) in the mutant brains the VHL expression was assessed at P0 (the day of birth) in the whole brain in order to obtain a reference. Up to that point we had been mainly interested in the cerebellum and had not looked at the rest of the brain that much and it was therefore very important to define whether there was localized expression of VHL in the rest of the brain. As shown in figure 49A, VHL expression at P0 seems to be ubiquitous in the brain, with enhanced staining at the periphery of the telencephalon, the hippocampus and the cerebellum (marked by arrowheads). There were no differences noticeable when comparing wt C57BL/6 brains with brains from nes-Cre;VHL$^{fl/+}$, VHL$^{fl/fl}$ or nes-Cre mice (data not shown). But when we compared pVHL expression in the brain of mutant nes-Cre;VHL$^{fl/fl}$ mice to the expression of pVHL in wt animals the first striking thing that was noticable was actually the severe brain abnormalities that could be seen in the overall structure. In addition there was also a strongly reduced VHL expression detectable especially in the outer regions of the brain mentioned before (FIG. 49).

As all these sites where enhanced VHL expression could be detected are developing strongly in the time frame around birth and as loss of VHL had such a severe impact on the

overall brain architecture, VHL seems to play a role somewhere in between the processes of proliferation, exit of cell cycle, migration and differentiation as already proposed by the result obtained from the expression study of VHL in the cerebellum and the retina.

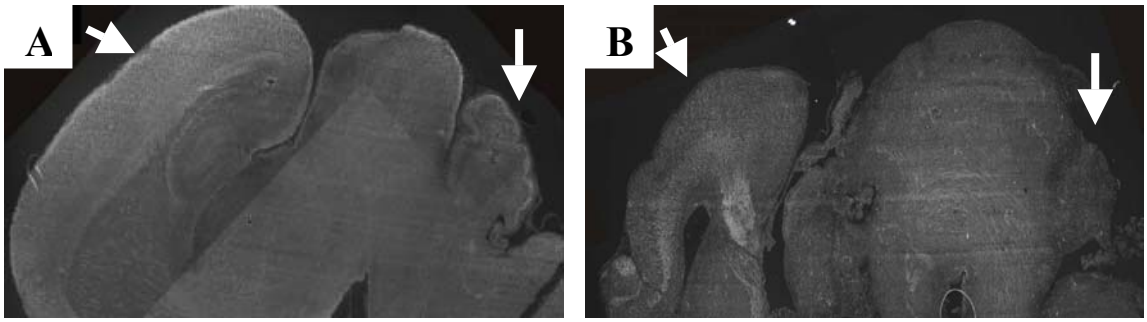

Figure 49. Brain section stained with α-pVHL$_{Mm}$ (CT). (A) VHL expression, as assessed by immunostaining utilising a mVHL-CT polyclonal antibody (see chapter 8), seems to be ubiquitous in wt mice at birth (PO). One can notice a strong expression of VHL on the outer borders of the cerebral and the cerebellar cortex (shown by arrows). B) The comparison of the brain at P0 of a nes-Cre;VHL$^{fl/fl}$ mouse with the wt brain depicted in A first of all shows much weaker overall VHL staining suggesting that the conditional inactivation of VHL has functioned properly. The signal was not expected to be lost completely as not all cell types are targeted by this conditional inactivation and there will still be residual VHL expression in these non-targeted cells or vessels. The two arrows point at the corresponding places in A) showing clearly that the brain development is somehow impaired in these mice leading in addition to open spaces within the brain.

In order to investigate in more detail the effect of VHL loss in the brain we focused on the telencephalon and the cerebellum. As seen in figure 50 the telencephalon of mutant nes-Cre;VHL$^{fl/fl}$mice (FIG. 50B) showed big holes which are ofter referred to in the literature as hydrocephalus, empty spaces probably filled by cerebrospinal fluid that upon fixation gets lost and appears as empty holes. In addition the outer layers seem to be thinner as in the wt control. Comparing the cerebella gives a similar picture: in the mutant mouse the cerebellum (FIG. 50D) seems to form but is perturbed and the surroundings again show larger holes and not the close compact structure seen in the wt (FIG. 50C).

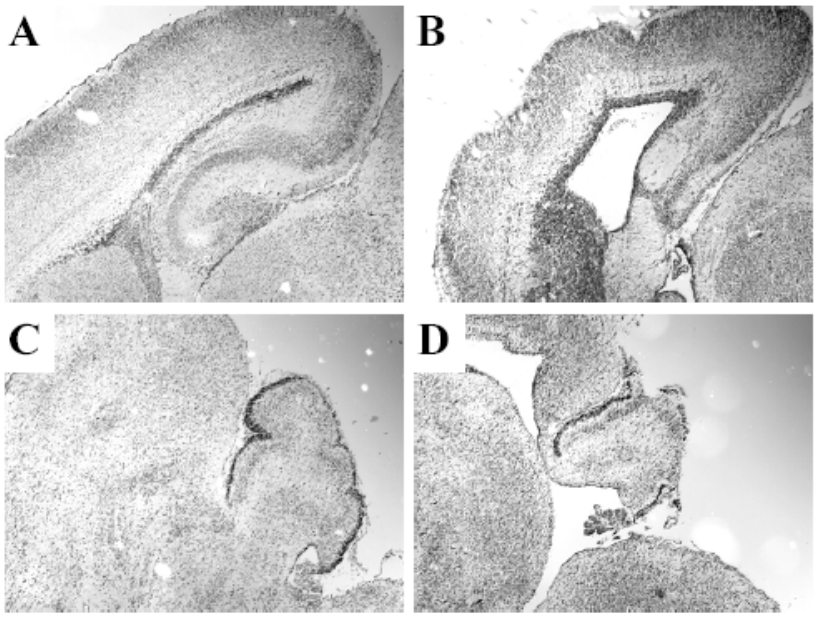

Figure 50. Hematoxylin and Eosin stainings of sagittal sections of the nes-Cre;VHL$^{fl/fl}$ brains in comparison to their wt control. A) and B) respresent a picture of the telencephalon with the hippocampal structure while C) and D) show the cerebellum and its surrounding. A) and C) are wt control whereas B) and D) represent a nes-Cre;VHL$^{fl/fl}$ brain. When comparing the telencephalons in A) and B) the difference is striking, showing that in the mutated brain the overall structure is perturbed and the same grade of perturbation can be seen also in the cerebellum.

3) Mice that lack VHL in the nervous system show a possible effect in the retina

As we had investigated VHL expression in the retina as well as in the cerebellum as part of this thesis it would have been interesting to specifically delete VHL in these cells. Unfortunately though due to the lack of a Mueller glia cell specific Cre-mouse we didn't have the chance to knock out VHL specifically in these cells. However, it was surprising to find that in one of the examined nes-Cre;$VHL^{fl/fl}$mice when we looked at the retina a strange involution could be noted that in addition stained positive for VHL. Now, it is known that Nestin is expressed specifically at E 12.5 in a part of the neuroretina, so it could be an effect of the deletion of VHL in the precursor cells. But this will have to be investigated further and will also need to be seen reproducibly. Nevertheless it is an interesting phenomenon.

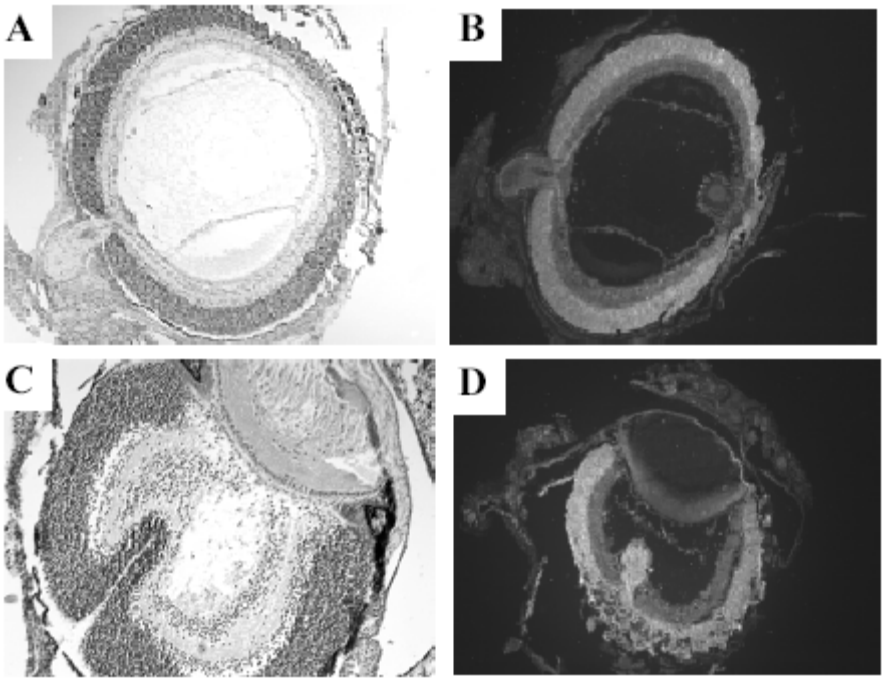

Figure 51. Hematoxylin /Eosin and pVHL staining of wt and mutant retinae. A) and B) represent a wt retina whereas C) and D) represent a mutant retina. A) and C) show Hematoxylin/Eosin stainings, while B) and D) depict pVHL expression as assessed by immunostaining with the α-$pVHL_{Mm}$ (CT) antibody. In the mutant brain an involution of the neuroretina can be seen that still seems to express VHL though.

In conclusion VHL seems to play a specific role during the development of the brain as loss of VHL, mimicked by a mouse model in which VHL was deleted specifically in neural precursor cells, leads to a severe brain phenotype and results ultimately in the death of newborns.

Chapter 10

Discussion and future perspectives

The most common lesions found in VHL disease include hemangioblastomas, which are neoplasms containing a mural nodule formed by noninvasive, vacuolated "stromal" cells of unknown origin that are embedded in a network of capillaries. VHL disease-associated hemangioblastomas can be found mainly in the retina and the cerebellum. Both lesions exhibit indistinguishable histological characteristics, with VHL loss restricted to stromal cells, suggesting that this is the neoplastic component. Given the central role of VHL in hypoxia signaling through regulation of HIF, these tumors consequently provide an *in vivo* view of HIF effects in a tumor.

Multiple mRNA expression studies, aiming at investigating VHL expression in tissues, have documented that VHL mRNA is present ubiquitously and not restricted only to tissues affected during the course of VHL disease. In addition immunolocalization studies utilizing poly- and mono-clonal VHL antibodies recognizing human pVHL additionally proved that the protein expression is not restricted to specific tissues either but can be found widespread, particularly within epithelial cells.

Although these studies provided an insight into pVHL expression in adult human tissues, so far no studies have addressed the issue of elucidating the VHL protein expression pattern and therefore its function during development. In addition, in-depth analysis of pVHL expression focusing in tissue-specific cell types e.g. in the retina was still pending. Knowing the identity of the cell that expresses VHL, and that is therefore prone to unforeseen misregulation by VHL loss, would definitely provide a better target for additional studies investigating cures or remedies for the disease.

To gain more insight into pVHL expression we decided to focus on two tissues that are heavily affected during the course of VHL disease, namely the retina and the cerebellum. We investigated the VHL protein expression in these two murine tissues during development and adulthood by immunostaining utilizing a newly characterized antibody that specifically recognizes murine pVHL.

pVhl expression in the retina was found throughout development. In addition, it was localized exclusively to a very specific cell type, the Müller glial cell, towards the end of development and in adulthood. As the so-called "stromal" cells in hemangioblastomas have

been hypothesized to be of glial cell origin, due to ultrastructural and immunohistochemical features (Lubinski *et al.*, 2003), the discovery that under normal conditions pVHL is expressed in the principal glial cell of the retina is striking.

Overall the finding that pVHL is expressed in retinal precursor cells and that its expression is unique to Müller glial cells in adult mice proves to be interesting for a variety of reasons:

First, the observed temporal expression pattern would suggest that VHL has some function during development, maybe even in directing glia differentiation. It has been shown that VHL plays a role in neuronal differentiation in the CNS (Murata *et al.*, 2002; Kanno *et al.*, 2000), but in these studies it was not linked to glial histogenesis. The finding that VHL expression is prominent in glial cells in the retina is though not really in contrast to these results in the CNS, because one has to keep in mind that VHL is already expressed throughout the retinal development in precursor cells, which are multipotent giving rise both to all the neurons and the glial cell type. Moreover it is likely that VHL anyway exerts different functions in different cell types.

The homeobox gene Chx10 has been shown to be expressed during development in most proliferating retinal cells. As cells exit the cell cycle, they downregulate Chx10 expression and shortly thereafter differentiating bipolar cells up-regulate and continue to express this protein again (Cunningham *et al.*, 2002). However, as a detailed analysis of the timing of the expression of Chx10 during cell cycle has not been carried out, it is thus not known whether Chx10 expression persists in a subset of retinal progenitor cells as they exit the cell cycle or if postmitotic neurons committed to becoming bipolar cells reinitiate expression as they differentiate. VHL follows a similar pattern of expression but being finally unique to the Müller glial cells. The expression of pVHL didn't seem to be always equally strong in retinal precursor cells as e.g. especially after/ around birth the signal intensity seemed to decrease (data not shown) and this time span is the one in which Müller glial cells are born together with bipolar cells and rods. It will be therefore interesting to have a closer look as to whether this phenomenon of signal reduction is reproducible. In addition by retroviral-mediated overexpression of VHL (coexpressed e.g. with GFP) in mitotic retinal progenitor cells one could monitor whether more cells become Müller glial cells. This would then confirm that VHL provides or relays a signal needed for specification to this cell type. When trying to unravel VHL function in this setting it will be necessary to find out which biological process is affected by VHL the most among proliferation (cell division/ multiplication), differentiation (into specialized retinal cell

types), and apoptosis (programmed cell death). Interestingly in the elegant survey focusing on the genomic analysis of mouse retinal development by serial analysis of gene expression (SAGE) VHL was not identified (Blackshaw *et al.*, 2004). However, in the same report they showed that mitotic retinal progenitor cells and Müller glia share a great degree of transcriptional overlap. Of the genes being specifically expressed in MG during the first postnatal week 68 % were found to be also enriched in mitotic progenitor cells. These two cell types resemble each other morphologically and based on the extensive overlap in gene expression it is interesting to speculate to which degree they also share a functional similarity. Müller glia are one of the last cell types to exit mitosis (Reh and Levine, 1998) and they are the only cell type in the mature retina that can reenter mitosis following retinal injury (Dyer and Cepko, 2000; Vetter and Moore, 2001). Moreover, data from chicken suggest that Müller glia can be induced to divide and give rise to some types of retinal neurons for a short period of time near the end of retinal development (Fischer & Reh, 2001). All these facts actually lead to the interesting, even more challenging question as to whether Müller glia are fundamentally multipotent progenitor cells that are simply quiescent regarding cell division and the production of neurons. Given the well-documented role of VHL in the control of gene expression primarily through HIF regulation and potentially other effectors, and the coupling of glial cell fate with specific gene expression patterns, it would be of interest to investigate the contribution of VHL-mediated gene expression in these processes.

Second, the fact that VHL is expressed solely in the Müller glial cells provides a model cell type in which to further analyze VHL function. Hypoxia has been shown to induce VEGF and TGF-β expression of Müller glial cells leading to neovascularization fitting therefore to the current knowledge about VHL: both VEGF and TGF-β are HIF target genes and HIF is active under hypoxia but normally degraded by VHL under normoxia. Interestingly it has been shown that p27 expression, which has been postulated to be linked to VHL expression by a yet unknown mechanism, is also restricted to the nucleus of müller glial cells in the adult retina. In addition, the fact that Mueller glia play a major role in every single disease or injury associated with the retina by initiating a process called reactive gliosis calls for further investigations of VHL expression in this context. Müller cell gliosis is characterized by a downregulation of p27 levels, by proliferation, changes in cell shape due to alterations in intermediate filament production and by secretion of signaling molecules such as VEGF, promoting neovascularisation in the surroundings. This setting now provides a great model system to unravel the role that VHL

plays in the retina. Our next aim is to further investigate whether reactive gliosis has an effect on VHL expression. This process can be induced by intraocular injections of ouabain utilizing subsequently immunostaining to monitor the changes in expression levels (Dyer & Cepko, 2000). It will be exciting to see whether the VHL pathway is downregulated in these cases because if this were the case one could envision a model of how actually hemangioblastomas could arise: Changes in the cellular redox status and the production of reactive oxygen species are associated with retinal injury. Under such conditions, it is likely that downstream VHL effectors are differentially modified thus evading destruction by the E3 ligase function of the protein. Such downregulation of the VHL pathway during the process of reactive gliosis would probably create a condition similar to that encountered in case of VHL loss due to mutation. The Müller glial cells would start proliferating again, probably expressing glial markers at the beginning, but then switching more to precursor markers again (that would explain the fact that there are controversial data regarding the markers expressed by stromal cells) and neovascularization would occur due e.g. to the expression of VEGF. Whether in reality it is as simple as this model would suggest the near future will tell.

As opposed to the retina, in the cerebellum we could show that pVHL expression seems to be localized to a specific subset of cells during development, whereas in adulthood the expression appeared more ubiquitously and overall reduced. Localizing pVHL expression to the non-proliferating subset of granule cell precursors is in complete accordance to an already proposed function of VHL in neuronal differentiation and is therefore not surprising. In addition some facts even further encourage the idea of a specific role played by VHL in these cells at that particular stage:

1) p27 expression has been shown to be high in GCP cells that have exited the cell cycle (Miyazawa *et al.*, 2000). Based on a proposed link between VHL and the cell cycle it is interesting to see that both in the retina and in the cerebellum VHL and p27 seem to be expressed in the same subset of cells. Whether this correlation translates into a true link at the molecular level needs further investigation. With regards to this, we are currently crossing floxed VHL mice with p27-/- mice to then delete VHL specifically in the brain by using again the Nestin-Cre mice discussed further down. As p27-/- mice have been shown to have enlarged organs (Fero *et al.*, 1996) including a larger cerebellum (Miyazawa *et al.*, 2000), it will be interesting to see whether knocking out VHL specifically in the brain reverts this phenotype or not.

2) expression of Cyclin D1 (or the brain-specific cyclin D2), which has been shown to be negatively regulated by VHL (Bindra *et al.*, 2002; Zatyka *et al.*, 2002), drops in postmitotic granule cell precursors.
3) CXCR4 expression, which is regulated by HIF that in turn is regulated by VHL (Staller *et al.*, 2003), has been shown to be present in proliferating granule cell precursors where it plays a role together with its ligand SDF1 (expressed from pial cells) to enhance the SHH-induced proliferation of granule cell precursors (Lewis *et al.*, 2004; Dahmane & Altaba, 1999). CXCR4 mRNA expression peaks in the first two postnatal weeks and from localization studies it seems that CXCR4 protein is localized only to the outer part of the EGL and not in the VHL expressing postmitotic GCPs. All these facts sustain a possible role for VHL in these precursor cells, due to the fact that it should not be possible for VHL and CXCR-4 to be expressed in the same cell type assuming that for CXCR4 expression on the membrane, HIF needs to be present and active. Maybe absence of CXCR4 expression due to the presence of VHL could even lead to the start of differentiation of granule cells (if the proliferation-driving signal provided by SHH is not sufficient).

The possible role of VHL played during differentiation in the cerebellum though, does still not explain what could happen in an adult cerebellum when lower VHL expression occurs.

In conclusion of the expression studies, the observed VHL expression during retinal and cerebellar development substantiates a previously suggested role of VHL in differentiation. The fact that VHL seems to be localized to glial cells in the retina while being present in neuronal cells is not in contrast as we could show that VHL is present throughout the retinal genesis in the precursor cells which are multipotent and can therefore generate glia and neuronal cells. In accordance to this, it is assumed that VHL exerts different functions in different tissues. This must be the case as it would be otherwise not explicable why despite widespread VHL expression only a small subset of organs are affected during the course of VHL disease. This assumption is further substantiated by the newly ascribed function of microtubule stabilisation to VHL (Hergovich *et al.,* 2003) which, however, despite the implications for a disease-type specific connection to particular VHL functions, is still pending evidence for a physiological role *in vivo*. Finally, the identification of Müller glia as the primary Vhl-expressing cell type in the adult retina provides a firm basis for the elucidation of the pathophysiological and molecular mechanisms that give rise to the observed VHL disease phenotypes.

A part of this thesis was dedicated to the creation of a conditional VHL knockout mouse model. The aim was to create a floxed VHL mouse, where exon 1 of the VHL gene would have been flanked by two loxP elements. This would have then allowed, by crossing these animals with cre-expressing mice, an excision of exon 1 leading therefore to the loss of VHL in the cre-expressing tissues. When this project was initiated in the year 2000 the only published report concerning a mouse model for VHL disease was the complete knockout that led to the death of the pups very early in gestation. Due to the lack of possibility to study VHL function more extensively in these mice the creation of floxed mice would have been a major achievement. During the course of this knockout project a conditional VHL knockout was though published by another laboratory (Haase *et al.*, 2001). Although this was a major adversity at that time, we decided nevertheless to continue in our intent because of the following: The complete knockout published by Gnarra in 1997 had shown that homozygous deletion of VHL in C57BL/6 mice led to vascular abnormalities in the placenta leading to the death of the embryos at 10-12.5 days of gestation. The conditional knockout published by Haase inactivated VHL in BALB/c mice. Comparing the heterozygous VHL mice showed that while the heterozygous VHL C57BL/6 mice didn't show any phenotype, heterozygous VHL mice on a BALB/c background developed hepatic hemangiomas. Reports in the literature have suggested that mouse models for human disease may develop variable phenotypes depending on the strain background, possibly due to the presence of polymorphic variants in certain modifier genes in some strain. As a recent example: the creation of a VHL conditional knockout mouse model on a C57BL/6 background was described which developed liver angiomas in 100% of animals within one year (Ma *et al.*, 2003). When this phenotype development was compared in different strains by introducing the VHL deleted allele also in BALB/c and A/J mouse strains a remarkable increase in development of hepatic vascular lesions was observed. Coming back to our original aim, we wanted to create a conditional knockout in the C57BL/6 background. Unfortunately though it proved to be impossible maybe due to unforeseen recombination events happening in the clones or due to adverse culturing conditions. It is also possible that the clone 117, which we picked for the second transfection, had a wild-type ES-cell contamination. However, at that point, given the availability of floxed VHL mice, we decided to use the information gained by our expression studies in the cerebellum to investigate the function of VHL in the central nervous system (No Müller glial cell specific Cre-strain exists so far). In order to do so a conditional knockout mouse was generated with the Cre/loxP system utilizing a nestin promoter-based neural precursor-specific Cre

recombinase. The thesis presented herein documents that neural cell-specific ablation of the VHL gene in mice leads to severe brain structure abnormalities resulting in premature death occurring shortly after birth. These are preliminary data from an ongoing study that needs further investigation as to HIF-1α- or related target genes expression levels either by immunostaining or by RT-PCR. Interestingly, in knockout animals of Hif-1α, which has been shown to be expressed in the brain, a brain phenotype was also encountered that resembles the one we found (Tomita *et al.*, 2003; Jain *et al.*, 1998; Ryan *et al.*, 1998). This phenotype is defined as hydrocephalus, the term coming from the greek words 'hydro' meaning water and 'cephalus' meaning head. The hydrocephalus is an abnormal build-up of cerebrospinal fluid in the brain. In sections it is recognizable by empty spaces as the one noticeable in figure 50. Based on our current knowledge VHL and HIF protein expression should be mutually exclusive. Furthermore, it is more and more appreciated that oxygen may act as a morphogen in neural tissues in that localised fluctuations in oxygen levels drive specific transcriptional programs (Acker & Acker, 2004; Sharp & Bernaudin, 2004). Given the similarities in the phenotypes of the two knock-out mice one could envision that differential VHL expression in the brain may create an antagonistic environment between high and low VHL-expressing cells, with varying responsiveness to surrounding oxygen levels and as such comprising a driving force in the differentiation of these brain compartments.

In addition the layers of the telencephalon in the VHL knockout mouse seemed to be smaller in size leading to the assumption of a probable effect of VHL on cell proliferation. In this case this would mean that VHL actually promotes proliferation. And therefore this finding would add up to the accumulating contrasting reports evaluating the effect of VHL on the cell cycle (see also the latest mouse model where VHL was knocked out in all cartilaginous elements to investigate its role in endochondral bone development (Pfander *et al.*, 2004). Given that these observations are still at a preliminary stage of investigation it would be premature to provide a definite answer as to which effect VHL exerts but our ongoing studies of the observed severe brain phenotype are warranted to elucidate novel functions associated with this interesting tumour suppressor.

References

Acker T. and Acker H. (2004). Cellular oxygen sensing need in CNS function: Physiological and pathological implications. J Exp Biol 207: 3171-3188.

Adryan B., Decker H.H., Papas T.S. and Hsu T. (2000). Tracheal development and the von Hippel-Lindau tumor suppressor homolog in *Drosophila*. Oncogene 19: 2803-2811.

Ahmad I., Dooley C.M., Thoreson W.B., Rogers J.A. and Afiat S. (1999). In vitro analysis of a mammalian progenitor that gives rise to neurons and glia. Brain Res 831: 1-10.

Aso Y., Yamazaki K., Aigaki T. and Kitajima S. (2000). *Drosophila* von Hippel-Lindau tumor suppressor complex possesses E3 ubiquitin ligase activity. Biochem Biophys Res Commun 276: 355-361.

Barry R.E. and Krek W. (2004). The von Hippel-Lindau tumour suppressor: a multi-faceted inhibitor of tumourigenesis. Trends Mol Med 10: 466-472.

Ben-Arie N., Bellen H.J., Armstrong D.L., McCall A.E., Gordadze P.R., Guo Q., Matzuk M.M. and Zoghbi H.Y. (1997). Math1 is essential for genesis of cerebellar granule neurons. Nature 390: 169-172.

Beroud B.U., Joly D., Gallou C., Staroz F., Orfanelli M.T. and Junien C. (1998). Software and database for the analysis of mutations in the VHL gene. Nucleic Acids Res. 26: 256-258.

Berra E., Benizri E., Ginouves A., Volmat V., Roux D. and Pouyssegur J. (2003). HIF prolyl-hydroxylase 2 is the key oxygen sensor setting low steady-state levels of HIF-1α in normoxia. EMBO J 22: 4082-4090.

Bindra R.S., Vasselli J.R., Stearman R., Linehan W.M. and Klausner R.D. (2002). VHL-mediated hypoxia regulation of cyclin D1 in renal carcinoma cells. Cancer Res 62: 3014-3019.

Bishop T., Lau K.W., Epstein A.C.R., Kim S.K., Jiang M., O'Rourke D., Pugh C.W., Gleadle J.M., Taylor M.S., Hodgkin J. and Ratcliffe P.J. (2004). Genetic analysis of pathways regulated by the von Hippel-Lindau tumor suppressor in *Caenorhabditis elegans*. PloS Biol 2: e289.

Blackshaw S.,Harpavat S., Trimarchi J., Cai L., Huang H., Kuo W.P., Weber G., Lee K., Fraioli R.E., Cho S., Asch E., Ohno-Machado L., Wong W.H. and Cepko C.L. (2004). Genomic Analysis of Mouse Retinal Development. PloS 2: e247.

Blackshaw S, Fraioli R.E., Furukawa T. and Cepko C.L. (2001) Comprehensive analysis of photoreceptor gene expression and the identification of candidate retinal disease genes. Cell 107: 579-589.

Blaess S., Graus-Porta D., Belvindrah R., Radakovits R., Pons S., Littlewood-Evans A., Senften M., Guo H., Li Y., Miner J.H., Reichardt L.F. and Mueller U. (2004). β1-integrins are critical for cerebellar granule cell precursor proliferation. J Neurosci 24: 3402-3412.

Blankenship C., Naglich J., Whaley J., Seizinger B. and Kley N. (1999). Alternate choice of initiation codon produces a biologically active product of the von Hippel Lindau gene with tumor suppressor activity. Oncogene 18: 1529-1535.

Bradley A., Evans M., Kaufman M.H. and Robertson E. (1984). Formation of germ-line chimaeras from embryo-derived teratocarcinoma cell lines. Nature 309: 255-256.

Brieger J., Weidt E.J., Schirmacher P., Storkel S., Huber C. and Decker H.J. (1999). Inverse regulation of vascular endothelial growth factor and VHL tumour suppressor gene in sporadic renal cell carcinomas is correlated with vascular growth: an *in vivo* study on 29 tumours. J Mol Med 77: 505-510.

Bringmann A. and Reichenbach A. (2001). Role of Mueller Cells in Retinal Degenerations. Frontiers in Biosciences 6: 77-92.

Bruick, R.K. and McKnight S.L. (2001). A conserved family of prolyl-4-hydroxylases that modify HIF. Science 294: 1337-1340.

Brusselmans K., Bono F., Maxwell P., Dor Y., Dewerchin M., Collen D., Herbert J.M. and Carmeliet P. (2001). Hypoxia-inducible factor 2-α (HIF-2α) is involved in the apoptotic response to hypoglycemia but not to hypoxia. J Biol Chem 276: 39192-39196.

Capecchi M.R. (1989). Altering the genome by homologous recombination. Science 244: 1288-1292.

Capecchi M.R. (1989). The new mouse genetics: altering the genome by gene targeting. Trends Genet 5: 70-76.

Cepko C.L., Austin C.P., Yang X., Alexiades M. and Ezzeddine D. (1996). Cell fate determination in the vertebrate retina. Proc Natl Acad Sci USA 93: 589-595

Chizkow V. and Millen K.J. (2003). Development and malformations of the cerebellum in mice. Mol Gen Met 80: 54-65.

Choyke P.L., Glenn G.M., Wagner J.P. *et al.*(1997). Epididymal cystadenomas in von Hippel-Lindau disease. Urology 49: 926-931.

Choyke P.L., Glenn G.M., Walther M.M., Patronas N.J., Linehan W.M. and Zbar B. (1995). Von Hippel-Lindau disease: genetic, clinical, and imaging features. Radiology 194: 629-642.

Clifford S.C., Cockman M.E., Smallwood A.C., Mole D.R., Woodward E.R., Maxwell P.H., Ratcliffe P.J. and Maher E.R. (2001). Contrasting effects of HIF-1-α regulation by disease-causing pVHL mutations correlate with patterns of tumourigenesis in von Hippel-Lindau disease. Hum Molec Genet 10: 1029-1038.

Cohen H., Zhou M., Welsh A., Zarghamee S., Scholz H., Mukhopadhyay D., Kishida T., Zbar B., Knebelmann B. and Sukhatme V. (1999). An important von Hippel-Lindau tumor suppressor domain mediates Sp1-binding and self-association. Biochem Biophys Res Commun 266: 43-50.

Corless C.L., Kibel A., Iliopoulos O. and Kaelin W.G. Jr (1997). Immunostaining of the von Hippel-Lindau gene product (pVHL) in normal and neoplastic human tissues. Hum Pathol 28: 459-464.

Corn P.G., McDonald E.R., Herman J.G. and El-Deiry W.S. (2003). Tat-binding protein-1, a component of the 26S proteasome, contributes to the E3 ubiquitin ligase function of the von Hippel-Lindau protein. Nat Genet 35: 229-237.

Cotta-de-Almeida V., Schonhoff S., Shibata T., Leiter A. and Snapper S.B. (2003). A New method for rapidly generating gene-targeting vectors by engineering BACs through homologous recombination in bacteria. Genome Res 32: 2190-2194.

Crossey P.A., Foster K., Richards F.M., Phipps M.E., Latif F., Tory K., Jones M.H., Bentley E., Kumar R., Lerman M.I., Zbar B., Affara N.A., Ferguson-Smith M.A. and Maher E.R. (1994). Molecular genetic investigations of the mechanism of tumourigenesis in von Hippel-Lindau disease: analysis of allele loss in VHL tumours. Hum Genet 93: 53-58.

Cunningham J.J., Levine E.M., Zindy F., Goloubeva O., Roussel M.F. and Smeyne R.J. (2002). The cyclin-dependent inhibitors p19Ink4d and p27Kip1 are coexpressed in select retinal cells and act cooperatively to control cell cycle exit. Mol Cell Neurosci 19: 359-374.

Dahmane N. and Altaba A.R. (1999). Sonic hedgehog regulates the growth and patterning of the cerebellum. Development 126: 3089-3100.

Davidowitz E.J., Schoenfeld A.R. and Burk R.D. (2001). VHL induces renal cell differentiation and growth arrest through integration of cell-cell and cell-extracellular matrix signalling. Mol Cell Biol 21: 865-874.

Deng C. and Capecchi M.R. (1992). Reexamination of gene targeting frequency as a function of the extent of homology between the targeting vector and the target locus. Mol Cell Biol 12: 3365-3371.

Duan D.R., Pause A., Burgess W.H., Aso T., Chen D.Y.T., Garrett K.P., Conaway R.C., Conaway J.W., Linehan W.M. and Klausner R.D. (1995). Inhibition of transcription elongation by the VHL tumor suppressor protein. Science 269: 1402-1406.

Dyer M.A. and Cepko C.L. (2001) $p27^{Kip1}$ and $p57^{Kip2}$ regulate proliferation in distinct retinal progenitor cell populations. J Neurosci 21: 4259-4271.

Dyer M.A. and Cepko C.L. (2001). Regulating proliferation during retinal development. Nat Rev Neurosci 2: 333-342.

Dyer M.A. and Cepko C.L. (2000). Control of Mueller glial cell proliferation and activation following retinal injury. Nat Neursci 3: 873-880.

Dymecki S.M. (1996). FLP recombinase promotes site-specific DNA recombination in embryonic stem cells and transgenic mice. Proc Natl Acad Sci USA 93: 6191-6196.

Eichler W., Kuhrt H., Hoffmann S., Wiedemann P. and Reichenbach A. (2000). VEGF release by retinal glia depends on both oxygen and glucose supply. Neuroreport 11: 3533-3537.

Epstein A.C., Gleadle J.M., McNeill L.A., Hewitson K.S., O'Rourke J., Mole D.R., Mukherji M, Metzen E., Wilson M.I., Dhanda A., Tian Y.M., Masson N., Hamilton D.L., Jaakola P., Barstead R., Hodgkin P.H., Pugh C.W., Schofield C.J. and Ratcliffe P.J. (2001). C. elegans EGL-9 and mammalian homologs define a family of dioxygenases that regulate HIF by prolyl hydroxylation. Cell 107: 43-54.

Esteban-Barragan M.A., Avila P., Alvarez-Tejado M., Gutierrez M.D., Garcia-Pardo A., Sanchez-Madrid F. and Landazuri M.O. (2002). Role of the von Hippel-Lindau tumor suppressor gene in the formation of β1-integrin fibrillar adhesions. Cancer Res 62: 2929-2936.

Evans M.J. and Kaufmann M.H. (1981). Establishment in culture of pluripotential cells from mouse embryos. Nature 292: 154-156.

Feldman D., Thulasiraman V., Ferreyra R. and Frydman J. (1999). Formation of the VHL-elonginBC tumor suppressor complex is mediated by the chaperonin TRiC. Mol Cell 4: 1051-1061.

Fero M.L., Rivkin M., Tasch M., Porter P., Carow A.E., Firpo E., Polyak K., Tsai J., Broudy V., Perlmutter R.M., Kaushansky K. and Roberts J.M. (1996). A syndrome of multiorgan hyperplasia with features of gigantism, tumourigenesis, and female sterility in $p27^{Kip1}$-deficient mice. Cell 85: 733-744.

Fischer A.J. and Reh T.A. (2003). Potential of Mueller Glia to become Neurogenic Retinal Progenitor Cells. Glia 43: 70-76.

Fischer A.J. and Reh T.A. (2001). Mueller glia are a potential source of neural regeneration in the postnatal chicken retina. Nat Neurosci 4: 247-252.

Furukawa T., Mukherjee S., Bao Z., Morrow E.M. and Cepko C.L. (2000). Rax, Hes1, and notch1 promote the formation of Mueller glia by postnatal retinal progenitor cells. Neuron 26: 383-394.

Furukawa T., Morrow E.M. and Cepko C.L. (1997). Crx, a novel otx-like homeobox gene, shows photoreceptor-specific expression and regulates photoreceptor differentiation. Cell 91: 531-541.

Gao J., Naglich J.G., Laidlaw J., Whaley J.M., Seizinger B.R. and Kley, N. (1995). Cloning and characterization of a mouse gene with homology to the human von Hippel-Lindau disease tumor suppressor gene: implications for the potential organization of the human von Hippel-Lindau gene. Cancer Res 55: 743-747.

Giordano F.J. and Johnson R.S. (2001). Angiogenesis: the role of the microenvironment in flipping the switch. Curr. Opin. Genet. Dev. 11: 35-40.

Gnarra J.R., Ward J.M., Porter F.D., Wagner J.R, Devor D.E., Grinberg A., Emmert-Buck M.R., Westphal H., Klausner R.D. and Linehan W.M. (1997). Defective placental

vasculogenesis causes embryonic lethality in VHL-deficient mice. Proc Natl Acad Sci USA 94: 9102-9107.

Gnarra J.R., Zhou S., Merrill M.J., Wagner J., Krumm A., Papavassiliou E., Oldfield E.H., Klausner R.D. and Linehan W.M. (1996). Post-transcriptional regulation of vascular endothelial growth factor mRNA by the VHL tumor suppressor gene product. Proc Natl Acad Sci USA 93: 10589-10594.

Gnarra J.R., Tory K., Weng Y., Schmidt L., Wei M.H. *et al.* (1994). Mutations of the VHL tumour suppressor gene in renal carcinoma. Nat Genet 7: 85-90.

Goda N., Ryan H.E., Khadivi B., McNulty W., Rickert R.C. and Johnon R.S. (2003). Hypoxia-inducible factor 1α is essential for cell cycle arrest during hypoxia. Mol Cell Biol 23: 359-369.

Goldowitz D. and Hamre K. (1998). The cells and molecules that make a cerebellum. TINS 21: 375-382.

Graus-Porta D., Blaess S., Senften M, Littlewood-Evans A., Damsky C., Huang Z., Orban P., Klein R., Schittny J.C. and Mueller U. (2001). β-1 integrins regulate the development of laminae and folia in the cerebral and cerebellar cortex. Neuron 31: 367-379.

Groulx I., Bonicalzi M. and Lee S. (2000). Ran-mediated nuclear export of the von Hippel-Lindau tumor suppressor protein occurs independently of its assembly with cullin-2. J Biol Chem 275: 8991-9000.

Haase V.H., Glickman J.N., Socolovsky M. and Jaenisch R. (2001). Vascular tumours in livers with targeted inactivation of the von Hippel-Lindau tumor suppressor. Proc Natl Acad Sci USA 98: 1583-1588.

Hamre K.M and Goldowitz D. (1997). meander tail acts intrinsic to granule cell precursors to disrupt cerebellar development: analysis of meander tail chimeric mice. Development 124: 4201-12.

Hansen W., Ohh M., Moslehi J., Kondo K., Kaelin W.G. Jr and Welch W. (2002). Diverse effects of mutations in exon II of the von Hippel-Lindau (VHL) tumor suppressor gene on the interaction of pVHL with the cytosolic chaperonin and pVHL-dependent ubiquitin ligase activity. Mol Cell Biol 22: 1947-1960.

Hatten M.E. (1999). Central nervous system neuronal migration. Annu Rev Neurosci 22: 511-539.

Hergovich A., Lisztwan J., Barry R., Ballschmieter P. and Krek W. (2003). Regulation of microtubule stability by the von Hippel-Lindau tumour suppressor protein pVHL. Nat Cell Biol 5: 64-70.

Hoffman M.A., Ohh M., Yang H., Kico J.M., Ivan M. and Kaelin W.G. Jr (2001). Von Hippel-Lindau protein mutants linked to type 2C VHL disease preserve the ability to downregulate HIF. Hum Mol Genet 10: 1019-1027.

Hon W.C., Wilson M.I., Harlos K., Claridge T.D., Schofield C.J., Pugh C.W., Maxwell P.H., Ratcliffe P.J., Stuart D.I. and Jones E.Y. (2002). Structural basis for the recognition of hydroxyproline in HIF-1 by pVHL. Nature 417: 975-978.

Iliopoulos O., Ohh M. and Kaelin W.G. Jr (1998). pVHL19 is a biologically active product of the von Hippel-Lindau gene arising from internal translation initiation. Proc Natl Acad Sci USA 95: 11661-11666.

Iliopoulos O., Jiang C., Levy A.P., Kaelin W.G. and Goldberg M.A. (1996). Negative regulation of hypoxia-inducible genes by the von Hippel-Lindau protein. Proc Natl Acad Sci USA 93: 10595-10599.

Iliopoulos O., Kibel A., Gray S. and Kaelin W.G. Jr. (1995). Tumour suppression by the human von Hippel-Lindau gene product. Nat Med 1: 822-826.

Ivan M., Kondo K., Yang H., Kim W., Valiando J., Ohh M., Salic A., Asara J.M., Lane W.S. and Kaelin W.G. Jr (2001). HIFα targeted for VHL-mediated destruction by proline hydroxylation: implications for O_2 sensing. Science 292: 464-468.

Ivanov S., Kuzmin I., Wei M., Pack S., Geil L., Johnson B., Stanbridge E. and Lerman M. (1998). Down-regulation of transmembrane carbonic anhydrases in renal cell carcinoma cell lines by wild-type von Hippel-Lindau transgenes. Proc Natl Acad Sci USA 95: 12596-12601.

Iwai K., Yamanaka K., Kamura T., Minato N., Conaway R.C., Conaway J.W., Klausner R.D. and Pause A. (1999). Identification of the von Hippel-Lindau tumor-suppressor protein as part of an active E3 ubiquitin ligase complex. Proc Natl Acad Sci USA 96: 12436-12441.

Iyer N.V., Kotch L.E., Agani F., Leung S.W., Laughner E., Wenger R.H., Gassmann M, Gearhart J.D., Lawler A.M., Yu A.Y. and Semenza G.L. (1998). Cellular and developmental control of O_2 homeostasis by hypoxia-inducible factor 1α. Genes Dev 12: 149-162.

Jaakola P., Mole D.R., Tian Y.M., Wilson M.I., Gielbert J., Gaskell S.J., von Kriegsheim A., Hebestreit H.F., Mukherji M., Schofield C.J., Maxwell P.H., Pugh C.W. and Ratcliffe P.J. (2001). Targeting of HIF-α to the con Hippel-Lindau ubiquitylation complex by O_2-regulated prolyl hydroxylation. Science 292: 468-472.

Jain S., Maltepe E., Lu M.M., Simon C. and Bradfield C.A. (1998). Expression of ARNT, ARNT2, HIF1α , HIF2α and Ah receptor mRNAs in the developing mouse. Mech Dev 73: 117-123.

Jensen P., Smeyne R. and Goldowitz D. (2004). Analysis of cerebellar development in math1 null embryos and chimeras. J Neurosci 24: 2202-2211.

Jeon C.J., Strettoi E. and Masland R.H. (1998). The major cell populations of the mouse retina. J Neuroscience 18: 8936-8946.

Jeong J.W., Bae M.K., Ahn M.Y., Kim S.H., Sohn T.K., Bae M.H., Yoo M.A., Song E.J., Lee K.J. and Kim K.W. (2002). Regulation and destabilization of HIF-1α by ARD1-mediated acetylation. Cell 111: 709-720.

Kaelin, W.J. Jr (2002). Molecular basis of the VHL hereditary cancer syndrome. Nat Rev Cancer 2: 673-682.

Kagami Y. and Furuichi T. (2001). Investigation of differentially expressed genes during the development of mouse cerebellum. Gene Exp Pat 1: 39-59.

Kamada M., Suzuki K., Kato Y., Okuda H. and Shuin T. (2001). Von Hippel-Lindau protein promotes the assembly of actin and vinculin and inhibits cell motility. Cancer Res 61: 4184-4189.

Kamura T., Conrad M., Yan Q., Conaway R. and Conaway J. (1999). The Rbx1 subunit of SCF and VHL E3 ubiquitin ligase activates Rub1 modification of cullins Cdc53 and Cul2. Genes Dev 13: 2928-2933.

Kamura T., Koepp D.M., Conrad M.N., Skowyra D., Moreland R.J., Iliopoulos O., Lane W.S., Kaelin W.G. Jr, Elledge S.J., Conaway R.C., Harper J. and Conaway J.W. (1999). Rbx1, a component of the VHL tumor suppressor complex and SCF ubiquitin ligase. Science 284: 657-661.

Kanno H., Saljooque F., Yamamoto I., Hattori S., Yao M., Shuin T. and U H. (2000). Role of the von Hippel-Lindau tumor suppressor protein during neuronal differentiation. Cancer Res 60: 2820-2924.

Kessler P., Vasavada S., Rackley R., Stackhouse T., Duh F., Latif F., Lerman M., Zbar B. and Williams B. (1995). Expression of the von Hippel-Lindau tumor-suppressor gene, VHL, in human fetal kidney and during mouse embryogenesis. Mol Med 1: 457-466.

Kibel A., Iliopoulos O., DeCaprio J.A. and Kaelin W.G. Jr (1995). Binding of the von Hippel-Lindau tumor suppressor protein to elongin B and C. Science 269: 1444-1446.

Kim M., Katayose Y., Li Q., Rakkar A., Li Z., Hwang S., Katayose D., Trepel J., Cowan K. and Seth P. (1998). Recombinant adenovirus expressing von Hippel-Lindau-mediated cell cycle arrest is associated with the induction of cyclin-dependent kinase inhibitor p27Kip1. Biochem Biophys Res Commun 253: 672-677.

Klein R.S., Rubin J.B., Gibson H.D., DeHaan E.N., Alvarez-Hernandez X., Segal R.A. and Luster A.D. (2001). SDF-1 α induces chemotaxis and enhances Sonic hedgehog-induced proliferation of cerebellar granule cells. Development 128: 1971-1981.

Kleymenova E., Everitt J.I., Pluta L., Portis M., Gnarra J.R. and Walker C.L. (2004). Susceptibility to vascular neoplasms but no increased susceptibility to renal carcinogenesis in Vhl knockout mice. Carcinogenesis 25: 309-315.

Knudson A.G. Jr (1971). Mutation and cancer: statistical study of retinoblastoma. Proc Natl Acad Sci USA 68: 820-823.

Koch C.A., Vortmeyer A.O., Huang S.C., Alesci S., Zhuang Y. and Pacak K. (2001). Genetic aspects of pheochromocytoma. Endocr Regul 35:43-52.

Komuro H. and Yacubova E. (2003). Recent advances in cerebellar granule cell migration. Cell Mol Life Sci 60: 1084-1098.

Kondo K., Kim W.Y., Lechpammer M. and Kaelin W.G. Jr (2003). Inhibition of HIF-2α is sufficient to suppress pVHL-defective tumor growth. PloS Biol 1:439-444.

Kondo K., Klco J.,Nakamura E., Lechpammer M. and Kaelin W.G. (2002). Inhibition of HIF is necessary for tumor suppression by the von Hippel Lindau protein. Cancer Cell 1: 237-246.

Kondo K. and Kaelin W.G. Jr (2001). The von Hippel-Lindau tumor suppressor gene. Exp Cell Res 264: 117-125.

Koochekpour S., Jeffers M., Wang P.H., Gong C. Taylor G.A., Roessler L.M., Stearman R., Vasselli J.R., Stetler-Stevenson W.G., Kaelin W.G. Jr, Linehan W.M., Klausner R.D., Gnarra J.R. and Woude G.F.V. (1999). The von Hippel-Lindau tumor suppressor gene inhibits hepatocyte growth factor/scatter factor-induced invasion and branching morphogenesis in renal carcinoma cells. Mol Cell Biol 19: 5902-5912.

Kuzmin I., Duh F., Latif F., Geil I., Zbar B. and Lerman M.I. (1995). Identification of the promoter of the human von Hippel-Lindau disease tumor suppressor gene. Oncogene 10: 2185-2194.

Kuznetsova A.V., Meller J., Schnell P.O., Nash J.A., Ignacak M.L., Sanchez Y., Conaway J.W., Conaway R.C. and Czyzyk-Krzeska M.F. (2003). Von Hippel-Lindau protein binds hyperphopsphorylated large subunit of RNA polymerase II through a proline hydroxylation motif and targets its ubiquitination. Proc Natl Acad Sci USA. 100: 2706-2711.

Lafleur M.A., Handsley M.M. and Edwards D.R. (2003) Metalloproteinases and their inhibitors in angiogenesis. Expert Rev Mol Med 5: 1-39.

Lando D., Peet D.J., Gorman J.J., Whelan D.A., Whitelaw M.L. and Bruick R.K. (2002). FIH-1 is an asparaginyl hydroxylase enzyme that regulates the transcriptional activity of HIF. Genes Dev 16: 1466-1471.

Latif F., Tory K., Gnarra J., Yao M., Duh F., Orcutt M.L. *et al.* (1993). Identification of the von Hippel-Lindau disease tumour suppressor gene. Science 260: 1317-1320.

Lee J., Bae S., Jeong J., Kim S. and Kim K. (2004). Hypoxia-inducible factor (HIF-1)α: its protein stability and biological functions. Exp Mol Med 36: 1-12.

Lee J.Y., Dong S.M., Park W.S., Yoo N.J., Kim C.S. *et al.* (1998). Loss of heterozygosity and somatic mutations of the VHL tumour suppressor gene in sporadic cerebellar hemangioblastomas. Cancer Res 58: 504-508.

Lee S., Chen D.Y.T., Humphrey J.S., Gnarra J.R., Linehan W.M. and Klausner R.D. (1996). Nuclear/cytoplasmic localization of the von Hippel-Lindau tumor suppressor gene product is determined by cell density. Proc Natl Acad Sci USA 93: 1770-1775.

Lendahl U., Zimmermann L.B. and McKay R.D.G. (1990). CNS stem cell express a new class of intermediate filament protein. Cell 60: 585-595.

Levine E.M., Close J., Fero M., Ostrovsky A. and Reh T.A. (2000). $p27^{Kip1}$ regulates cell cycle withdrawal of late multipotent progenitor cells in the mammalian retina. Dev. Biol. 219: 299-314.

Lewis P.M., Gritli-Linde A., Smeyne R., Kottmann A. and McMahon A.P. (2004). Sonic hedgehog signalling is required for expansion of granule neuron precursors and patterning of the mouse cerebellum. Dev Biol 270: 393-410.

Li Z., Wang D., Na X., Schoen S.R., Messing E.M. and Wu G. (2003). The VHL protein recruits a novel KRAB-A domain protein to repress HIF-1α transcriptional activity. EMBO J 22: 1857-1867.

Li Z., Wang D., Na X., Schoen S.R., Messing E.M. and Wu G. (2002). Identification of a deubiquitinating enzyme subfamily as substrates of the von Hippel-Lindau tumor suppressor. Biochem Biophys Res Commun 294: 700-709.

Lindau A. (1927). Zur Frage der Angiomatosis Retinae und ihrer Hirnkomplikation. Acta Opthalmol 4: 193-226.

Lisztwan J., Imbert G., Wirbelauer C., Gstaiger M. and Krek W. (1999). The von Hippel-Lindau tumor suppressor protein is a component of an ubiquitin-protein ligase activity. Genes Dev 13: 1822-1833.

Livesey F.J., Young T.L. and Cepko C.L. (2004). An analysis of the gene expression program in mammalian neural progenitor cells. Proc Natl Acad Sci USA, 101: 1374-1379

Livesey F.J. and Cepko C.L. (2001). Vertebrate neural cell-fate determination: Lessons from the retina. Nat Rev Neurosci 2: 109-118.

Lolkema M.P., Mehra N., Jorna A.S., van Beest M., Giles R.H. and Voest E.E. (2004). The von Hippel-Lindau tumor suppressor protein influences microtubule dynamics at the cell periphery. Exp Cell Res 301: 139-146.

Lonser R.R., Glenn G.M., Walther M., Chew E.Y., Libutti S.K., Linehan W.M. and Oldfield E. (2003). von Hippel-Lindau disease. Lancet 361: 2059-2067.

Los M., Jansen G.H., Kaelin W.G. Jr, Lips C.J.M., Blijham G.H. and Voest E.E. (1996). Expression pattern of the von Hippel-Lindau protein in human tissues. Lab Invest 75: 231-238.

Lubinski W., Krzystolik K., Cybulski C., Szych Z., Penkala K., Palacz O. and Lubinski J. (2003). Retinal function in the von Hippel-Lindau disease. Doc Ophthalmol 106: 271-280.

Ma W., Tessarollo L., Hong S., Baba M., Southon E., Back T.C., Spence S., Lobe C.G., Sharma N., Maher G.W., Pack S., Vortmeyer A.O., Guo C., Zbar B. and Schmidt L.S. (2003). Hepatic vascular tumors, angiectasis in multiple organs, and impaired

spermatogenesis in mice with conditional inactivation of the VHL gene. Cancer Res 63: 5320-5328.

Mack F., Rathmell W.K., Arsham A.M., Gnarra J., Keith B. and Simon M.C. (2003). Loss of pVHL is sufficient to cause HIF dysregulation in primary cells but does not promote tumor growth. Cancer Cell 3: 75-88.

Maher E.R and Kaelin W.G. Jr (1997). Von Hippel-Lindau disease. Medicine (Baltimore) 76: 381-191.

Maher E.R., Iselius L., Yates J.R. (1991). Von Hippel-Lindau disease: a genetic study. J Med Genet 28: 443-447.

Maher E.R., Yates J.R.W. and Ferguson-Smith M.A. (1990). Statistical analysis of the two stage mutation model in von Hippel-Lindau disease, and in sporadic cerebellar hemangioblastoma and renal cell carcinoma. J Med Genet 27: 311-314.

Mahon P.C., Hirota K. and Semenza G.L. (2001). FIH-1: a novel protein that interacts with HIF-1α and VHL to mediate repression of HIF-1 transcriptional activity. Genes Dev 15: 2675-2686.

Makino Y., Kanopka A., Wilson W.J., Tanaka H. and Poellinger L. (2002). Inhibitory PAS domain protein (IPAS) is a hypoxia-inducible splicing variant of the hypoxia-inducible factor-3α locus. J Biol Chem 277: 32405-32408.

Manski T., Heffner D., Glenn G., Patronas N., Pikus A., Katz D., Lebovics R., Sledjeski K., Choyke P., Zbar B., Linehan W. and Oldfield E. (1997). Endolpymphatic sac tumors-A source of morbid hearing loss in von Hippel-Lindau disease. JAMA 277: 1461-1466.

Mansour S.L., Thomas K.R. and Capecchi M.R. (1988). Disruption of the proto-oncogene int-2 in mouse embryo-derived stem cells: a general strategy for targeting mutations to non-selectable genes. Nature 336, 348-

Martin G.R. (1981). Isolation of a pluripotent cell line from early mouse embryos cultured in medium conditioned by teratocarcinoma stem cells. Proc Natl Acad Sci USA 78: 7634-7638.

Masland R.H. (2001). The fundamental plan of the retina. Nat. Neurosci. 4(9):877-886.

Masson N., William C., Maxwell P.H., Pugh C.W. and Ratcliffe P.J. (2001). Independent function of two destruction domains in hypoxia-inducible factor-α chains activated by prolyl hydroxylation. EMBO J 20: 5197-5206.

Matzuk M.M., Finegold M.J., Su J.G., Hsueh A.J. and Bradley A. (1992). A-inhibin is a tumour-suppressor gene with gonadal specificity in mice. Nature 360: 313-319.

Maxwell P.H., Wiesener M.S., Chang G.W., Clifford S.C., Vaux E.C., Pugh C., Maher E.R. and Ratcliffe P.J. (1999). The von Hippel-Lindau gene product is necessary for oxygen-dependent proteolysis of hypoxia-inducible factor α subunits. Nature 399: 271-275.

Maynard M.A. and Ohh M. (2004). Von Hippel-Lindau tumor suppressor protein and hypoxia-inducible factor in kidney cancer. Am J Nephrol 24: 1-13.

Maynard M.A., Qi H., Chung J., Lee E.H.L., Kondo Y., Hara S., Conaway R.C., Conaway J.W. and Ohh M. (2003). Multiple splice variants of the human HIF-3α locus are targets of the von Hippel-Lindau E3 Ubiquitin Ligase complex. J Biol Chem 278: 11032-11040.

Melmon K.L. and Rosen S.W. (1964). Lindau's disease. Am J Med 36: 595-617.

Meyers E.N., Lewandoski M. and Martin G.R. (1998). An Fgf8 mutant allelic series generated by Cre- and FLP-mediated recombination. Nature Genet. 18: 136-141.

Min J., Yang H., Ivan M., Gertler F., Kaelin W.G. Jr and Pavletich N.P. (2002). Structure of an HIF-1α-pVHL complex: hydroxyproline recognition in signaling. Science 296: 1886-1889.

Miyazawa K., Himi T., Yamagashi H., Sato S. and Ishizaki Y. (2000). A role for p27/Kip1 in the control of cerebellar granule cell precursor proliferation. J Neurosci 20: 5756-5763.

Morrow E.M., Furukawa T. and Cepko C.L. (1998). Vertebrate photoreceptor cell development and disease. Trends Cell Biol 8: 353-358.

Mueller U. (1999). Ten years of gene targeting: targeted mouse mutants, from vector design to phenotype analysis. Mech Dev 82: 3-21.

Murata H., Tajima N., Nagashima Y., Yao M., Baba M., Goto M., Kawamoto S., Yamamoto I., Okuda K. and Kanno H. (2002). Von Hippel-Lindau tumor suppressor protein transforms human neuroblastoma cells into functional neuron-like cells. Cancer Res 62: 7004-7011.

Na X., Duan H.O., Messing E.W., Schoen S.R., Ryan C.K., di Sant'Agnese P.A., Golemis E.A. and Wu G. (2003). Identification of the RNA polymerase II subunit hsRPB7 as a novel target of the von Hippel-Lindau protein. EMBO J 22: 4249-4259.

Neumann H.P. and Wiestler O.D. (1991). Clustering of features of von Hippel-Lindau syndrome: evidence for a complex genetic locus. Lancet 337: 1052-1054.

Newman E. and Reichenbach A. (1996). The Mueller cell: a functional element of the retina. TINS 19:307-312

Ohh M., Park C.W., Ivan M., Hoffman M.A., Kim T., Huang L. E., Pavletich N., Chau V. and Kaelin W.G. Jr (2000). Ubiquitination of hypoxia-inducible factor requires direct binding to the β-domain of the von Hippel-Lindau protein. Nat Cell Biol 2: 423-427.

Ohh M., Yauch R.L., Lonergan K.M., Whaley J.M., Stemmer-Rachamimov A.O., Louis D.N., Gavin B.J., Kley N., Kaelin W.G. Jr and Iliopoulos O. (1998). The von Hippel-Lindau tumor suppressor protein is required for proper assembly of an extracellular fibronectin matrix. Mol Cell 1: 959-968.

Okuda H., Hirai S., Takaki Y., Kamada M., Baba M., Sakai N., Kishida T., Kaneko S., Yao M., Ohno S. and Shuin T. (1999). Direct interaction of the β-domain of VHL tumor

suppressor protein with the regulatory domain of atypical PKC isotypes. Biochem Biophys Res Commun 263: 491-497.

Park S., Dadak A.M., Haase V.H., Fontana L., Giaccia A.J. and Johnson R.S. (2003). Hypoxia-induced gene expression occurs solely through the action of hypoxia-inducible factor 1α (HIF-1α): role of cytoplasmic trapping of HIF-2α. Mol. Cell. Biol. 23: 4959-4971.

Pause A., Lee S., Lonergan K.M. and Klausner R.D. (1998). The von Hippel-Lindau tumor suppressor gene is required for cell cycle exit upon serum withdrawal. Proc Natl Acad Sci USA 95: 993-998.

Pause A., Lee S., Worrell R.A., Chen D.Y., Burgess W.H., Linehan W.M. and Klausner R.D. (1997). The von Hippel-Lindau tumor-suppressor gene product forms a stable complex with human CUL-2, a member of the Cdc53 family of proteins. Proc Natl Acad Sci USA 94: 2156-2161.

Peng J., Zhang L., Drysdale L. and Fong G.H. (2000). The transcription factor EPAS-1/hypoxia-inducible factor 2α plays an important role in vascular remodeling. Proc Natl Acad Sci USA 97: 8386-8391.

Pfander D., Kobayashi T., Knight M.C., Zelzer E., Chan D.A., Olsen B.J., Giaccia A.J., Johnson R.S., Haase V.H. and Schipani E. (2004). Deletion of Vhlh in chondrocytes reduces cell proliferation and increases matrix deposition during growth plate development. Development 131: 2497-2508.

Rafty L.A. and Khachigian L.M. (2002). Von Hippel-Lindau Tumor suppressor protein represses platelet-derived growth factor B-chain expression via the Sp1 binding element in the proximal PDGF-B promoter. J Cell Biochem 85: 490-495.

Reh T.A. and Levine E.M. (1998). Multipotential stem cells and progenitors in the vertebrate retina. J Neurobiol 36: 206-220

Richards F.M. (2001). Molecular pathology of von Hippel-Lindau disease and the VHL tumour suppressor gene. Expert Rev Mol Med 1-27.

Richards F.M., Schofield P.N., Fleming S. and Maher E.R. (1996). Expression of the von Hippel-Lindau disease tumour suppressor gene during human embryogenesis. Hum Mol Genet 5: 639-644.

Ryan H.E., Lo J. and Johnson R.S. (1998). HIF-1 α is required for solid tumor formation and embryonic vascularization. EMBO J. 17: 3005-3015.

Sakashita N., Takeya M., Kishida T., Stackhouse T.M., Zbar B. and Takahashi K. (1999). Expression of von Hippel-Lindau protein in normal and pathological human tissues. Histochem J 31:133-44.

Schoenfeld A., Davidowitz E.J. and Burk R.D. (2001). Endoplasmic reticulum/cytosolic localization of von Hippel-Lindau gene products is mediated by a 64-amino acid region. Int J cancer 91: 457-467.

Schoenfeld A., Davidowitz E.J. and Burk R.D. (1998). A second major native von Hippel-Lindau gene product, initiated from an internal translation start site, functions as a tumor suppressor. Proc Natl Acad Sci USA 95: 8817-8822.

Sharp F.R. and Bernaudin M. (2004). HIF1 and oxygen sensing in the brain. Nat Rev Neurosci 5: 437-448.

Sherr C.J. and Roberts J.M. (1999). CDK inhibitors: Positive and negative regulators of G1-phase progression. Genes Dev 13: 1501-1512.

Singh A.D., Shields C.L. and Shields J.A. (2001). Von Hippel-Lindau disease. Surv Opthalmol 46: 117-142.

Sotelo C. (2004). Cellular and genetic regulation of the development of the cerebellar system. Prog Neurobio 72: 295-339.

Staller P., Sulitkova J., Lisztwan J., Moch H., Oakeley E.J. and Krek W. (2003). Chemokine receptor CXCR4 downregulated by von Hippel-Lindau tumor suppressor pVHL. Nature 425: 307-311.

Stebbins C.E., Kaelin W.G. Jr and Pavletich N.P. (1999). Structure of the VHL-ElonginC-elonginB complex: implications for VHL tumor suppressor function. Science 284: 455-461.

Stickle N.H., Chung J., Klco J.M., Hill R.P., Kaelin W.G. Jr and Ohh M. (2004). pVHL modification by NEDD8 is required for fibronectin matrix assembly and suppression of tumor development. Mol Cell Biol 24: 3251-61.

Sufan R.I., Jewett M.A.S. and Ohh M. (2004). The role of von Hippel-Lindau tumor suppressor protein and hypoxia in renal clear cell carcinoma. Am J Physiol Renal Physiol 287: F1-F6.

Tanimoto K., Makino Y., Pereira T. and Poellinger L. (2000). Mechanism of regulation of the hypoxia-inducible factor-1α by the von Hippel-Lindau tumor suppressor protein. EMBO J 19: 4298-4309.

te Riele H., Maandag E.R. and Berns A. (1992). Highly efficient gene targeting in embryonic stem cells through homologous recombination with isogenic DNA constructs. Proc Natl Acad Sci USA 89: 5128-5132.

Thomas K.R. and Capecchi M.R. (1987). Site-directed mutagenesis by gene targeting in mouse embryo-derived stem cells. Cell 51: 503-512.

Tian H., Hammer R.E., Matsumoto A.M., Russell D.W. and McKnight S.L. (1998). The hypoxia-responsive transcription factor EPAS1 is essential for catecholamine homeostasis and protection against heart failure during embryonic development. Genes Dev. 12: 3320-3324.

Tian H., McKnight S.L. and Russell D.W. (1997). Endothelial PAS domain protein 1 (EPAS1), a transcription factor selectively expressed in endothelial cells. Genes Dev 11: 72-82.

Tomita S., Ueno M., Sakamoto M., Kitahama Y., Ueki M., Maekawa N., Sakamoto H., Gassmann M., Kageyama R., Ueda N., Gonzalez F.J. and Takahama Y. (2003). Defective brain development in mice lacking the Hif-1α gene in neural cells. Mol Cell Biol 23: 6739-6749.

Tronche F., Kellendonk C., Kretz O., Gass P., Anlag K., Orban P.C., Bock R., Klein R. and Schuetz G. (1999). Disruption of the glucocorticoid receptor gene in the nervous system results in reduced anxiety. Nat Gen 23: 99-103.

Turner D.L. and Cepko C.L. (1987). A common progenitor for neurons and glia persists in rat retina late in development. Nature. 328: 131-6.

Van der Harst E., de Krijger R.R., Dinjens W.N., Weeks L.E., Bonjer H.J., Bruining H.A., Lamberts S.W. and Koper J.W. (1998). Germline mutations in the vhl gene in patients presenting with phaeochromocytomas. Int J Cancer 77: 337-340.

Vetter M.L. and Moore K.B. (2001). Becoming glial in the neural retina. Dev Dyn 221: 146-153.

Von Hippel E. (1904). Ueber eine sehr seltene Erkrankung der Netzhaut. Graefe Arch Opthalmol 59: 83-106.

Voyvodic J.T., Burne J.F. and Raff M.C. (1995). Quantification of normal cell death in the rat retina: implications for clone composition in cell lineage analysis. Eur J Neurosci 7: 2469-2478.

Wahlin K.J., Lim L., Grice E.A., Campochiaro P.A., Zack D.J. and Adler R. (2004). A method for analysis of gene expression in isolated mouse photoreceptor and Muller cells. Mol Vis 10: 366-75.

Wang G., Reisdorph R., Clark R.E., Miskimins R., Lindahl R. and Miskimins W.K. (2003). Cyclin dependent kinase inhibitor p27Kip1 is upregulated by hypoxia via an ARNT dependent pathway. J Cell Biochem 90: 548-560.

Wang V.Y. and Zoghbi H.Y. (2001). Genetic regulation of cerebellar development. Nat Rev Neurosci 2: 484-491.

Wassle H. and Boycott B.B. (1991). Functional Architecture of the Mammalian Retina. Physiological Reviews 71 (2): 447-447.

Wiesener M.S., Jurgensen J.S., Rosenberger C., Scholze C.K., Horstrup J.H., Warnecke C., Mandriota S., Bechmann I., Frei U.A., Pugh C.W., Ratcliffe P.J., Bachmann S., Maxwell P.H. and Eckardt K.U. (2003). Widespread hypoxia-inducible expression of HIF-2α in distinct cell populations of different organs. FASEB J. 17: 271-273.

Woodward E.R., Buchberger A., Clifford S.C., Hurst L.D., Affara N.A. and Maher E.R. (2000). Comparative sequence analysis of the VHL tumor suppressor gene. Genomics 65: 253-265.

Yang J., Bian W., Gao X., Chen L. and Jing N. (2000). Nestin expression during mouse eye and lens development. Mech. Dev. 94: 287-291.

Young, R.W. (1985). Cell proliferation during postnatal development of the retina in the mouse. Brain Res 353: 229-239.

Zatyka M., Morrissey C., Kuzmin I., Lerman M.I., Latif F., Richards F.M. and Maher E.R. (2002). Genetic and functional analysis of the von Hippel-Lindau (VHL) tumour suppressor gene promoter. J Med Genet 39: 463-472.

Zatyka M., da Silva N.F., Clifford S.C., Morris M.R., Wiesener M.S., Eckardt K.U., Houlston R.S., Richards F.M., Latif F. and Maher E.R. (2002). Identification of cyclin D1 and other novel targets for the von Hippel-Lindau tumor suppressor gene by expression array analysis and investigation of cyclin D1 genotype as a modifier in von Hippel-Lindau disease. Cancer Res 62: 3803-3811.

Plasmid Maps

pET-16b Vector

TB046 2/00

The pET-16b vector (Cat. No. 69662-3) carries an N-terminal His•Tag® sequence followed by a Factor Xa site and three cloning sites. Unique sites are shown on the circle map. Note that the sequence is numbered by the pBR322 convention, so the T7 expression region is reversed on the circular map. The cloning/expression region of the coding strand transcribed by T7 RNA polymerase is shown below.

pET-16b sequence landmarks	
T7 promoter	466-482
T7 transcription start	465
His•Tag coding sequence	360-389
Multiple cloning sites	
(*Nde* I -*Bam*H I)	319-335
T7 terminator	213-259
lacI coding sequence	869-1948
pBR322 origin	3885
bla coding sequence	4646-5503

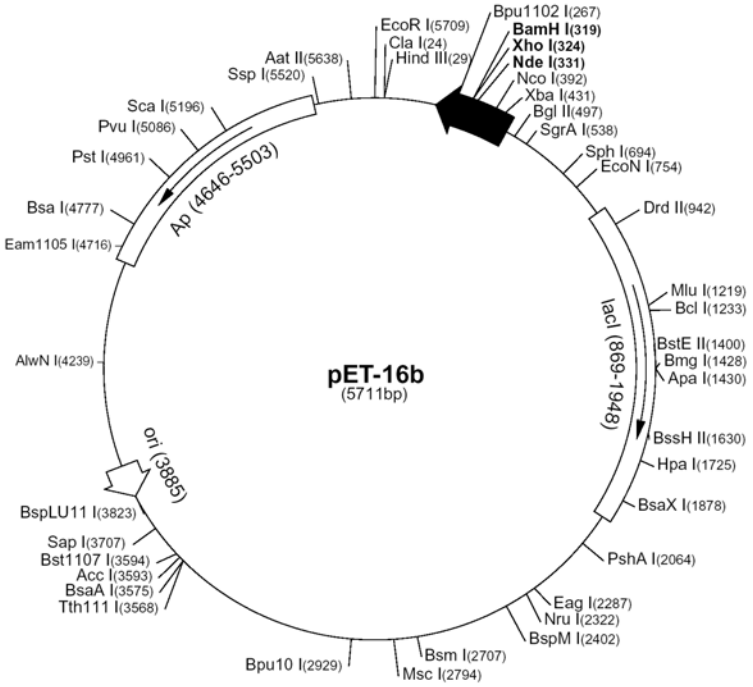

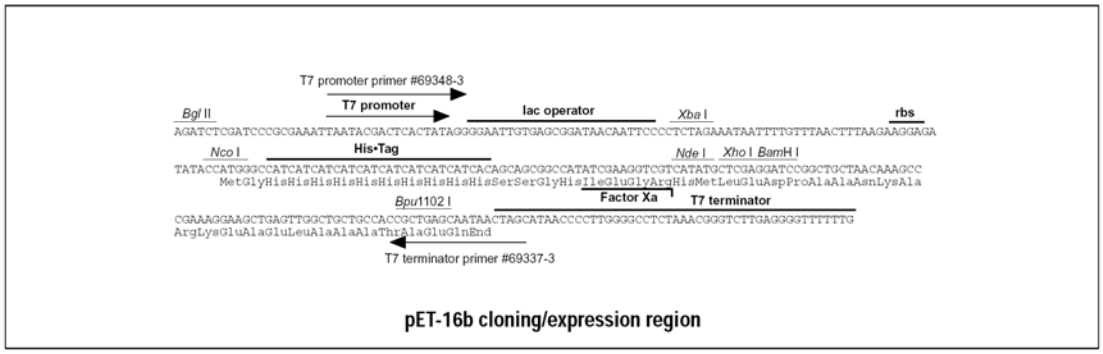

pET-16b cloning/expression region

pET-17b Vector

TB047 12/98

The pET-17b vector (Cat. No. 69663-3) carries an N-terminal 11aa T7•Tag® sequence followed by a region of useful cloning sites. Included in the multiple cloning region are dual *BstX* I sites, which allow efficient cloning using an asymmetric linker (1). Unique sites (except for the two *BstX* I sites) are shown on the circle map. Note that the sequence is numbered by the pBR322 convention, so the T7 expression region is reversed on the circluar map. The cloning/expression region of the coding strand transcribed by T7 RNA polymerase is shown below.

1. Seed, B. (1987) *Nature* **329**, 840.

pET-17b sequence landmarks	
T7 promoter	333-349
T7 transcription start	332
T7•Tag coding sequence	237-269
Multiple cloning sites	
(*Hin*d III - *Xho* I)	141-228
T7 terminator	28-74
pBR322 origin	1480
bla coding sequence	2241-3098

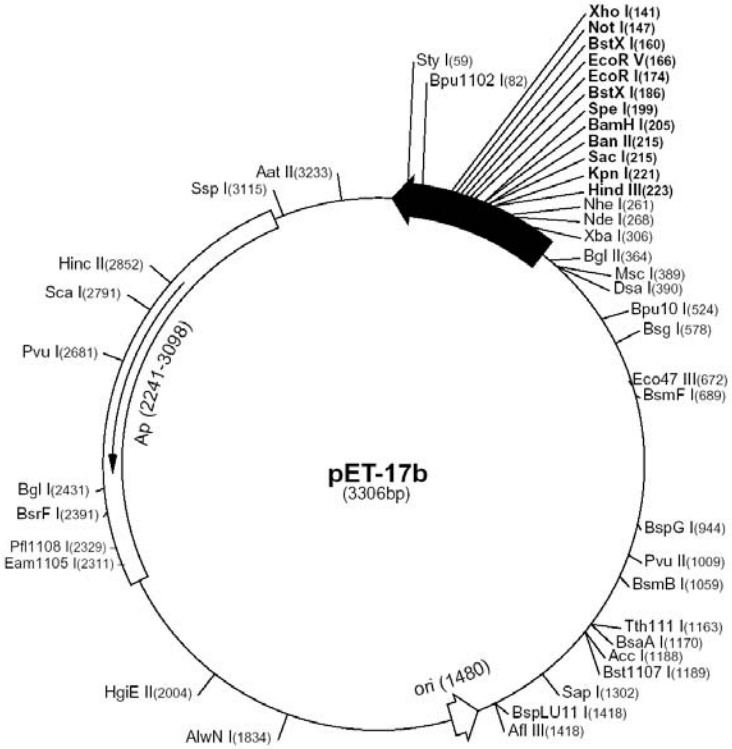

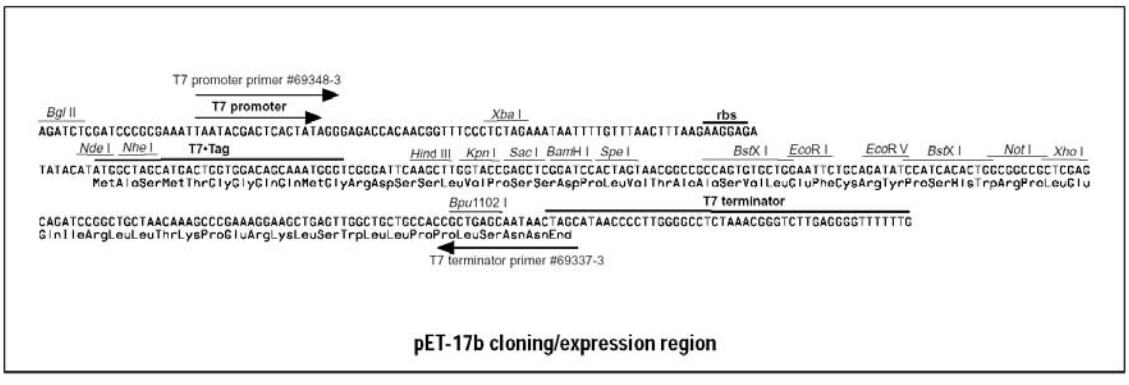

pET-17b cloning/expression region

pET-28a-c(+) Vectors

TB074 12/98

	Cat. No.
pET-28a DNA	69864-3
pET-28b DNA	69865-3
pET-28c DNA	69866-3

The pET-28a-c(+) vectors carry an N-terminal His•Tag®/thrombin/T7•Tag® configuration plus an optional C-terminal His•Tag sequence. Unique sites are shown on the circle map. Note that the sequence is numbered by the pBR322 convention, so the T7 expression region is reversed on the circular map. The cloning/expression region of the coding strand transcribed by T7 RNA polymerase is shown below. The f1 origin is oriented so that infection with helper phage will produce virions containing single-stranded DNA that corresponds to the coding strand. Therefore, single-stranded sequencing should be performed using the T7 terminator primer (Cat. No. 69337-3).

pET-28a(+) sequence landmarks	
T7 promoter	370-386
T7 transcription start	369
His•Tag coding sequence	270-287
T7•Tag coding sequence	207-239
Multiple cloning sites	
(*Bam*H I - *Xho* I)	158-203
His•Tag coding sequence	140-157
T7 terminator	26-72
lacI coding sequence	773-1852
pBR322 origin	3286
Kan coding sequence	3995-4807
f1 origin	4903-5358

The maps for pET-28b(+) and pET-28c(+) are the same as pET-28a(+) (shown) with the following exceptions: pET-28b(+) is a 5368bp plasmid; subtract 1bp from each site beyond *Bam*H I at 198. pET-28c(+) is a 5367bp plasmid; subtract 2bp from each site beyond *Bam*H I at 198.

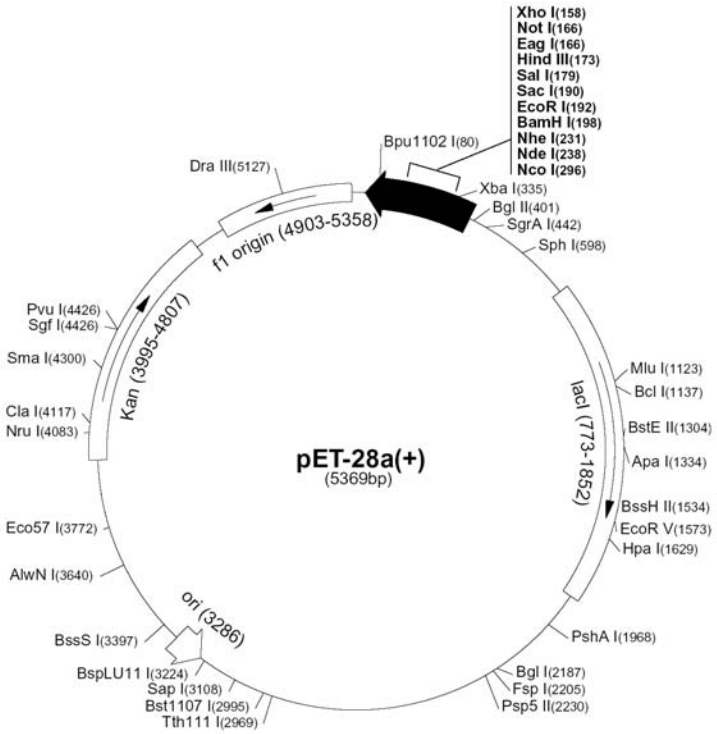

pET-28a-c(+) cloning/expression region

f1 (+) origin 135–441
β-galactosidase α-fragment 460–816
multiple cloning site 653–760
***lac* promoter** 817–938
pUC origin 1158–1825
ampicillin resistance (*bla*) ORF 1976–2833

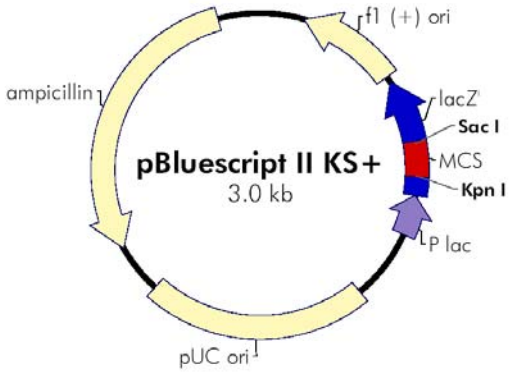

pBluescript II KS (+/–) Multiple Cloning Site Region (sequence shown 598–826)

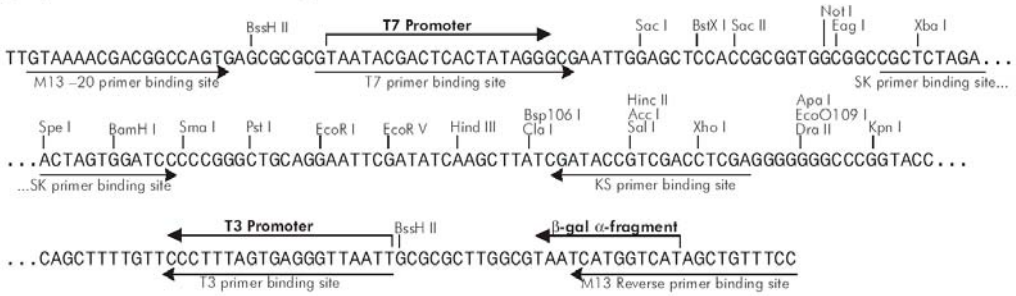

Acknowledgements

To begin with I would like to thank Prof. Dr. Wilhelm Krek for giving me the opportunity to carry out my thesis in his laboratory. I will be always grateful for what I have learned in these few years, because I learned much more than just dealing with everyday scientific problems and challenging questions…..I started understanding who I am, who I can be and who I want to be (*Jitka, I love you for verbalising this perspective*…) . For this "swimming lesson" and for the opportunity to finish my ongoing works as a postdoc I sincerely thank you Willy.

A big thank you goes also to Prof. Dr. Thomas Bickle as my Fakultätsverantwortlicher and to Prof. Dr. Holger Moch as Korefferent, who, in the occasions that I had the pleasure to meet them, were very enthusiastic and interested in my ongoing work and who made it possible to fix a date for my final exam so easily.

I want to thank Melanie Sticker for her great work in regards to the localization studies. Whenever she came there was a positive result coming…..so I wish that good things will keep on coming on now that we are together again. ☺

I need to thank Christiane Wirbelauer for making it easy for me when I first started in the lab by providing loads of help and advice regarding any kind of method. She really had it all under control….. In addition I want to thank Robert E. Barry for being a special colleague, apart from being the only normal PhD student when I started….☺. My sincere gratitude goes also to all the other members of the Krek Lab for providing advice, help and entertainment, each of them in different occasions. Manuela Hitz needs a special thank you for being a great lab-companion and for doing a good job with all those squirky mice. I am happy she joined this lab. In regards to mice, especially regarding the knockout strategy and the isolation of retinas, I want to thank Prof. Dr. Ulrich Müller for his invaluable help and advice. Thanks also to Dr. Philippe Bugnon for being the nicest and most helpful vet I have ever met and to all the people who have helped me in moments of need and that are too many to be all mentioned by name. I just hope that whenever I was helped I made sure to show my gratitude then……..

Thank you to Jitka Sulitkova for being my "companion of (dis)adventure" besides being a friend. Vanda Pogacic, there are no words to express my happiness to have met you and to have you as a friend (….and true friends last forever…..). *Girls, I miss the good old times, but I believe they will come again. Thank you for making me so often smile and think about other things, like LIFE, and for being simply your way*.

Many thanks go also to Francesca Cesari for her support during the writing of this thesis.

Last, but not least the three most important people in my life have to be thanked:

I thank my parents for their continuous support and advice throughout whatever I was doing or going through and for their unconditional love that always kept me warm. You were the best, you are the best and you will always be the best and most adorable parents in the world. Vi voglio un mondo di bene…

Dimitris Anastasiou has proven to be the most valuable and amiable person I have ever met. I need to thank him for giving me strength, love, help and support and for being, on top of all this, an inspiration at work. You complete me…